Durham E-Theses

Optimisation of Fluid Properties and Process Parameters for Batch Slot Die Coating of Dilute Polymer Systems

STOBO, ANNA-MARIE

Optimisation of Fluid Properties and Process Parameters for Batch Slot Die Coating of Dilute Polymer Systems

MSc Thesis

Department of Chemistry

Anna-Marie Stobo

2017

Abstract

The effects of viscosity and surface tension are well documented in the case of roll-to-roll slot die systems. However their influence in combination with process parameters for batch scale coaters are less often discussed. Lack of coating uniformity attained using a bespoke slot die coater at the CPI National Printable Electronics Centre led to the requirement for an investigation to identify the sources of error.

This project outlines a method used to determine the effects of material and process parameters on coating quality without the requirement for modification of equipment. It also describes the development of a series of versatile formulations containing polyethylene oxide that can be used to mimic similar polymer formulations for cost-effective initial process development of new materials.

Various dilute polymer systems were developed whereby solids loading, viscosity and surface tension were all fully controlled. Design of Experiments techniques were employed to determine relationships between parameters and fluid properties. Chosen parameters included coating velocity, coating acceleration, coating gap (gap between slot die lips and substrate), volume infuse (volume of material initially infused) and flow infuse (flow rate of material initially infused). Their effects on coating thickness and thickness uniformity were quantified for the bulk region of the coating, resulting in the development of a statistical model to aid optimisation of parameters for new materials.

Surface tension had a minimal effect on coating thickness and uniformity during the screening study so this was not included in the final model. Coating acceleration and flow infuse exhibited a proportional relationship relating to coating thickness uniformity. Volume infuse did not have a significant effect on coating thickness or uniformity. Particular focus was placed on viscosity and coating velocity; in the case of this bespoke tool they were found to be inversely proportional in relation to coating thickness and uniformity. They strongly influenced the flow rate and the resultant coating thickness due to the effects of fluid resistance, though the wet coat thickness parameter was held at a constant value. This suggested that the system does not work by a feedback loop to correct the flow rate for fluid resistance and internal pressure effects. Regardless of this, an operating window was found in which coating thickness and uniformity can be controlled for polymer solutions with a range of viscosities.

Acknowledgements

Firstly I would like to thank my manager Dave Barwick for making this MSc project happen and for his support and advice through the whole process. I would also like to thank CPI and the Catapult for funding this project, I hope this process has been as valuable for you as it has for me.

As always my colleagues at CPI have been very helpful, in particular John for all of the DOE advice you've given me. Thanks team process for sputtering substrates at short notice and team maintenance (mainly Lee!) for working so hard with me to coordinate slot die head setups.

Thank you Richard and Colin for your supervision, I hope we can keep in touch in the future. I'm grateful to Richard and Colin's groups for helping me while working in unfamiliar labs at Durham, particularly Beth for carrying out formulation analysis and answering my silly questions.

Finally I would like to thank my family for all of their love and support. In particular my mum for her valuable feedback and error checking, and my boyfriend Adam who kept me sane and well fed during those final few months.

Contents

Glossary of Terms - English Alphabet

$a = Acceleration$

$A = Area$

$Av = Mean\ thickness$

$B = Coating\ width$

$\dfrac{dV_p}{dt} = Flow\ rate\ of\ the\ pump$

$D = Distance\ between\ anode\ and\ cathode$

$E = Electric\ field$

$E_0 = Amplitude\ of\ electric\ field$

$f = Frequency$

$F = Force$

$G' = Storage\ modulus$

$G'' = Loss\ modulus$

$G_N^0 = Plateau\ modulus$

$G_x = Crossover\ modulus$

$h = Height$

$I = Slot\ area\ height\ (distance\ between\ downstream\ edge\ of\ manifold\ and\ slot\ exit)$

$J = Current\ density$

$k = Excinction\ coefficient$

$K = Constant$

$L = Length$

$M = Mass$

$M_e = Entanglement\ molecular\ weight$

$M_n = Number\ average\ molecular\ weight$

$Mn_c = Calculated\ number\ average\ molecular\ weight$

$M_w = Weight\ average\ molecular\ weight$

$Mw_c = Calculated\ weight\ average\ molecular\ weight$

$Mw_H = Weight\ average\ molecular\ weight\ of\ high\ molecular\ weight\ polymer$

$Mw_L = Weight\ average\ molecular\ weight\ of\ low\ molecular\ weight\ polymer$

$n = Refractive\ index$

$N = Number\ Fraction$

$N_H = Number\ fraction\ of\ high\ molecular\ weight\ polymer$

$N_L = Number\ fraction\ of\ low\ molecular\ weight\ polymer$

$p = Deflection\ path$

$PDI = Polydispersity\ index$

$r = Radius$

$R = Ideal\ gas\ constant$

$Rf = Fluid\ resistance$

$s = Shim\ thickness$

$S = Distance\ from\ the\ start\ of\ the\ coating$

$SD = Thickness\ standard\ deviation$

$T = Temperature$

$t = Time$

$H_d = Dry\ coat\ thickness$

$H_w = Wet\ coat\ thickness$

$TABLE_{\gamma\eta} = Results\ table, shear\ rate\ v.s.\ viscosity$

$TRUE = Find\ closest\ match$

$U\% = Uniformity$

$v = Velocity$

$v\% = Volume\ percent\ of\ solids$

$V_d = Potential\ difference\ (between\ anode\ and\ cathode)$

$wt\% = Weight\ percent\ of\ solids$

$x = Distance\ travelled\ by\ light$

Glossary of Terms - Greek Alphabet

$\gamma = Strain$

$\dot{\gamma} = Shear\ rate$

$\dot{\gamma}_L = Shear\ rate\ in\ lips$

$\dot{\gamma}_{min} = Lowest\ experimental\ shear\ rate\ value$

$\Delta p = Change\ in\ pressure/Internal\ pressure$

$\eta = Viscosity$

$\theta = Contact\ angle$

$\lambda = Wavelength\ of\ light$

$\rho = Density$

$\sigma = Surface\ tension$

$\sigma_l = Surface\ tension\ of\ the\ liquid$

$\sigma_s = Surface\ free\ energy\ of\ the\ solid$

$\sigma_{sl} = Interfacial\ tension\ between\ liquid\ and\ solid$

$\tau = Shear\ stress$

$\varphi = Deflection\ angle$

List of Tables

1. Introduction

Thin-film coating is prominent in many technology areas; from wearable devices to supercapacitor batteries to packaging medical products. A number of solution coating techniques are employed depending on the application such as slot die coating, spin coating, inkjet printing and screen printing. Slot die coating has the potential to become the most widely used wet coating technique for the blanket coating of high performance materials, however the difficulty of developing a robust process sometimes hinders its popularity growth. It requires an understanding of chemistry and engineering to fully exploit its potential to produce highly uniform coatings. In addition to this many systems have a large number of parameters to optimise that will interact with coating material properties to affect coating quality. The referenced parameters include wet coat thickness, coating speed, coating acceleration and coating gap, others will be described in detail in section 1.a.

In the field of printable electronics, coating thickness uniformity is particularly critical to the fabrication of organic light-emitting diode (OLED) devices, an example of a simple device stack is shown in Figure 1. The organic emitting and hole injection layers are deposited via solution processed techniques, either spin coating or slot die coating. Spin coating applies thin coatings by dispensing ink into the centre of the substrate and spinning at high speeds (500 – 3000 rpm) causing the material to spread uniformly across the surface. Slot die coating incorporates a polished stainless steel head with a slit of set width through the centre; fluid is fed through this gap at a controlled flow rate to form a meniscus where it meets the substrate. The substrate is moved at a defined speed underneath the head so that ink is dispensed across the plate. The indium tin-oxide (ITO) anode is commonly applied via sputter coating techniques as described in Sivaji Reddy (2006)[1]. Thermal evaporation is the usual method of deposition for the silver cathode, as detailed in Lv (2006)[2]. See appendix 4 for an example set of processing steps.

Barrier e.g. Glass - 0.7 mm
Adhesive e.g. DELO glue
Cathode e.g. Silver – 100 nm
Organic emitting layer e.g. Polymer-based ink – 100 nm
Hole injection layer (HIL) e.g. PEDOT: PSS ink – 100 nm
Anode e.g. ITO - 100 nm
Substrate e.g. Glass – 0.7 mm

Figure 1: Schematic cross-section of an example OLED device structure

When a voltage is applied to an OLED device electrons leave the cathode and positively charges 'holes' leave the anode, both moving towards one another. The HIL layer facilitates the movement of holes towards the emissive layer. Electrons travel to the lowest unoccupied molecular orbital (LUMO) and holes inhabit the highest occupied molecular orbital (HOMO), within the semiconducting emissive layer; species recombine and photons are released.[3] The thickness of the emissive layer is critical due to the mobility of the charged species; ideally recombination will occur in the centre of the emissive region, thicker or thinner layers will result in species recombining towards an edge of the emissive region. Usually 80 – 100 nm is ideal for solution processed emissive polymers.[4]

Low uniformity of the emitting layer and HIL will result in variable distances between the anode and cathode across the device. Due to the proportional relationship of current density and luminance[5], Childs Law[6] dictates that deviations in distance between the anode and cathode will cause light variations i.e. bright and dark regions, making the device not fit for purpose. In addition to this, light emitting polymers (LEPs) are expensive; ranging from £500 - £1500 per gram. The high cost of these material often hinders the amount of process development that can occur.

$$J = \frac{KV_d^{\frac{3}{2}}}{D^2}$$

Equation 1: Childs Law.

where:

- $J = Current\ density$

- $V_d = Potential\ difference\ (between\ anode\ and\ cathode)$

- $D = Distance\ between\ anode\ and\ cathode$

- $K = Constant$

Non-uniformity is often observed at the Printable Electronics platform of the Centre for Process Innovation (CPI) where this project was carried out. The aim was to develop an understanding of how material properties interact with process parameters to determine coating quality and uniformity. Slot die coating is favoured for the blanket coating of a variety of polymer-based formulations due to the vast variation in production scale, viscosity capabilities and wet coat thickness control. It also results in low levels of waste and operates in a closed environment. The advantages and disadvantages of slot die coating will be compared with other wet coating techniques in section 1.b.

The equipment that was investigated is a batch slot die coater built into a bespoke Large Area Coating Equipment (LACE) line, designed to produce OLED and OPV devices on a 4", 6" and 8" scale. The prototyping line comprises four modules each with a different function, see appendices 1 and 2 for an overview of the system and a description of each unit. Wet coating is carried out in the ambient module and the inert module. Processing in the ambient module is carried out in air under minimal extraction; this is used for non-air sensitive materials and chemicals without inhalation risks, usually water-based inks. The inert module has adequate extraction for use with hazardous solvents and is fully sealed with a glass cover incorporating rubber gloves. It can be filled with nitrogen for use with oxygen and moisture sensitive materials, however this was not necessary for this project. Substrates are moved through the system using an automated robotics system and equipment can be operated individually to allow for process development on specific tools. There is more detailed information regarding the LACE line and its integrated coating equipment in appendices 2 and 3.

This project focussed on the solution processing of polymer materials by slot die coating. The LACE slot die system is controlled by 24 parameters that, when optimised, should result in highly uniform coatings i.e. coating thickness variation of less than 5% across a substrate, while affording very little waste. For the purpose of this project, uniformity was defined as:

$$U\% = \frac{SD}{Av} \times 100$$

Equation 2: Definition of uniformity

where:

- $U\% = Uniformity$
- $SD = Thickness\ Standard\ Deviation$
- $Av = Mean\ thickness$

To put into context the challenges involved, the slot die coating process must be described in detail. In the next section each parameter will be explained alongside an illustration and the parameter ranges. In some cases the typical values have been stated.

a. Mode of Operation and Description of Parameters
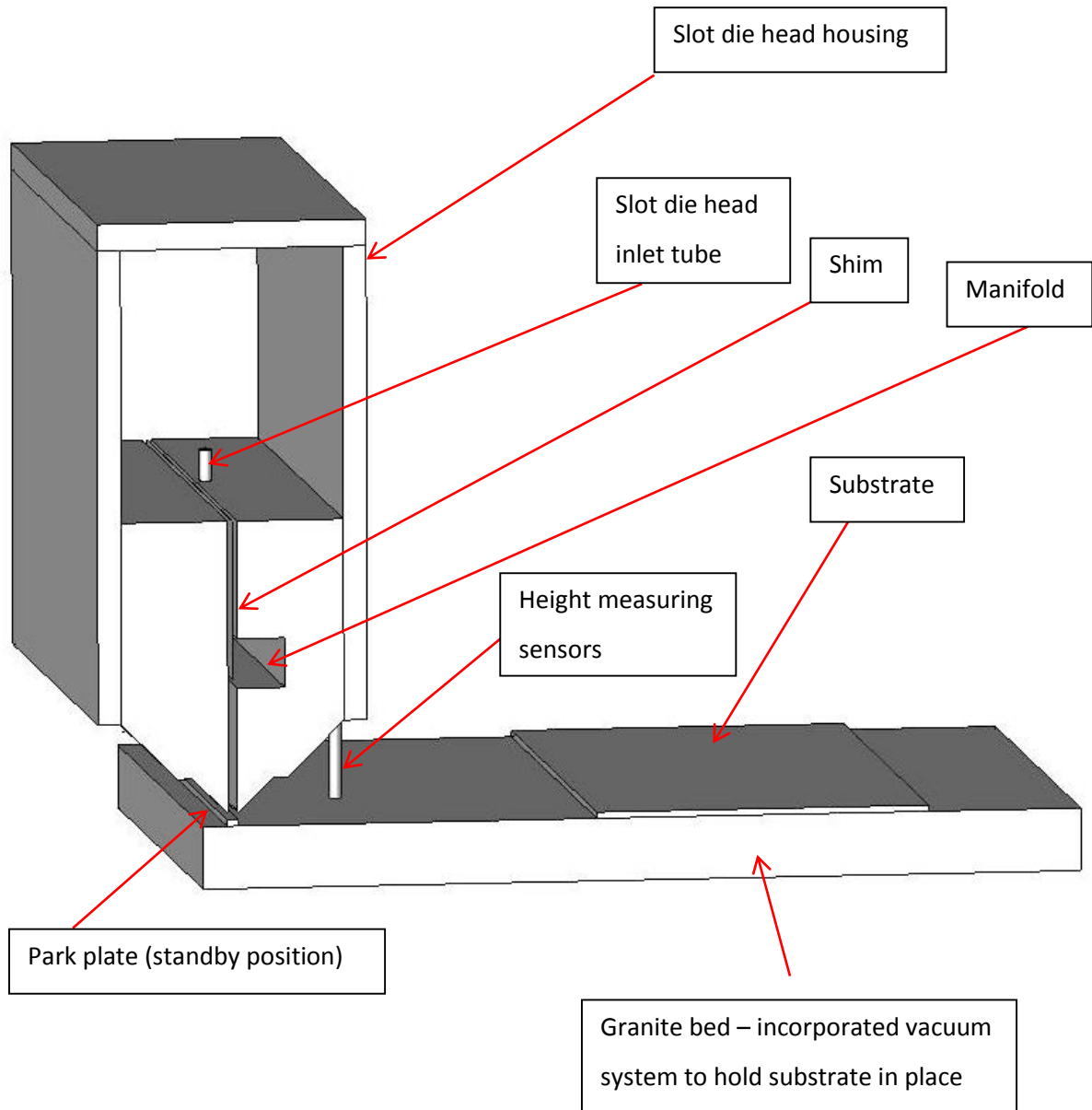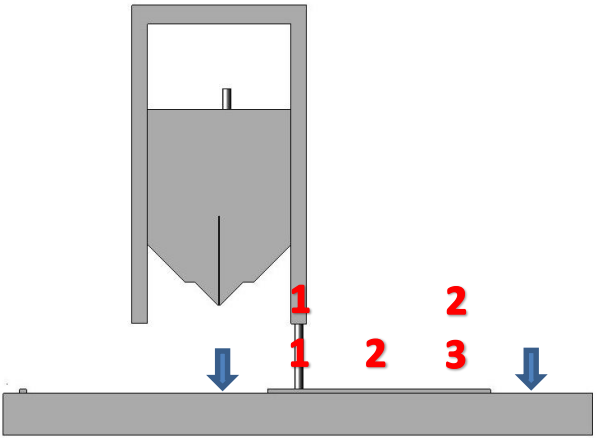
Figure 2: Simplified 3D CAD rendering of the LACE slot die system and labelled components.
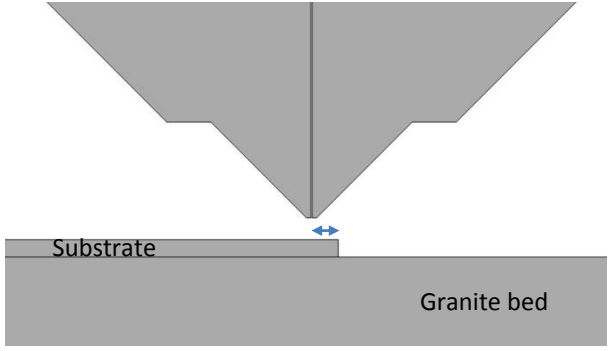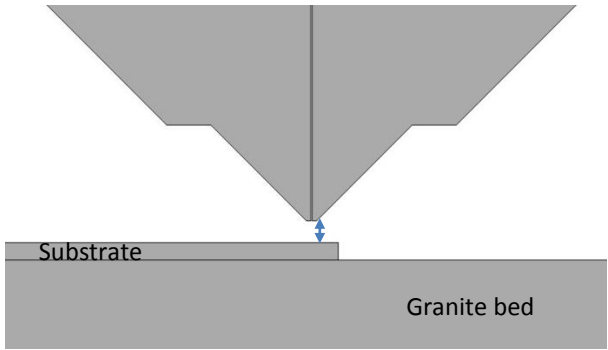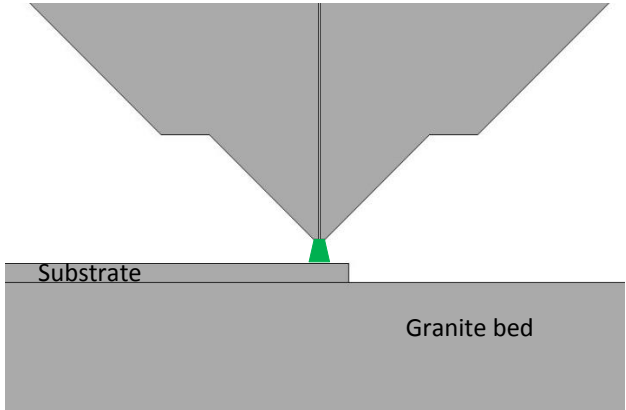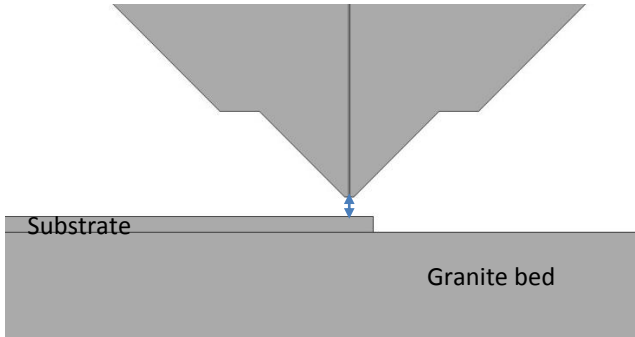
Figure 3: Photographic image of the slot die coater
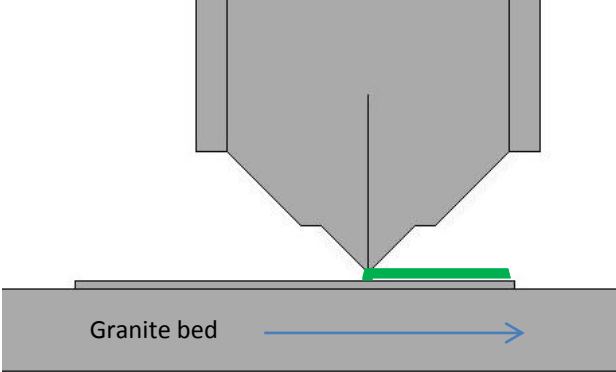
The system works by batch processing i.e. sheet-to-sheet coating. The fluid feeding system is controlled by Harvard syringes which are attached to the inlet tube via approximately 500 mm of 3.3 mm internal diameter tubing. The volume required to fill the tubing and the head (known as the dead volume) is 10 mL. The syringes and slot die head are controlled by the internal software. The granite bed is flat to a tolerance of ±2 μm to ensure the substrate-die lips gap remains constant. The slot die head lips and internal faces are polished flat, the mean roughness was measured to be Sa – 28.9 nm ± 0.9 nm, Sq – 51.6 nm ± 2.5 nm (see section 3.c.ii for description of roughness parameters); any defects could drastically impact coating quality. The two slot die faces are separated by a shim which defines the slot width that material flows through; this is critical to providing control over the fluid as it is dispensed. Low viscosity materials require a thin shim e.g. 50 μm to prevent material from 'falling' through the head. High viscosity materials require a thicker shim e.g. 150 μm to keep pressure in the system at a manageable level i.e. below 700 N/m^2.
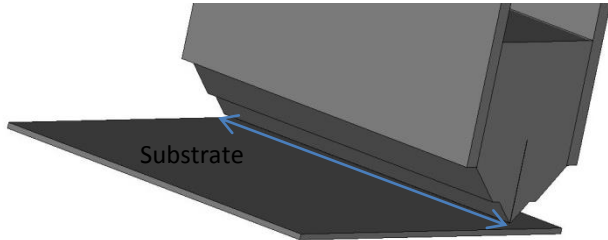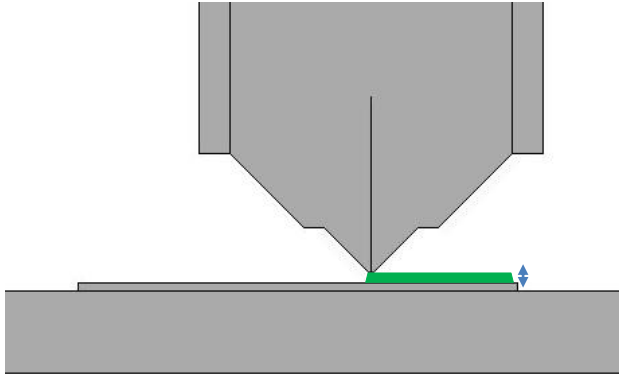
Each of the slot die parameters will be explained alongside a picture to show their relevance at each stage of coating, Table 1. Parameters are input prior to coating and cannot be controlled during processing.
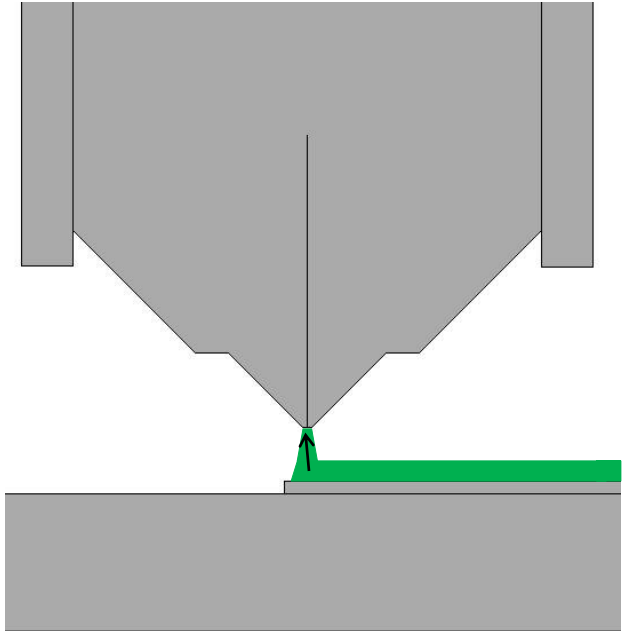
Stage	Diagram	Operation/Description	Parameter	Range	Units
Stage 1 – Bead formation		There are two positions on the inert slot die and one on the ambient; the correct position of the head must be selected. For the ambient module this is always 1.	Slot die selection	1 or 2	None
		A substrate of chosen size is placed in position on the slot die system and is held in place with vacuum. The system will not work if there is no substrate in place i.e. vacuum is not achieved.	Substrate size	4, 6 or 8	Inches
		The head lifts and the bed begins to move to the left, sensors come down to touch the bed and substrate; this detects the distance between the slot die head housing and substrate/granite bed. The red numbers signify distance checks on the substrate which is either carried out at 2 or 3 points. The blue arrows represent distance checks on the bed; the bed and substrate distances are used to calculate the substrate thickness. Generally 2 points are measured for a 4 inch substrate, 3 for an 8 inch substrate.	Number of substrate measure points	2 or 3	None
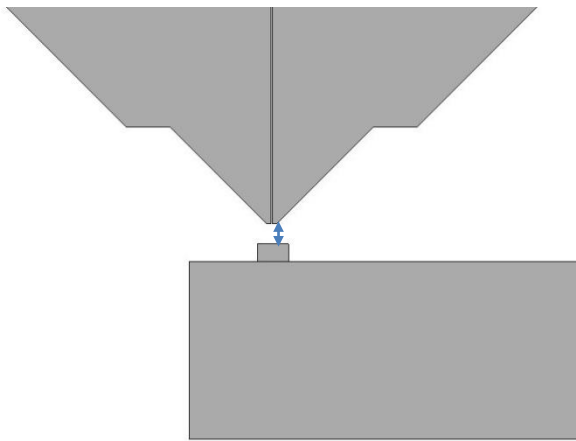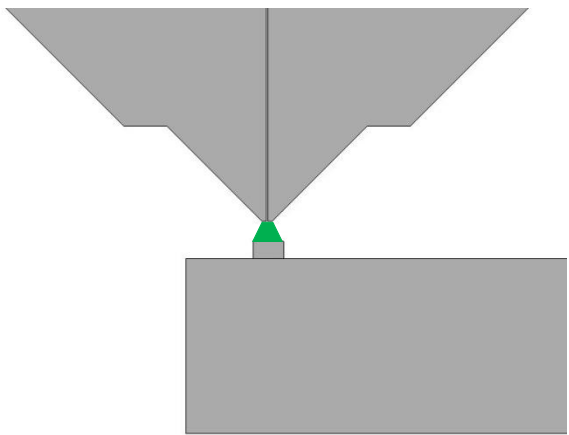
Stage 1 – Bead formation		The bed moves the substrate so that the slot die lips are situated near the start of the substrate; a gap will be left between the edge of the plate and the start of the coating. The gap is left at the start and end of the plate to prevent material from spilling over the substrate. This is usually set to 1 mm.	Coating border	0 - 40	mm
		The head is moved so that the lips and substrate are a controlled distance apart to aid bead formation. Coating gaps larger than 200 µm often result in a meniscus not being formed.	Coating priming gap	0 – 4,000	µm

Stage 1 – Bead formation		The material syringe feeds formulation to the head to allow a bead to form between the die lips and the substrate.	Material bead volume infuse	0 – 100,000	μL
			Material bead flow infuse	0 – 150,000	μL/min
		The head will stay in this position for a defined time.	Coating start delay	0 – 30,000	ms
Stage 2 - Coating		The head will move to the defined coating gap as it starts moving.	Coating gap	0 – 4,000	μm

Stage 2 - Coating		The bed will move and accelerate at the set speed and rate.	Coating velocity	1 – 30	mm/s
			Coating acceleration	1 – 450	mm/s²
		The material pump can start as soon as the bed begins to move, or after a defined time/distance.	Pump start offset	0 – 2,000	ms
			Coating material pump start offset	0 – 50	mm

Granite bed

Stage 2 - Coating		The width of the coating is defined by the width of the shim; there is usually a small gap at the top and bottom of the coating i.e. ~1 mm to prevent material from spilling over the edge.	Coating width	100, 150 or 200	mm
		The amount of material to be deposited (i.e. wet coat thickness) is set and the flow rate is adjusted automatically by the syringe control units.	Coating film thickness	0 – 400	µm
		The material pump can be stopped a defined distance before the end of the plate to reduce the amount of material left at the end of the plate.	Coating material pump stop offset	0 – 50	mm

Stage 3 – Lifting the head				
	The head may begin lifting before the end of the coating (0 or 1 i.e. off or on), the distance before the end of the plate is defined.	Slot die take-off mode	0 or 1	None
		Take-off offset	0 – 50	mm
	Any leftover material can be drawn back into the head, the volume and flow rate are defined.	Material bead volume withdraw	0 – 100,000	µL
		Material bead flow withdraw	0 – 150,000	µL/min

Stage 4 - Standby		Once the head has lifted it will return to the standby (park) position with the lips a defined distance from the park plate.	Standby gap	10 – 4,000	µm
		A bead is formed between the lips and park plate to ensure the lips stay wet, volume and flow rate of infused material is defined.	Standby bead volume	0 – 100,000	µL
			Standby bead flow	0 – 150,000	µL/min
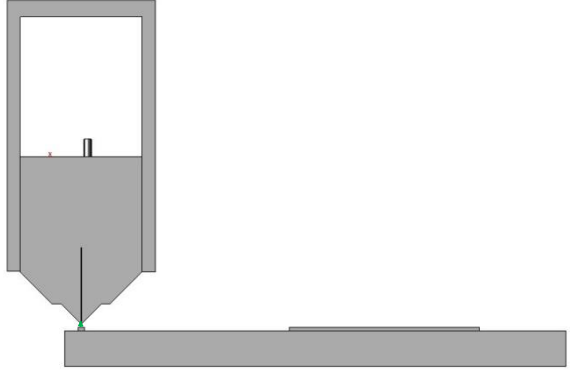
			Standby material flow	0 – 150,000	μL/min
Stage 4 - Standby		Once the bead has formed material will be fed through the head at a defined rate. This prevents formulations from drying and the head from becoming blocked.			

Table 1: Mode of action of the LACE slot die coater and description of parameters.

To evaluate the benefits of slot die it must be compared with other techniques. A number of techniques ranging in scale will be discussed in the next section.

b. Comparison With Other Coating Techniques

Spin coating is a common technique in the field of thin-film research as it produces highly uniform coatings and process development is minimal. It works by placing a substrate on a vacuum chuck; material is dispensed in the centre of the substrate and it is spun at a high speed, usually 500 – 3000 rpm, to allow spreading across the substrate.

Lid is closed once fluid is dispensed to contain material while coating is in progress

Arm moves to an area above and in the centre of the substrate to dispense coating media

Vacuum chuck holds substrate using vacuum and spins at a defined speed causing the material to spread across the substrate
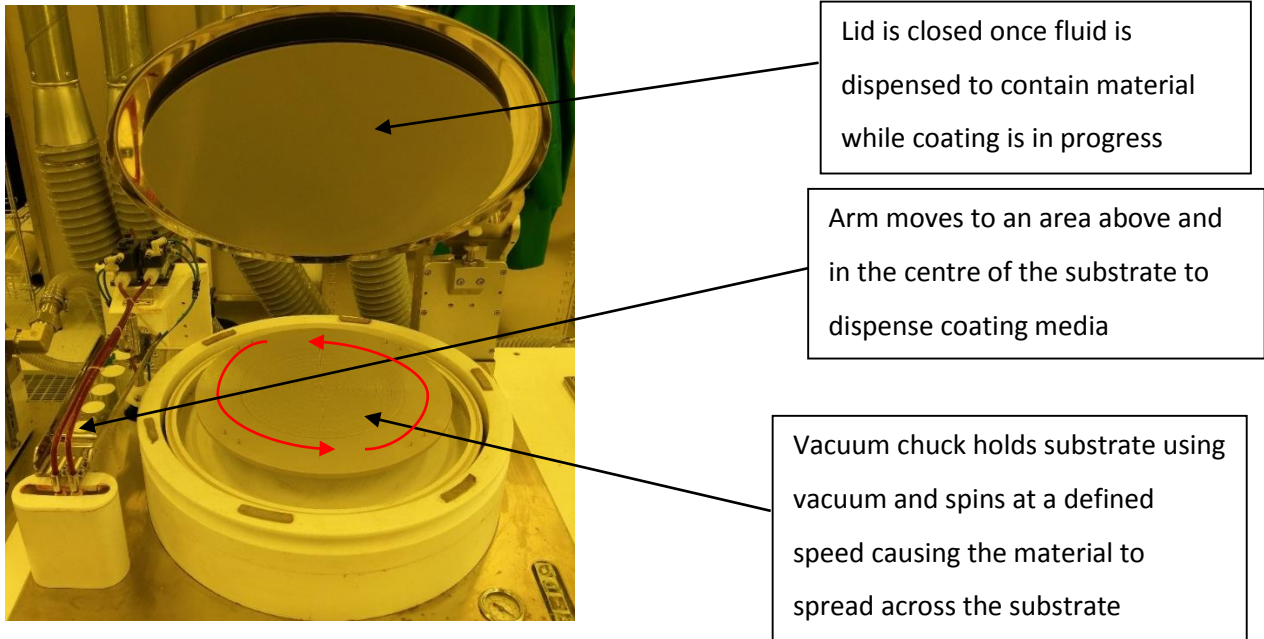
Figure 4: Image describing the spin coating process

Spin coating is ideal for small scale research. When attempting to upscale processes the excessive level of wastage becomes apparent; up to 95% of the coated fluid is spun off and washed away, making this method commercially unviable at an industrial scale. It is also not possible to integrate spin coating with a roll-2-roll system which is possible for many other coating techniques.[7] Spin coating is only suitable for Newtonian fluids; the shear rate gradient across the plate results in low uniformity for non-Newtonian fluids, Figure 5.

a = Low shear region

b = High shear
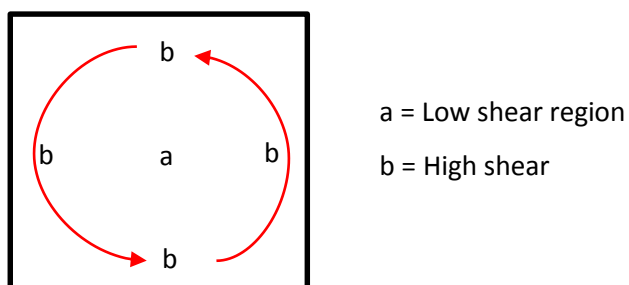
Figure 5: Shear gradient across a substrate during spin coating

Inkjet printing is an additive manufacturing process that works by applying a 'drop-on-demand' using a piezoelectric element to afford a high level of control over fluids, Figure 6[8].

A charge is applied to the piezoelectric element causing it to change shape. This causes ink to be drawn from the main chamber and a meniscus will form at the print nozzle.

The applied electrical charge is inverted causing an ink droplet to be dispensed. Once a droplet has been printed the piezoelectric element will return to its original shape.
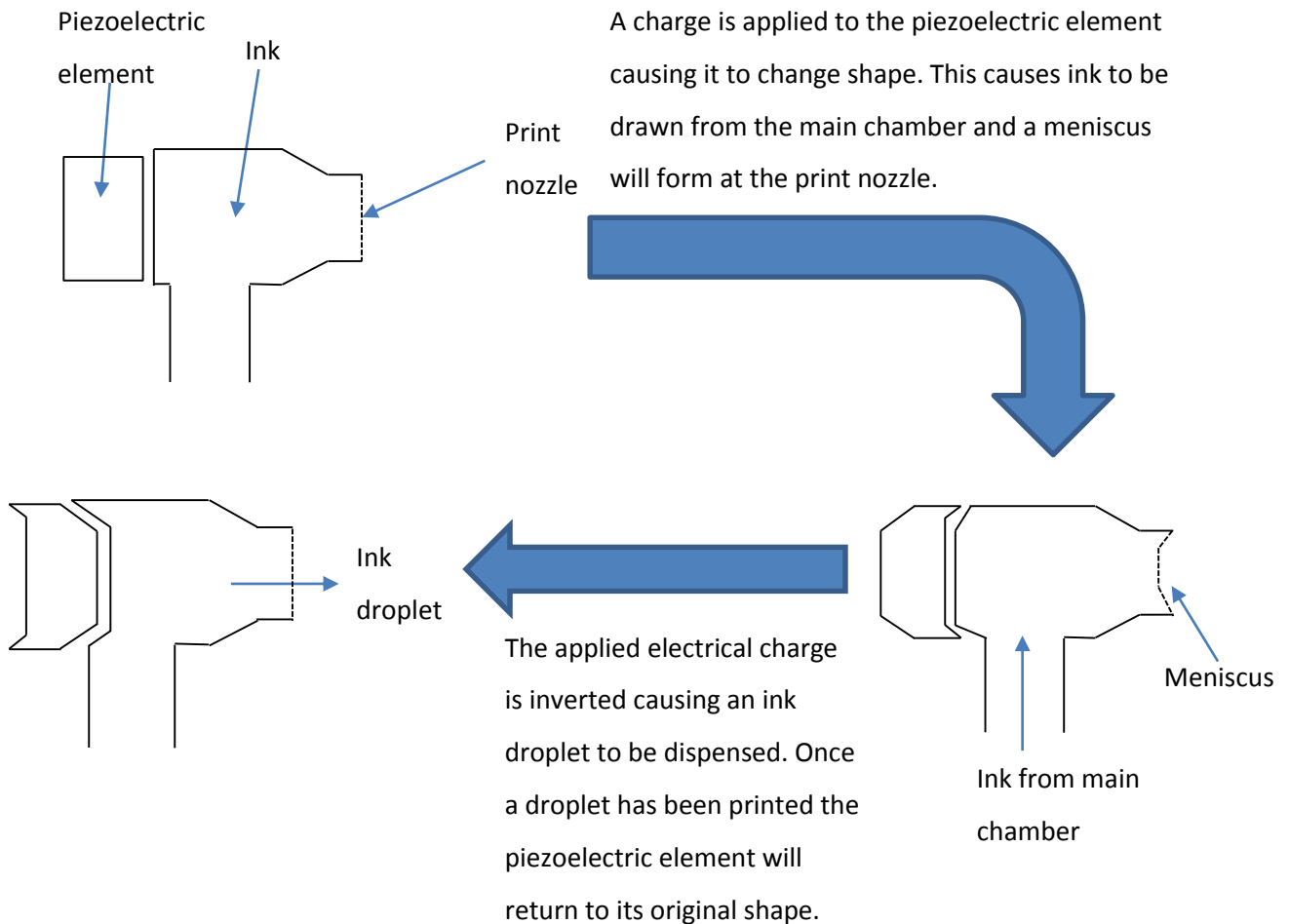
Figure 6: Inkjet printing droplet formation and deposition

The coffee-ring effect (see section 3.b.i) is often observed during inkjet printing due to the small amount of material that is being deposited i.e. a few picolitres. Suitable inks are usually <14 mPa.s and systems cannot process high molecular weight polymers (> 50,000 g/mol) making the formulation processing range quite small. Inkjet printing is an additive manufacturing process resulting in little to no waste and new materials can be trialled in very small volumes i.e. a few millilitres. This technique is a digital process allowing for complicated designs to be coated without the need for lithographic patterning. It can be used to coat large areas as multiple print heads can be incorporated on a batch or roll-to-roll scale. However thickness of coatings can only be controlled by modifying the concentration of the active material; reformulation can be a lengthy process.

Aerosol jet printing is another method that requires the use of a nozzle. It works by atomising inks into femtoliter sized drops which are passed through the head to meet argon sheath gas. The mist is focussed into a thin beam by the high flow rate gas for deposition onto the substrate, Figure 7. [9]
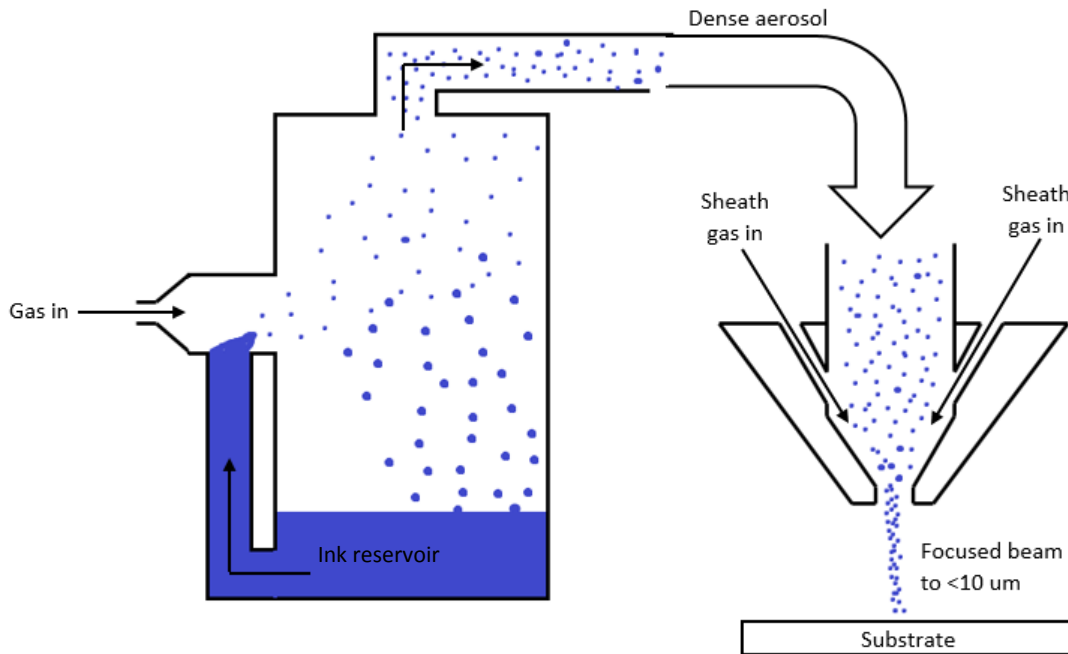
Figure 7: Aerosol jet printing process

Unlike inkjet printing, viscosity is not a limiting factor as viscous materials (up to 1000 mPa.s) can be atomised using pneumatics or ultrasonics to overcome the viscosity, allowing the material to pass through the print head. However this can destabilise formulations and, in the case of particulate dispersions, cause particles to break apart. Aerosol jet printing can be upscaled and used for blanket coating by incorporating multiple print heads into a system, though generally is it preferred for patterned printing. The process affords very little waste and is not affected by the coffee-ring effect to the same degree as inkjet printing. However, as with inkjet printing, coating thickness can only be controlled by modulating the concentration of the active material.

A common batch and roll-to-roll production process in the printing industry is **screen printing**. The setup comprises a screen which incorporates a pattern to be printed in the form of a porous mesh; the area around the pattern is not porous so that ink cannot pass through. Ink is dispensed at the start of the coating and a squeegee is drawn across the screen while applying a pressure. Screen printing inks must be of high viscosity (1,000 – 40,000 mPa.s) with an extremely pseudoplastic profile i.e. the ink dramatically reduces in viscosity when shear stress is applied with a gradually recovering viscosity once the stress is no longer applied. Due this rheological phenomenon the ink is able to sit on top of the screen before the process begins, once pressure is applied the viscosity of the ink dramatically reduces and it passes through the pores of the mesh onto the substrate to create a printed pattern.[10] The slow recovery time allows the ink to level-out after it has been forced through the mesh before being dried or cured, leaving a uniform coating without residual mesh marks. Continuous processes work by the same principle.
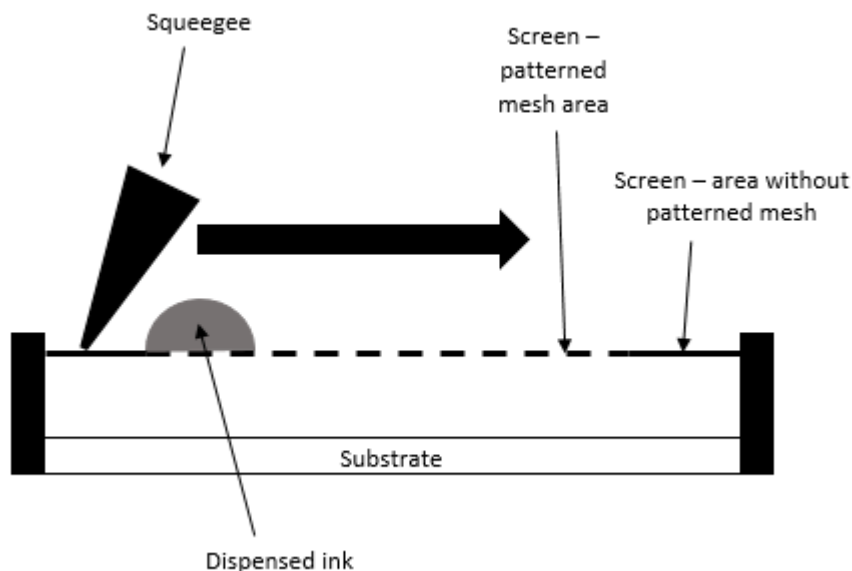
Figure 8: Screen printing process

This process can be used for small quantities of fluid as well as being upscaled to rotary printing systems without the hindrance of large amounts of wastage. It also offers the ability to apply inks to a variety of substrates such as paper, metals and fabrics. The main disadvantage however is the requirement for fluids with a specific rheological profile. The rheological nature of screen printing inks also results in high dry coat thicknesses after one pass i.e. >5 µm making it unsuitable for many thin film applications including OLED emissive layer processing.

Other rotary printing techniques include **flexographic and gravure** printing which work by transferring ink to a reel of substrate using patterned rollers. In flexographic printing the ink is picked up by the anilox roller and is metered by the blade i.e. excess ink is removed. The anilox roller will be selected depending on the desired thickness of the final coating, this translates to a defined volume of ink per meter squared being uniformly transferred onto the photopolymer plate. The photopolymer plate comprises a thick polymer sheet wrapped around a cylinder. The polymer sheets are patterned by etching the area outside of the design i.e. the print pattern is raised ~1 mm above the non-patterned area. The ink transfers to the patterned areas and is subsequently printed onto the substrate. A set pressure is applied using the impression cylinder to ensure sufficient contact between the photopolymer plate and substrate.[11]
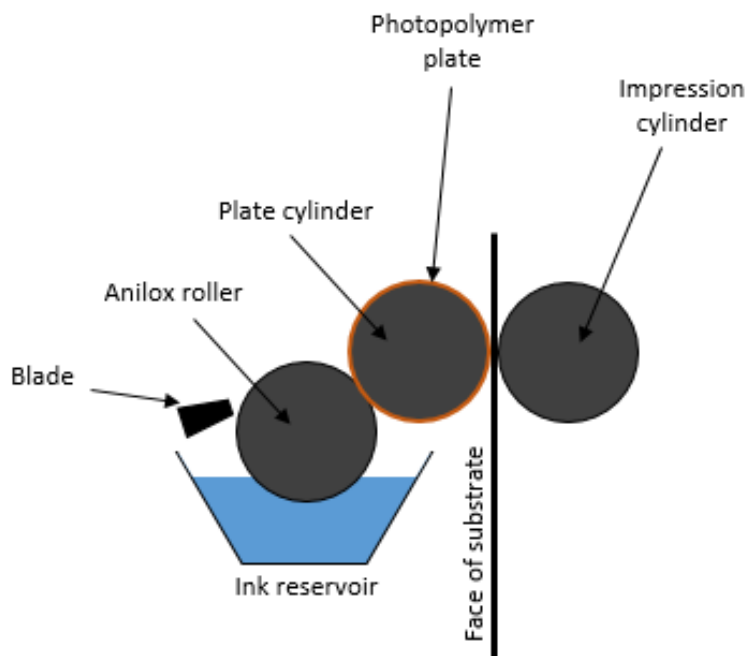
Figure 9: Flexographic printing process[12]

Gravure printing uses two rollers; a printing cylinder and impression cylinder. As with flexographic printing the impression cylinder is used to achieve a set pressure between the printing cylinder and the substrate. The printing cylinder is a metal roller that has been engraved with the pattern, the depth of the engraving dictates the coating thickness onto the substrate. The printing cylinder essentially has the same role as the anilox roller and photopolymer plate in flexographic printing. The blade is used to remove excess material on the roller so that only the engraved areas contain ink, affording neat and uniform coatings; this is known as an intaglio process.[13]
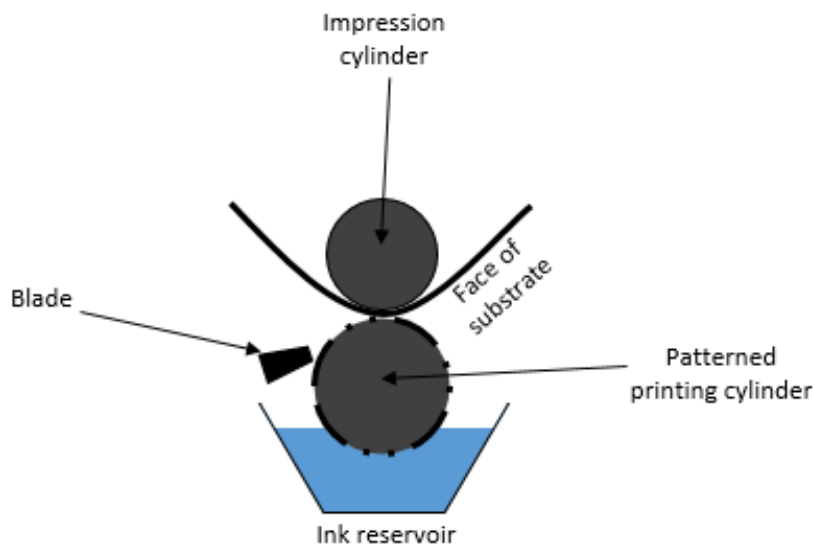
Figure 10: Gravure printing process [14]

Flexographic printing allows more flexibility and the photopolymer plates are cheaper to produce than gravure printing cylinders. Gravure printing is favoured for longer runs.

Flexographic and gravure printing are heavily used in the manufacturing industry due to their high speed production processes. They do however require large amounts of material (>2 litres) making them unsuitable for lab scale research using expensive materials. Material is recirculated preventing large amounts of waste but this introduces further problems such as solvent evaporation and ink contamination. The solvent evaporation is commonly counteracted by the addition of further base solvent, but this may introduce dispersion instability into the formulation. The wet coat thickness of flexo/gravure printed inks can be controlled by choosing the correct setup i.e. volume anilox and printing multiple times.[15] Flexographic and gravure printing are highly dependent on the material properties of the ink; low viscosity can result in material falling off the rollers and the surface energies of ink and substrate have to be carefully tuned.[16]

Slot die coating has a number of advantages over the described techniques, one being the low level of waste. Slot die coating results in less than 10% wastage of material; this is due to the precise delivery of fluid during coating. This coating technique is not without its limits; dewetting and the coffee staining effect can become apparent during coating but this is often minimised using a more appropriate solvent system; this will be further explained in section 3.b.i. Slot die coating is limited to blanket coating, striped coating (using a striped shim to dictate where fluid flows) or patch coating (stopping and starting the fluid flow). However it allows for the coating of most common fluids without complex formulation work being required to attain a specific rheological profile. This technique operates within a closed system and fresh material is fed through as required preventing contamination. Modulation of coating thickness is simply controlled by changing the wet coat thickness parameter in the software. Some systems do not allow the wet coat thickness to be input but it can be controlled using flow rate and coating speed settings. In summary, slot die coating is the most suitable process for the blanket coating of polymer materials with a wide range of properties. [17]

c. Mechanics of Slot-Die Coating

It is important to understand the forces acting during slot die coating to allow for identification of potential sources of error. The initial force encountered by the fluid is the maximum shear rate created in the pipes during fluid delivery[18];

$$\dot\gamma = \frac{4\left(\frac{dV_p}{dt}\right)}{\pi r^3}$$

Equation 3: Shear rate in pipes

where:

- $\dot\gamma = Shear\ rate$

- $\frac{dV_p}{dt} = Flow\ rate\ of\ the\ pump$

- $r = Radius$

The shear rate is an important force to calculate as this can be used in conjunction with rheological characterisation to understand the viscosity changes of a fluid as it is travelling through the system.

When the material reaches the slot die head, there will be a build-up of internal pressure which is influenced by the viscosity of the fluid. A suitable shim thickness must be selected to prevent an unmanageable pressure being created in the head i.e. high viscosities will require a thick shim;

$$\Delta p = \frac{12\eta I\left(\frac{dV_p}{dt}\right)}{s^3 B}$$

Equation 4: Internal pressure

where:

- $\Delta p = Change\ in\ pressure$

- $\eta = Viscosity$

- $I = Slot\ area\ height\ (distance\ between\ downstream\ edge\ of\ manifold\ and\ slot\ exit)$

- $s = Shim\ thickness$

- $B = Coating\ width$

The fluid will then be forced through the lips in three stages; during infuse, during coating and back into the slot die head during withdraw;

$$\dot{\gamma} = \frac{6\left(\frac{dV_p}{dt}\right)}{s^2(B+s)}$$

Equation 5: Shear rate in head

The flow rate is a value input to the software during infuse and withdraw stages. The flow rate during coating is calculated using;

$$\frac{dV_p}{dt} = B\ v\ t_w$$

Equation 6: Flow rate

where:

- $v = Velocity$
- $t_w = Wet\ coat\ thickness$

All equations are critical to understanding the fluid dynamics of slot die coating, they will be related to coating success and uniformity at various stages in this project.

d. Industrial Applications of Slot-Die Coating

Slot die coating is used for the blanket, striped or patch coating of an increasing number of high performance materials in academic research and in industry.

i. Large Area Lighting and Display Technology

OLED polymers are complex molecules that require a large number of steps to synthesise; this is reflected in the cost which is usually in the region of £500 – £1,500 per gram (at the time of writing). Spin coating of an 8" plate requires 12-15 mL, slot die coating requires <1 mL. Consider a 2 wt% formulation of a green emitting polymer, costing £600 per gram, in a solvent (cost of the solvent is negligible compared to the polymer); spin coating this formulation would cost £144 - £180 per plate, slot die coating would cost <£12 per plate. The low level of waste during slot die coating and the potential for upscale makes this process desirable for the wet coating of these materials. Collaborative UK R&D projects, such as the High Performance Lighting Project, are using slot die coating to reduce the cost of producing high performance OLED lighting using polymer active materials. This three year project involved Cambridge Display Technology (a polymer manufacturer), Tridonic (a provider of lighting management solutions), Pilkington (a glass manufacturer) and Durham University.[19]

PEDOT: PSS is commonly used as a hole injection layer; 1 kg of formulated ink usually costs £500 – £1,000. Plextronics are developing ways to reduce the cost of production of their OLED devices via slot die coating for the processing of PEDOT: PSS.[20]

Choi et al (2015)[21] processed the hole injection and hole transport layers of their OLED stack via slot die coating and used coating thickness, roughness and uniformity to assess coating quality. They utilised methods such as substrate heating, addition of surfactant and variation of coating speed to improve coating quality. They found that the performance of OLEDs produced via slot die coating were comparable to those produced by more convention coating methods i.e. spin coating and vacuum-evaporation.

Raupp et al (2017)[22] investigated the reproducibility of slot die coating for the deposition of the emissive layer and hole injection layer. Coating processes were developed by optimising the coating speed, coating thickness and coating gap to improve the stability of the fluid meniscus. They concluded that it was possible to produce highly uniform and reproducible coatings; therefore achieving repeatable device performance.

ii. Light Energy Harvesting

Krebs (2009)[23] used a bespoke slot die coater incorporating cameras and humidity sensors to coat a number of layers for the roll-to-roll fabrication of an OPV device in ambient conditions. He describes the importance of solvent selection and meniscus stability. Due to the speed limitations of the equipment a meniscus guide was used to pin the material to the substrate.

Krebs et al (2013) [24] built upon previous work using roll-to-roll striped slot die coating to produce fully solution-processed flexible organic photovoltaic (OPV) cells. Using striped coatings allows for simple isolation of devices without the requirement for any post processing. Devices are fabricated using a continuous process producing large quantities which reduces the overall cost, making their integration into everyday products more feasible.

Machui et al (2014) [25] observed reduced device efficiency when upscaling their lab-scale process to roll-to-roll using slot die coating. The electron injection layer, absorbing layer and hole injection layer were processed by doctor blade at lab scale. Device performance was increased by using a combination of solvent blends to improve film formation. This showed the challenges of process upscale but in turn the suitability of slot die coating to do so.

iii. Lithium-ion Batteries

Lithium-ion battery manufacturers, such as Siemens, use slot die coating to apply the anode and cathode to their chosen substrate. The electrode formulations are usually supplied as a slurry so the processing range of slot die coating is a big advantage. Slot die also allows both sides of the substrate on a roll-to-roll setup. Siemens are exploiting the use of striped coating and patch (intermittent) coating to create blocks of coating.[26]

Other methods include the use of multilayer deposition via slot die coating incorporating multiple heads. Liu et al (2016)[27] describe a process that allows for improved adhesion between electrodes and the substrate by applying binder materials and active particles separately.

The relevance of slot die coating and its complications have been described, therefore it is now important to ascertain where current research stands and how my work can complement previous findings.

2. Objectives

A range of studies have been carried out to determine the operating window of slot die coating. Many publications, such as Lin et al (2010)[28] measure coating quality in terms of defects i.e. incomplete coatings. In this project coating success will be measured by thickness uniformity as it is directly applicable to the OLED application previously described. In addition to this, there will be no cameras or computational modelling used therefore thickness data is critical. The described articles focus on the limits of the machine whereas this project will work within a reasonable operating window where defect free films i.e. no uncoated areas, can be achieved. The emphasis will be on optimising within this region to obtain coatings of uniform thickness. This will be realised using a statistical Design of Experiments approach whereby a number of experiments were carried out to determine relationships between inputs (factors) and outputs (responses i.e. coating thickness). Experimentation will be carried out using a simple polymer system comparable to materials used to fabricate OLED devices. Materials will be used as an analogue so that data will be transferable to new materials, reducing the process development time required.

Carvalho and Khesghi (2000)[29] discuss the low flow limit of slot die coating which is characterised by the capillary number. The capillary number is a ratio of the viscous and surface tension forces. The model described in their study is relevant for Newtonian fluids and dictates that for low viscosity fluids a high flow rate should be used to increase bead stability. In reality most materials are not completely Newtonian; polymers form pseudoplastic formulations of different degrees depending on concentration and molecular weight. Romero et al (2005)[30] found that a mild level of pseudoplasticity was not only acceptable, but it lowered the low flow limit reported for Newtonian materials. In the case of the LACE coater, the flow rate cannot be controlled directly so it is reasoned that the flow rate changes with the wet coat thickness and coating speed parameters. The wet coat thickness will be held at a constant value for experimentation to allow for comparison between substrates, also to ensure that when the coating speed is modified the resulting coating thickness remains unchanged. Another often discussed coating phenomenon is the minimum wet coat thickness achievable at a particular viscosity, flow rate and coating speed. Chang et al (2007)[31] state speeds in the region of meters per second; the coater used for this study can only achieve a maximum of 30 mm/s so this is not thought to be a concern. The main issues encountered on the LACE coater are described below.

Excess material at the beginning and end of coatings

Large amounts of material are often observed at the start and the end of coatings causing material to run into the bulk of the coating, which increases the degree of non-uniformity. This suggests a lack of control over the fluid due to rheological and/or interfacial tension issues. Some changes to the setup can be made, such as shim thickness, and to the formulation to improve stability and compatibility with the surrounding solid interfaces.

Lengthy process development timescales

The parameters can be electronically altered and many will impact one another; often changing one parameter can have unexpected and currently unexplained effects on the coating which results in long process development timescales. For example, consider a 4 inch substrate coated at a velocity of 5 mm/s and acceleration of 5 mm/s^2. If the velocity was increased to 20 mm/s without changing the acceleration the head would have travelled further along the plate before full speed was reached, Figure 11.
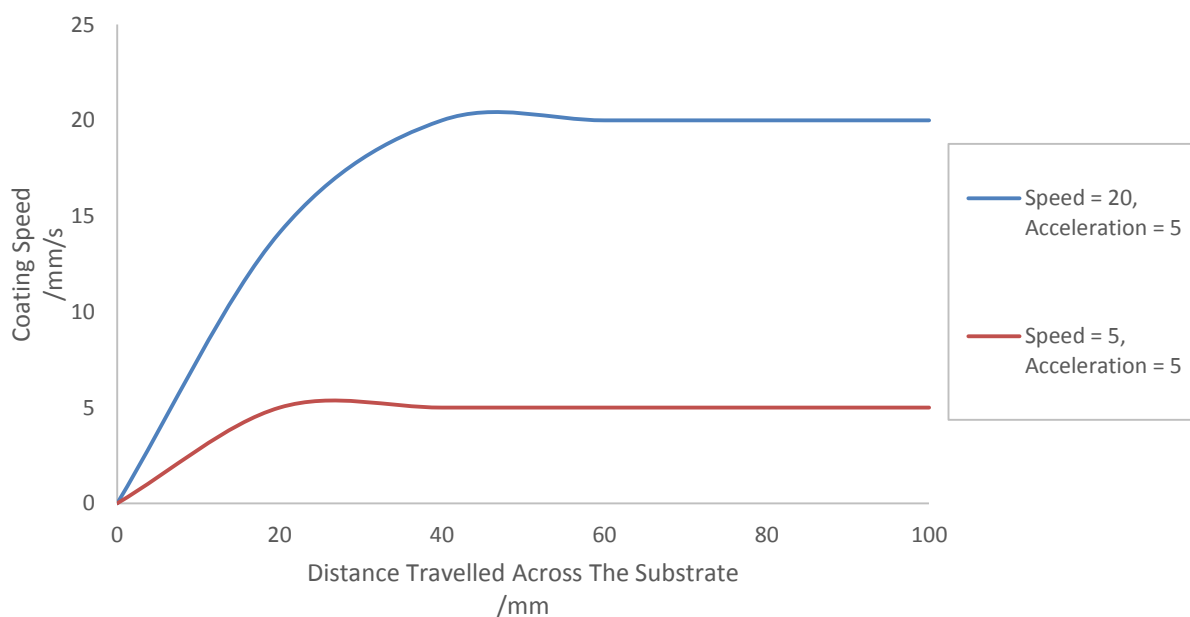
Figure 11: Interaction between coating velocity and acceleration

A better understanding of the parameters and how they impact one another will result in more time effective process development and potentially a more robust processes.

Material Issues

Dewetting i.e. receding of the wet coat in the bulk of the coating or at the edges is often observed when i) using a low molecular weight material, ii) a low concentration of active material, iii) when surfactant is omitted from the formulation and iv) when the substrate's surface energy is lower than the surface tension of the formulation. This suggests that viscosity and surface tension heavily impact on coating success; this needs to be better understood so that methods can be setup to allow for more successful formulation of inks for slot die coating. In addition to this, some highly polydisperse polymers when coated reveal a wavy/mottled pattern which is not yet understood. This mottled effect results in severe light deviations across fabricated devices.

The described concerns will be investigated in a methodical manner; the steps to be taken are outlined below.

- Development of multiple low cost polymer solutions (relative to LEP polymer cost) with close to Newtonian (mildly pseudoplastic) rheology that can be slot die coated. Safety implications will be taken into consideration when choosing experimental materials;
- Viscosity will be modulated by changing the molecular weight, surface tension will be controlled using different concentrations of a suitable surfactant;
- Development of a suitable coating process for the chosen formulations by changing process parameters by trial-and-error;
- Development of a method for analysing the thickness variations across coated substrates to understand the source of observed issues;
- Development of a method for understanding the relationship between process parameters using a design of experiments (DOE) approach;
- Correlation of material properties to process parameters in an easily useable format e.g. Microsoft Excel Macro, MiniTab.

At the end of this project the goal is to have developed a model relating relevant parameters and material properties to coating thickness uniformity. This should be applicable for formulations at a range of viscosities and surface tensions. This allows for the model to be used for costly LEP formulations and a range of other potential inks, facilitating efficient process development for new materials.

3. Experimental Techniques

A number of techniques were used in this project for preparation and analysis. Rheology and surface tension measurements will be described in the most detail as they are most relevant to this project.

a. Rheology

Rheology is the study of flow and deformation[32]; understanding how a fluid flows is critical to developing a coating process. Rotational and oscillatory rheology have been used in this study to understand how stresses inherent to the process may alter the flow of a fluid and how this impacts coating uniformity.

i. Shear Rheology

Shear rheology uses the 'Two-Plates Model', Figure 12, to determine how a fluid's viscosity is affected by composition (or molecular weight) and imposed shear stress, measured most commonly using a rotational rheometer.
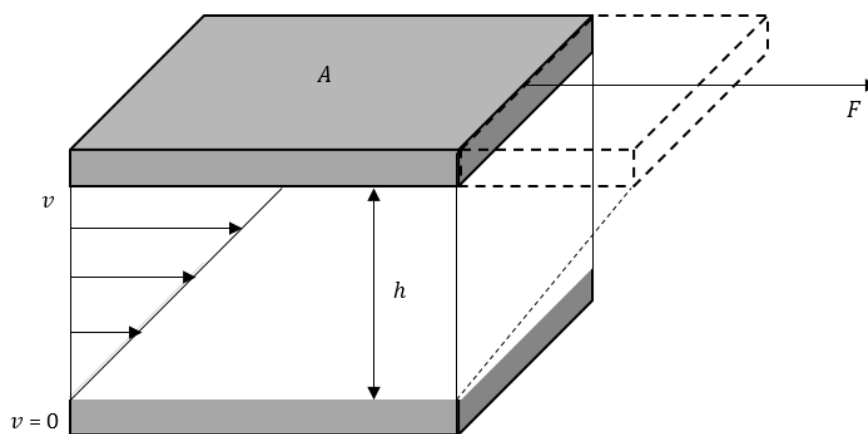
Figure 12: Two-Plates model[33]
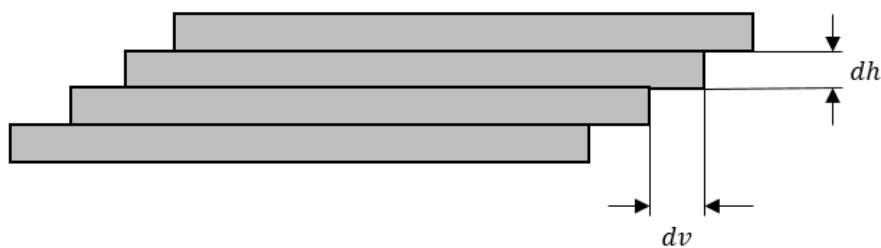
Figure 13: Laminar flow[33]

The region between the two plates (labelled h) is filled with a fluid; the bottom plate remains stationary and the top plate i.e. the shear area (labelled A) is moved to apply a shear force. The velocity (labelled v) is measured; this displays changes in relation to the viscous behaviour of the fluid.

This model assumes there will be no 'slipping' at the interface between the plates and the fluid. It also assumes that the fluid moves by laminar flow, Figure 13, i.e. in planar layers without the presence of turbulence i.e. chaotic movements.

Shear viscosity is defined as shear stress applied per shear rate:

$$\eta = \frac{\tau}{\dot{\gamma}}$$

Equation 7: Shear viscosity

where:

- $\tau = Shear\ stress$

Shear stress is defined as the force per unit area:

$$\tau = \frac{F}{A}$$

Equation 8: Shear stress

where:

- $A = Area$
- $F = Force$

Shear rate is defined as velocity over a given distance:

$$\dot{\gamma} = \frac{v}{h}$$

Equation 9: Shear rate

where:

- $h = Height$

There are three main types of viscous behaviour that can be determined using a shear rate/viscosity curve[34]:

- Newtonian behaviour – viscosity is independent of shear rate
- Pseudoplastic behaviour – viscosity decreases with increasing shear rate
- Dilatant behaviour – viscosity increases with increasing shear rate
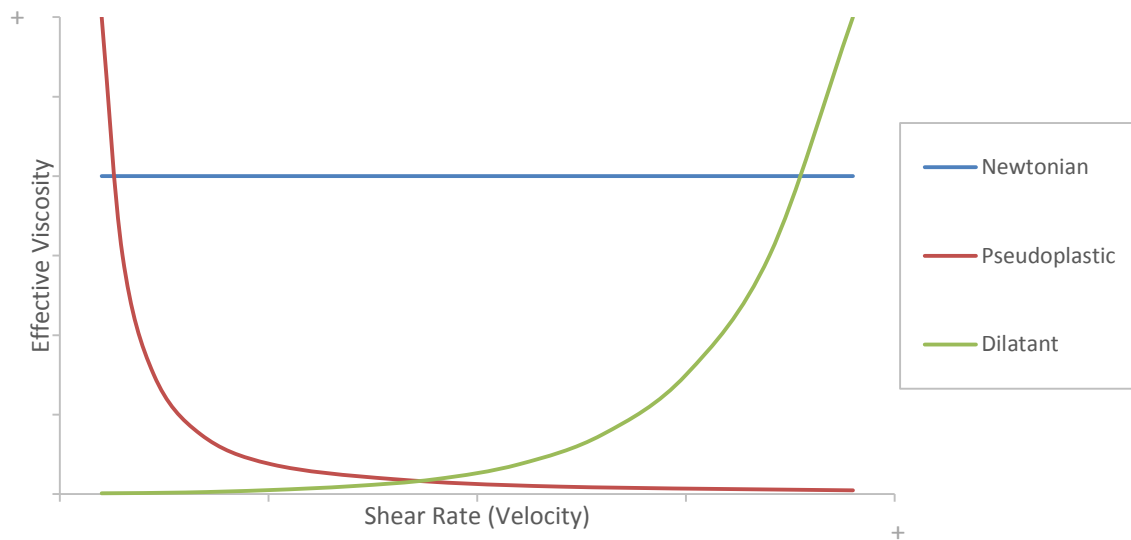
Figure 14: Three types of viscous behaviour

Newtonian behaviour is ideal for slot die coating; any changes in shear rate within the system will not affect viscosity. Severe pseudoplasticity may result in non-uniformity across the plate in the direction of the slot die head; pressure changes across the head will result in the material being infused at different viscosities, lower viscosities will pass through the head at a quicker rate hence more material will be fed to those regions of the substrate, Figure 15. Dilatancy may cause the system to become blocked should the viscosity increase due to high shear rates.
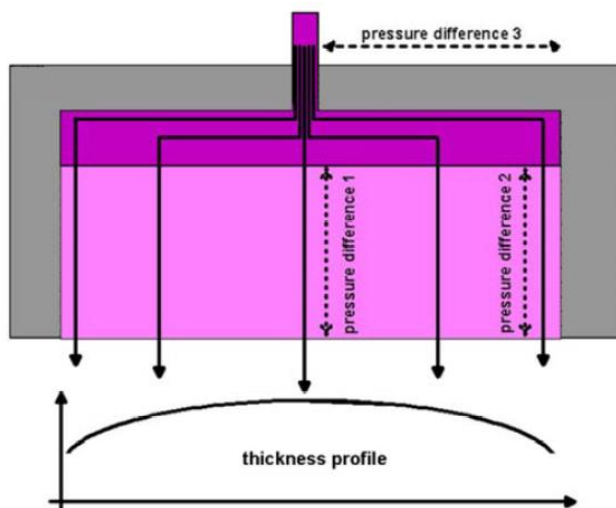
Figure 15: The effect of pseudoplasticity on slot die coating.[18]

Reprinted with permission from (Crone, Klaus P. (2014) Slot Die Coating for organic photovoltaics and other high tech applications, Germany: Coatema). Copyright (2014) Coatema Coating Machinery GmbH.

Rheological testing was carried out using a TA Instruments AR1500s fitted with a 60 mm parallel plate geometry, Figure 16, which was set to a 500 µm geometry gap.
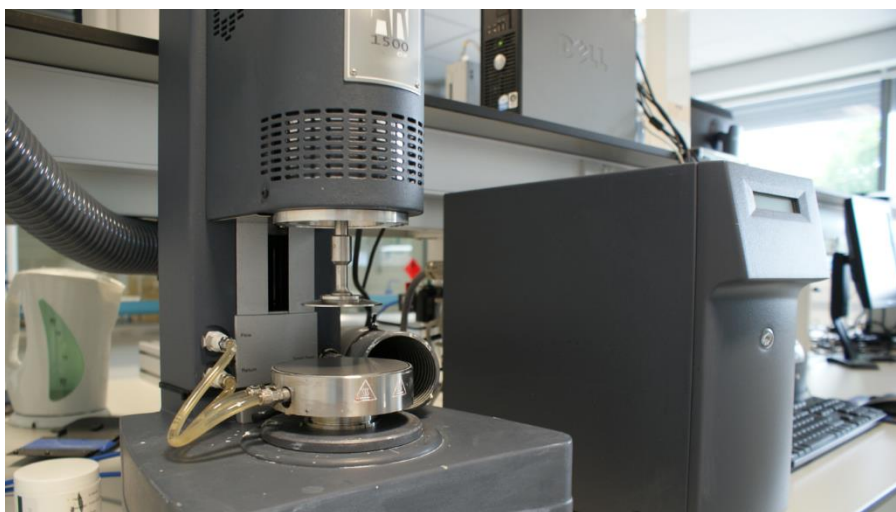
Figure 16: TA Instruments AR1500 Rheometer

The procedure entailed the use of a steady state flow regime whereby the shear rate was ramped from 10 – 2,000 1/s. Measurements were spaced logarithmically and ten points were taken per decade at 20°C. Steady state was achieved when three consecutive readings were within a five percent tolerance; maximum point time was set to one minute. Prior to each rheology run a conditioning step was applied; this entailed a two minute equilibration at 20°C.

ii. Oscillatory Rheology

Oscillatory rheology is used to investigate the viscoelasticity of a material, in particular polymer systems. The two-plates model can be used to describe the movement of the rheometer geometry during an oscillation test.
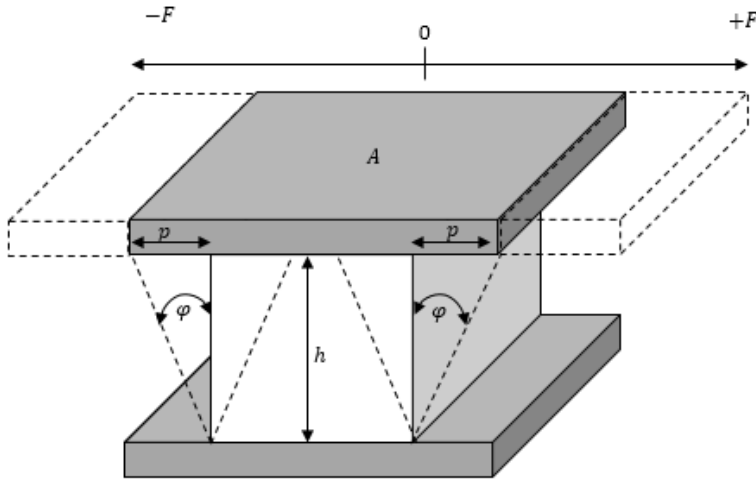
Figure 17: Two-plates model used to describe oscillatory shear tests[33]

The bottom plate remains stationary while the upper plate with shear area is pushed forward and backwards by the shear force. The movement of the plate causes shearing of the medium between the plates, via the deflection path and deflection angle.

$$\pm\tau = \pm\frac{F}{A}$$

Equation 10: Shear stress in oscillation rheology

$$\pm\gamma = \pm\frac{p}{h} = \pm\tan\varphi$$

Equation 11: Shear strain in oscillation rheology

where:

- $\gamma = Strain$

- $p = Deflection\ path$

- $\varphi = Deflection\ angle$

There are three categories that materials fall into; elastic, viscous and viscoelastic. An ideally elastic material is completely solid, viscous material is fluid and a viscoelastic material has characteristics of a solid and a fluid. Oscillatory testing in this project focused on viscoelastic behaviour.

Formulations were analysed by first determining the linear viscoelastic region (LVR).[35] The LVR is the region in which a materials response is independent of strain and is characteristic for each polymer. Within the LVR, properties of the material can be calculated using oscillatory frequency sweeps to determine changes to modulus values (a measure of elasticity) with increasing frequency of strain.

Many instruments are limited by torque and angular frequency, however more data can be acquired by running scans at different temperatures and combining them using time temperature superposition (TTS).[36] When exposed to a constant load over a period of time, deformation/strain will increase; the system will undergo molecular rearrangement to minimise local stress. TTS allows for a master curve to be created that shows a range of values spread over much larger frequency range. This is produced by combining profiles taken at different temperatures. The underlying basis for this theory is:

- Processes involved in molecular rearrangement in viscoelastic materials will occur faster at higher temperatures;

- There is a direct equivalency between time and temperature, provided there are no changes in structure or phase transitions.

Models that are used to do this use either the WLF (Williams–Landel–Ferry) or the Arrhenius equation. WLF is more accurate in the region of the T_g of the polymer, Arrhenius is more reliable at temperatures well above the T_g (at least 100°C) or when using a small range of temperature values.

b. Interfacial Effects

Interfacial effects are important at the interface between 2 media of any type. For slot die coating they dictate how stable the meniscus is, how easily a formulation wets onto a substrate and how uniformly the coating dries.

i. The 'Coffee-Ring' Effect

The coffee-ring effect is an interfacial phenomenon that usually occurs at a liquid-gas interface. It is described as the flow of fluid in response to a surface tension gradient, in this case it is a result of changing concentration due to solvent evaporation. It is responsible for drying issues observed in wet coating and is usually something that formulators have to overcome. It can be observed most readily at the region of a fluid droplet where it meets the substrate, known as the contact line; the edges of the droplet are away from the bulk of the material and most in contact with air so the evaporation rate is higher. Whereas material in the centre is surrounded by fluid reducing the evaporation rate, Figure 18.
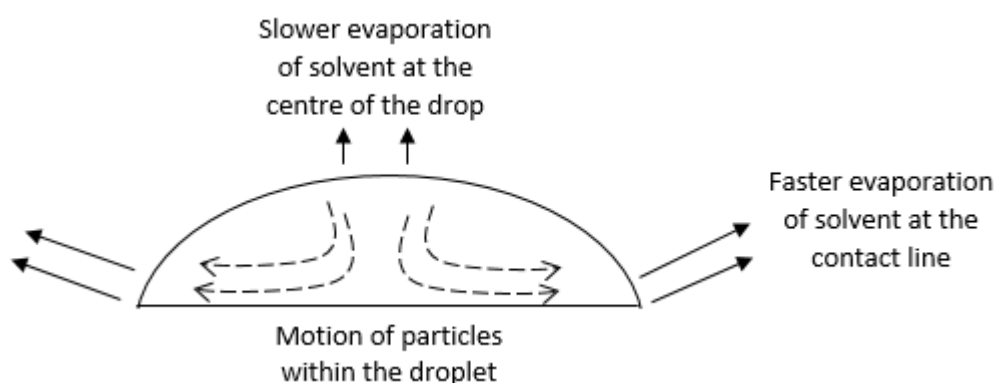
Figure 18: The coffee-ring effect

This causes internal motion of the fluid i.e. surface tension driven flows to push material to the edges of the drop, resulting in the bulk of the solid material being deposited at the edges of the drop.[37] This can be overcome by using high boiling point solvents or multiple solvent systems to better control the rate of solvent drying.

ii. Surface Tension

The surface tension of formulations was measured and calculated using a pendant drop method; a drop of fluid is suspended from a needle tip, the surface tension is calculated from the shape of the drop using the Young-Laplace equation.

When a drop is formed it becomes deformed due to gravity and Laplace pressure; the pressure difference between inside and outside of the drop, labelled Δp. This is calculated by using the density difference between the two phases, in this case one of the phases is air. For circularly symmetrical drops, the radii (labelled r) of each half is the same hence $2\,r$ applies.[38]

$$\sigma = \frac{\Delta p}{2r}$$

Equation 12: Young-Laplace Equation

where:

- $\sigma = Surface\ tension$

 A standard pendant drop setup was used incorporating a 50 µL glass gas tight syringe and a Navitar camera. The plunger was mechanically moved and liquid was released in multiples of 0.167 µL. The software used was FTA32 Video 2.0 which allowed changes in density to be incorporated into surface tension calculations.
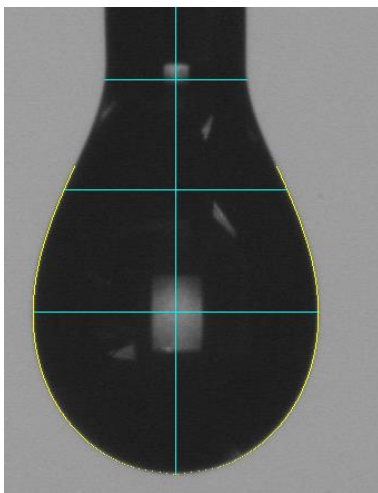
Figure 19: Image of a pendant drop

iii. Critical Micelle Concentration (CMC)

The CMC is the surfactant concentration in a solvent at which and any further addition of surfactant will have no effect on the surface tension. Initial addition of surfactant will result in amphiphilic molecules adsorbing to the interface between the hydrophilic (in this case water) and the hydrophobic region (in this case air surrounding the droplet), resulting in a lowered surface tension of the liquid. An increase in surfactant concentration up to the point of CMC will result in more molecules adsorbing to the interface up to a critical concentration. Once this concentration has been reached, free surfactant molecules will begin to form aggregates. Due to their size the activity of these aggregates will not significantly rise with increasing concentration, therefore the interface remains constant.[39]

iv. Surface Free Energy

The free energy of a surface is used as a measure of how a liquid will wet onto a substrate. Contact angle measurements are taken using a polar (water) and a dispersive solvent (diiodomethane) to measure the contribution of polar and dispersion forces. Surface free energy is related to contact angles by the following equation.

$$\sigma_s = \sigma_{sl} + \sigma_l . \cos \theta$$

Equation 13: Surface free energy

where:

- $\sigma_s = Surface\ free\ energy\ of\ the\ solid$
- $\sigma_{sl} = Interfacial\ tension\ between\ liquid\ and\ solid$
- $\sigma_l = Surface\ tension\ of\ the\ liquid$
- $\theta = Contact\ angle$

Measurements were carried out using a KSV CAM101 contact angle meter incorporating a 5 mL glass airtight syringe and an 18 gauge needle.
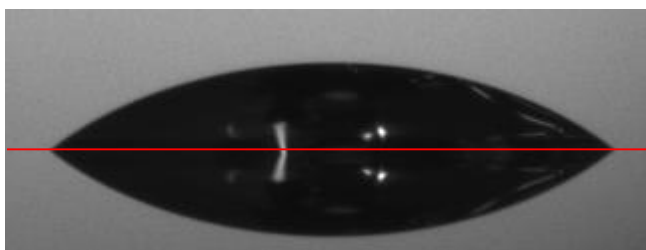
Figure 20: Image of a contact angle. The red line is the substrate surface i.e. the contact line, the image shown below the line is a reflection

c. Optical Characterisation of a Film

In this project optical film characterisation methods have been selected due to their high resolution output data and their non-contact nature; this study will investigate polymers which may be susceptible to damage from contact measurement methods.

Spectral reflectance and interferometry will be explained and the reason for choosing to use them for different purposes will be discussed.

i. Spectral Reflectance

When light propagates through a medium it will be partly absorbed and partly reflected; the degree to which this occurs is characteristic of that medium. This optical identity is described by two optical constants; 'n' and 'k'.

- 'n' is the refractive index and is described as the ratio of the speed of light in a vacuum and the speed of light in a medium.
- 'k' is the extinction coefficient which is a measure of how much light has been absorbed by the medium. [40]

The two relate to one another through the following time-dependant equation:

$$E(x,t) = E_0 Cos\, 2\pi \left(\frac{nx}{\lambda} - ft \right) . e^{\left(\frac{-2\pi kx}{\lambda} \right)}$$

Equation 14: Light propagation through a medium

where:
- $E = Electric\ field$
- $E_0 = Amplitude\ of\ electric\ field$
- $n = Refractive\ index$
- $k = Excinction\ coefficient$
- $\lambda = Wavelength\ of\ light$
- $x = Distance\ travelled\ by\ light$
- $f = Frequency$
- $t = Time$

The 'n' and 'k' values are adjusted by the software until a profile that closely fits the measured reflected light is obtained and input to the model, the compatibility is described by 'goodness of fit' which should be as close to 1 as possible, Figure 21. The blue line is the reflected light; the red line is the model that is optimised to closely fit the blue line across as much of the spectrum as possible. This is carried out at a range of coating thicknesses to ensure the model is robust. Separate profiles are created for the surrounding interfaces i.e. substrate and air which are added to the measurement procedure to account for reflected light from each interface at normal incidence.
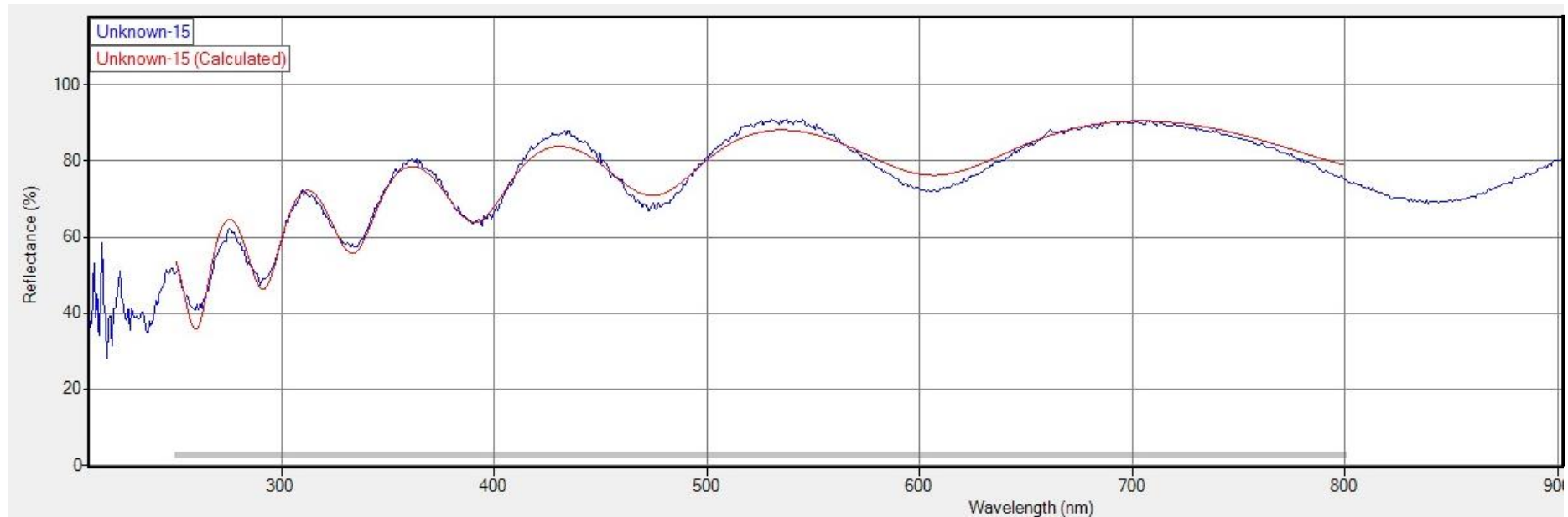
Figure 21: Spectral reflectance of polyethylene oxide (100,000 Mw) at 300 nm thickness, optical model (red line) compared with the measured data (red line). This model exhibited 0.9803 goodness of fit, out of 1.

Spectral reflectance is favoured for large area coating as it allows detailed thickness mapping across a whole substrate. Data is output in a pictorial format alongside calculated values such as mean, standard deviation and uniformity, Figure 22.
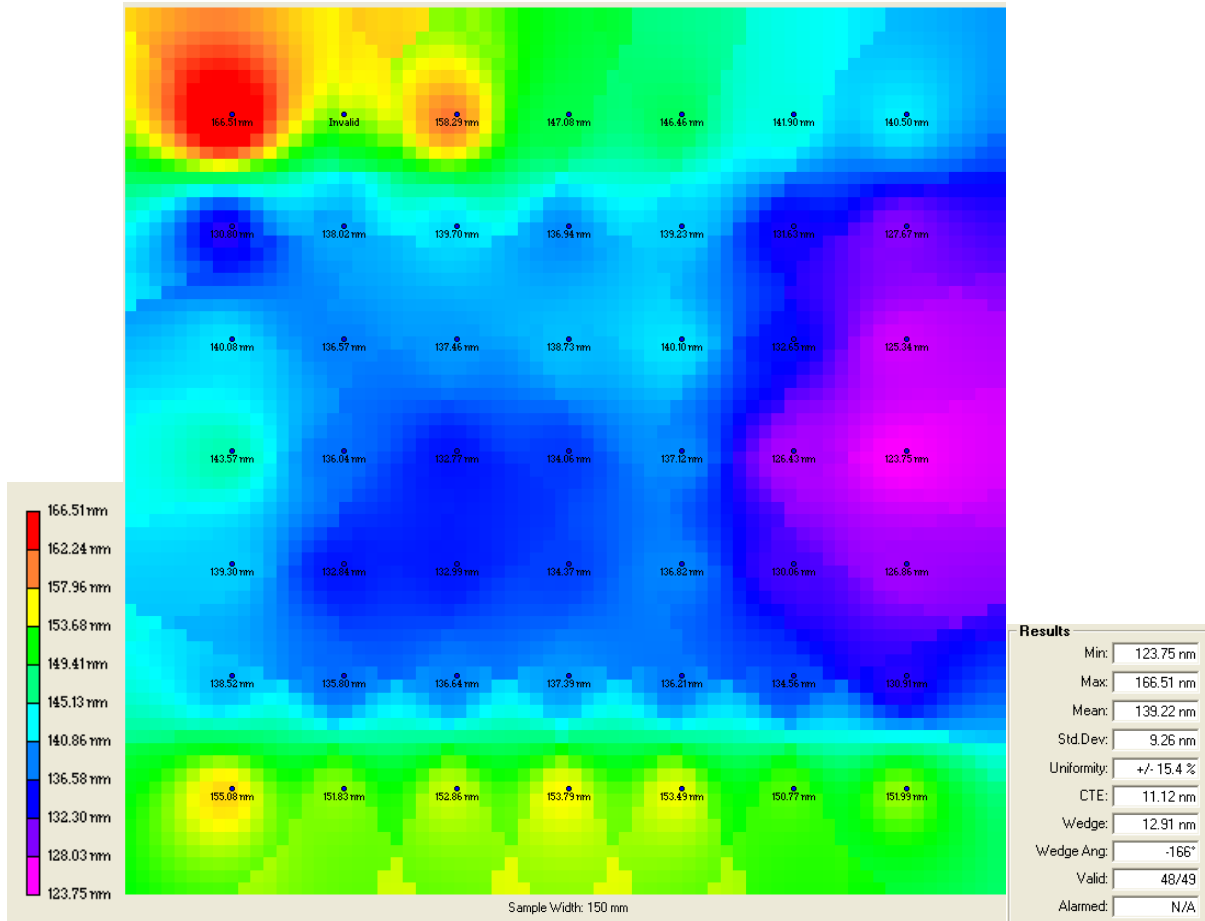
Figure 22: An example of Filmetrics data output

Data can also be saved as a Filmetrics map file (.map) which separates values by commas; it can be imported into Microsoft Excel or other data manipulation software for analysis. The tool can process substrate sizes up to 600 mm x 600 mm.
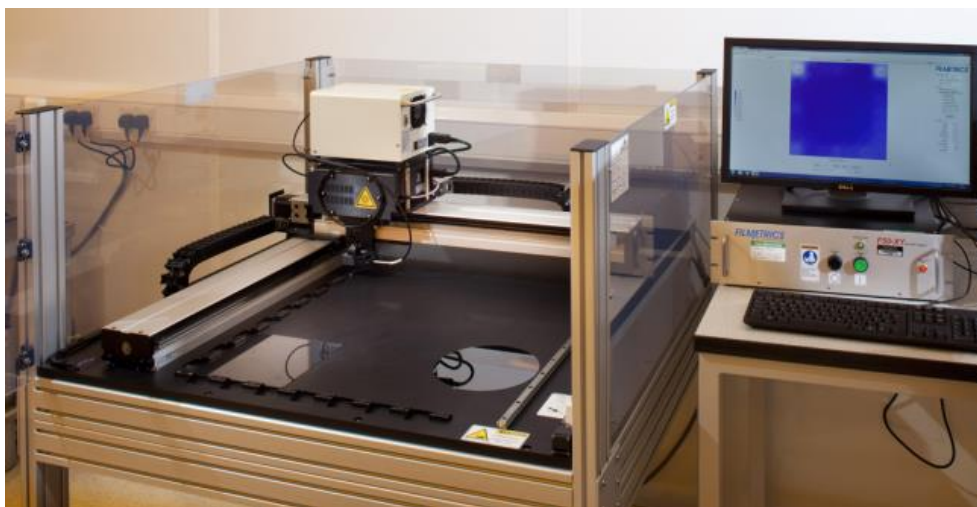
Figure 23: Filmetrics optical thickness analysis tool

ii. Coherence Correlation Interferometry (CCI)

Coherence correlation interferometry exploits the low-coherence of white light by comparing the signal to a reference beam to produce interference patterns. This allows for the position of a number of points to be determined creating a surface profile.[41]

A Taylor Hobson Talysurf CCI 6000 was used for interferometry analysis in this study. The CCI tool offers substrate mapping analysis, however due to the small viewing window of 1.8 mm x 1.8 mm and scan time of 2 minutes per point it is extremely slow. Filmetrics analysis is preferred for thickness mapping. The CCI however is useful for attaining roughness data. A 10x lens was used for roughness values greater than 5 nm, a 50x lens was used for anything less. Roughness was defined by the two following statistical descriptors:

- The arithmetic mean height (S_a) – this describes the mean of absolute values of height deviations from the mean, it's essentially the average of the peaks and valleys of a surface.
- Root mean square deviation (S_q) – this is the root mean square of the height deviations from the mean, this is much more affected by a single large peak.

In the illustration below the S_a value is constant.
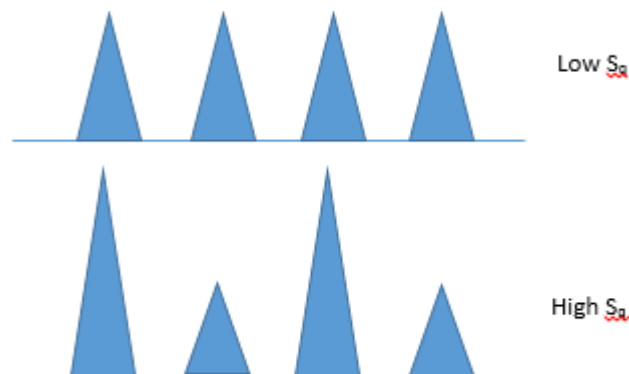
Figure 24: Root mean square deviation

d. Thermogravimetric Analysis (TGA)

TGA entails measuring mass change of a sample with temperature. A TA Instruments TGA Q50 tool was used; samples were loaded into a platinum pan, nitrogen gas was purged at a rate of 90 mL/min and the temperature was ramped from 20 – 500°C at a rate of 10°C/min. The temperature at which materials began to decompose i.e. mass was lost, was recorded and compared.

e. Wirebar Coating

This is commonly used as a short-loop draw-down method to ascertain the suitability of a formulation for use in slot die coating as it will identify compatible surfaces and fluids. It has the advantage of only requiring 1 mL of solution and it can be setup to wet coat at a number of thicknesses using different bars.[42] The bars have a wire wrapped around that has a defined gap between the wires, Figure 25, which will collect a volume of material corresponding to the chosen wet coat thickness. The wire diameter essentially controls the wet thickness of material applied to the substrate. The bar is dragged across the surface using the inbuilt motor set to an arbitrary speed of 1 – 6 and the liquid within the wirebar gaps will be deposited.
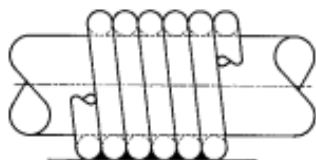
Figure 25: Wirebar coater, bar structure[42]

Figure 26: An RK wirebar coater

f. Plasma Treatment

Plasma treatment is often used to aid wetting when carrying out wet coating by increasing the free energy of a substrate. Plasma is an ionised gas created by subjecting a gas to an electric or microwave field, usually within a vacuum. When enough energy is in the system electrons will be removed from the outer shell of the gas atom resulting the production of reactive species, which interact with the surface of a substrate.[43] In this case oxygen plasma was used to increase the polarity of a surface by removing hydrophobic organic contaminants, therefore increasing the polar component to the surface free energy. This was carried out using an Alpha Plasma Microwave Etcher.

g. Sputter Coating

Sputter coating is a vacuum deposition technique that is used to apply a highly uniform thin-film of metal. A plasma is created, as described in the previous section, using an inert gas such as argon. A negative charge is applied to the target (material to be coated) causing free electrons to be released. The electrons collide with the inert argon atoms to remove outer shell electrons. The now positively charged argon atoms are drawn to the negatively charged target which knock off particles. These particles condense onto a substrate to form a thin and uniform film.[44] Coatings were applied using an SCT AXIS sputtering tool.

An opaque surface is often required for spectral reflectance due to refractive indices of materials; if the analysed material has a refractive index close to that of glass then it will not be able to distinguish between the two. In this case aluminium-sputtered glass substrates were used.

Material	'n' value @ 435.8 nm	'k' value @ 435.8 nm	'n' value @ 632.8 nm	'k' value @ 632.8 nm
Glass	1.5276	0.0000	1.5156	0.0000
Aluminium	0.5795	5.2994	1.3762	7.6162

Table 2: Refractive index of substrate materials

4. Materials and Procedures

The aim is to establish a series of well-defined formulations in terms of viscosity, surface tension and solids loading in order to carry out a systematic analysis of process parameters. The development of a suitable range of formulations was carried out as described:

- Polymers will be combined with solvents and compatibility will be determined;
- The effect of changing the molecular weight on viscosity and surface tension will be quantified;
- The effect of changing concentration of polymers on viscosity and surface tension will be measured;
- The effect of addition of surfactant on surface tension will be quantified.

a. Polymer and Surfactant Selection

There are a wide range of polymers available to buy from a number of suppliers so it was necessary to decide on a set of criteria. Suitable polymer candidates had to be readily available and low cost; materials in the price range of the LEP's described in the introduction would be unsuitable. Materials were sourced from Sigma Aldrich.

Three polymers were chosen to be investigated; polystyrene, polyisobutylene and polyethylene oxide. None of the purchased polymers investigated exceeded £100 per 100 g; a fraction of the cost of the light emitting polymers.
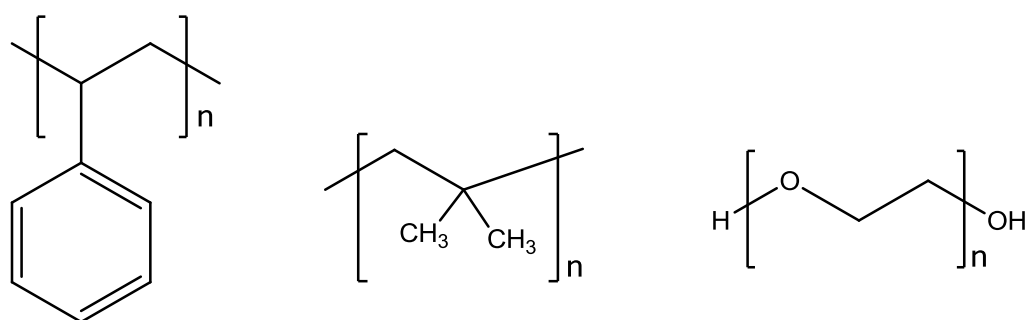
Figure 27: Chemical structure of styrene (left) isobutylene (middle) and ethylene oxide (right) repeating units, drawn using ChemDraw

Polystyrene is a readily available polymer that is often supplied in a variety of molecular weights allowing for simple modulation of viscosity. Three polystyrene grades were sourced from Sigma Aldrich; chemical information was not available for all grades, Table 3.

Name	Weight average molecular weight (g/mol)	Number average molecular weight	Polydispersity Index (PDI)	Density @ 25°C (g/mL)
PS35K	35,000	-	-	1.06
PS192K	192,000	-	-	-
PS350K	350,000	170,000	2.06	1.06

Table 3: Molecular weight data for polystyrene grades sourced from Sigma Aldrich[45]

Two further polystyrene grades were obtained from Durham University for comparison to the commercially available grades. Materials had been analysed using gel permeation chromatography (GPC) to determine the molecular weight distribution, Table 4.

Name	Weight average molecular weight (g/mol)	Number average molecular weight	Polydispersity Index (PDI)
PS348K	348,000	155,000	2.25
PS885K	884,875	707,900	1.25

Table 4: Molecular weight distribution for polystyrene grades sourced from Durham University

One polyisobutylene grade was sourced from Sigma Aldrich, Table 5, and assessed; viscosity would be modulated by changing the solids loading.

Name	Weight average molecular weight (g/mol)	Number average molecular weight	Viscosity average molecular weight (g/mol)	Polydispersity Index (PDI)	Density @ 25°C (g/mL)
PIB500K	500,000	200,000	420,000	2.5	0.92

Table 5: Molecular weight data for polyisobutylene grade sourced from Sigma Aldrich

Polyethylene oxide (PEO) was selected due to its ability to dissolve in water; this was desirable from a safety perspective and would also allow for manual processing of substrates. This will be further explained in section 5.a.

Several polyethylene oxide (PEO) grades were available from Sigma Aldrich, five of which were sourced, Table 6. Four of the five grades that were sourced contained butylated hydroxytoluene (BHT) which acted as an antioxidant.

Name	Viscosity average molecular weight (g/mol)	Number average molecular weight	Polydispersity Index (PDI)	Density @ 25°C (g/mL)
PEO37K	37,100 (calculated)	35,000	1.04	-
PEO100K (BHT)	100,000	-	-	1.13
PEO200K (BHT)	200,000	-	-	1.21
PEO300K (BHT)	300,000	-	-	1.21
PEO8000K (BHT)	8,000,000	-	-	-

Table 6: Molecular weight data for polyethylene oxide grades sourced from Sigma Aldrich

Polyethylene oxide is readily soluble in water, however the surface tension of water is high and the addition of polyethylene oxide would result in a marginal reduction.[46] It was anticipated that a surfactant would be required to allow the formulated material to wet onto a substrate. Two non-ionic surfactants were trialled; Triton X-100 and Span 20 as they had previously worked well in water-based systems, Table 7.

Name	CMC (mM)	Weight average molecular weight (g/mol)	Density @ 25°C (g/mL)	Chemical structure
Triton X-100	0.2-0.9[45]	625.00	1.07	
Span 20	0.024[47]	346.47	-	
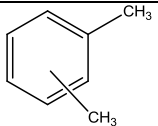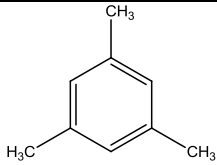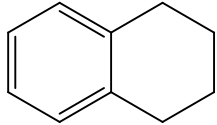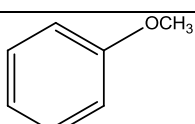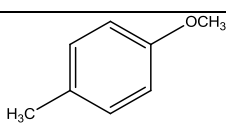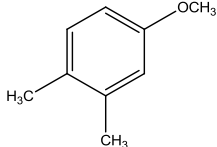
Table 7: Chemical information for surfactants sourced from Sigma Aldrich, chemical structures drawn with ChemDraw

A number of polymers had been selected at a wide range of molecular weights; this enabled formulation development work to be detailed in section 5.a, 5.c and 5.f. The next section describes the solvents chosen and the criteria that resulted in their selection. The surfactants would be later studied as part of the polyethylene oxide formulation development, section 5.a.iii.

b. Solvent Selection

The main criteria for solvent selection were i) ability to dissolve the polymers and ii) high boiling point i.e. >100°C. Polystyrene and polyisobutylene has been used in previous CPI studies with aromatic hydrocarbons and ketones; a number of solvents from those two categories with high boiling points were selected. Low boiling point and volatile solvents are unsuitable for use with the LACE slot die coater due to the high chance of the solvent drying when the die head is in motion between processing stages i.e. when there is no fluid being pumped through. This can lead to the slot die lips getting blocked with dried polymer. As a result of increasing drying time, high boiling point solvents often counteract the effects of surface tension driven flows, which was explained in section 3.b.i of this document. Solvents were also purchased from Sigma Aldrich.

Ten aromatic solvents were selected according to the above criteria, Table 8.

Name	Safety Statements	Boiling Point (˚C)	Density @ 25°C (g/mL)	Chemical Structure
1. Xylenes	Flammable, irritant	137	0.86	
2. Mesitylene	Flammable, irritant, harmful to the environment	163	0.864	
3. 1,2,3,4-Tetrahydronaphthalene	Harmful, environment, possible carcinogen	207	0.973	
4. Anisole	Flammable	154	0.995	
5. 4-Methylanisole	Flammable, harmful, irritant	174	0.969	
6. 3,4-Dimethylanisole	Harmful, irritant	200	0.974	
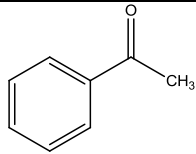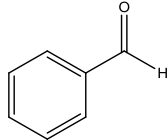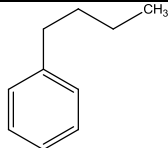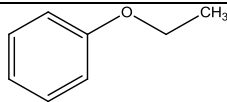
7. Acetophenone	Harmful, irritant	202	1.03	
8. Benzaldehyde	Harmful	178	1.044	
9. Butylbenzene	Flammable, harmful to the environment	183	0.86	
10. Ethoxybenzene	Flammable	169	0.966	

Table 8: Chemical and safety information for solvents sourced from Sigma Aldrich, chemical structures drawn on ChemDraw

In order to ascertain suitability, polymers were mixed with the chosen solvents at a 1 weight percent (wt%) loading and were dropped using a pipette onto cleaned glass. This is known as the 'drop test'. Figure 28 describes the drying of polystyrene particles (500 nm diameter) dispersed in water using surfactants. [48] The image on the left shows the coffee-ring effect whereby polymer has collected around the edges. The image on the right is an example of uniform drying where the effects of surface tension flows were mitigated.

Figure 28: Dried droplets highly affected by surface tension flows (left) and unaffected by surface tension flows (right) Reprinted with permission from (Anyfantakis, Manos et al (2015) Modulation of the Coffee-Ring Effect in Particle/Surfactant Mixtures: the Importance of Particle–Interface Interactions, 31: 4113-4120). Copyright (2015) American Chemical Society.

Dried droplets were inspected visually and were rated on a scale of 1 – 4 depending on drying quality; 1 being good i.e. not affected by surface tension flows, 4 being poor i.e. highly affected by surface tension flows. Images were taken to show examples of a drop for each rating alongside a description, Table 9.
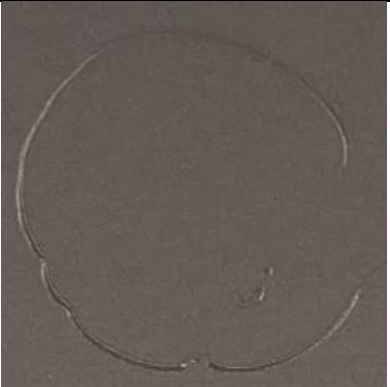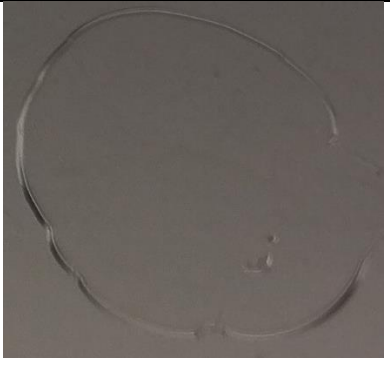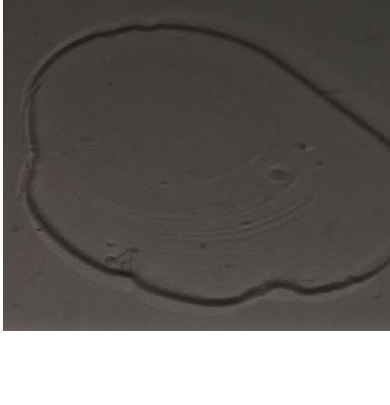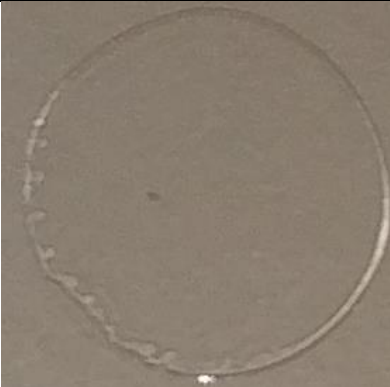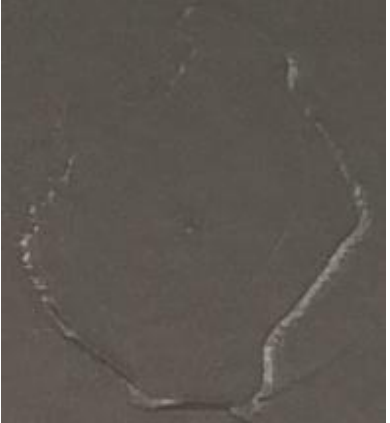
1			Smooth coating, it apears that the coffee ring effect has been mitigated.
2			Almost smooth coating, mildly affected by surface tension flows.
3			Thicker coating around the edges of the drop, typical effect of surface tension flows.
4			Very poor drying, affected by surface tension flows and potentially polymer/solvent compatibility.

Table 9: Example of drop rest ratings for polystyrene

Once a suitable solvent had been selected, a range of concentrations were made up and rheologically tested to find mixtures with a range of mean viscosities between 5 and 50 mPa.s. Samples were subjected to $10 - 2000$ s^{-1} as the shear rate at various stages of slot die coating fall between these two values. Shear rate values were calculated for standard parameter settings using the equations described in section 1.c:

- Fluid delivery piping @ 3.3 mm internal diameter – 13 s^{-1}
- Slot die lips during infuse @ 2,000 µL/min – 800 s^{-1}
- Slot die lips during coating @ 50 µm shim thickness – 1,080 s^{-1}
- Slot die lips during withdraw @ 3,000 µL/min – 1,200 s^{-1}

All materials had been identified and could now be assessed for compatibility with other components. Formulation development will be detailed in the next section, trials are be grouped by polymer.

5. Results and Discussion

The findings of this project have been presented in a methodical order beginning with the development of the fluids required to proceed with subsequent work. Following on from that some initial slot die coating trials were carried out to identify potential issues when processing the selected materials. Two isolated studies were completed to investigate some of the issues highlighted in the objectives section; dewetting and 'wavy' coatings. Some time was spent developing an efficient method to carry out detailed analysis of a large number of substrates, followed by a baselining study to identify the inherent error at each stage of the process. Finally a number of statistical trials were completed to determine which parameters and material properties were interacting and how this was affecting coating thickness uniformity.

a. Formulation Development

All three polymers were studied and their suitability for use in this study was assessed according to the criteria stated in section 4. First was polystyrene (PS), followed by polyisobutylene (PIB) and finally polyethylene oxide (PEO).

i. Polystyrene Formulation Development

Polystyrene formulation development began by carrying out a drop test using the mid-range Sigma Aldrich molecular weight grade of polystyrene; 192,000 g/mol (PS192K). The polymer was mixed with the solvents from Table 8 and dropped onto a glass substrate. They were visually inspected for drying quality and it was observed that polystyrene produced better drying profiles with branched aromatic hydrocarbons. The best drying profile was obtained using 3,4-dimethylanisole (34DMA), Table 10, so subsequent polystyrene development was carried out using 34DMA as the solvent.

Solvent number	Solvent name	Drop test quality
1	Xylenes	3
2	Mesitylene	2
3	1,2,3,4-Tetrahydronaphthalene	4
4	Anisole	3
5	4-Methylanisole	2
6	3,4-Dimethylanisole	1
7	Acetophenone	4
8	Benzaldehyde	3
9	Butylbenzene	2
10	Ethoxybenzene	2

Table 10: Polystyrene drop test results

Four polystyrene grades were added to 3,4-dimethylanisole at a 10 weight percent (wt%) loading to ascertain the effect of molecular weight on viscosity, Figure 29.
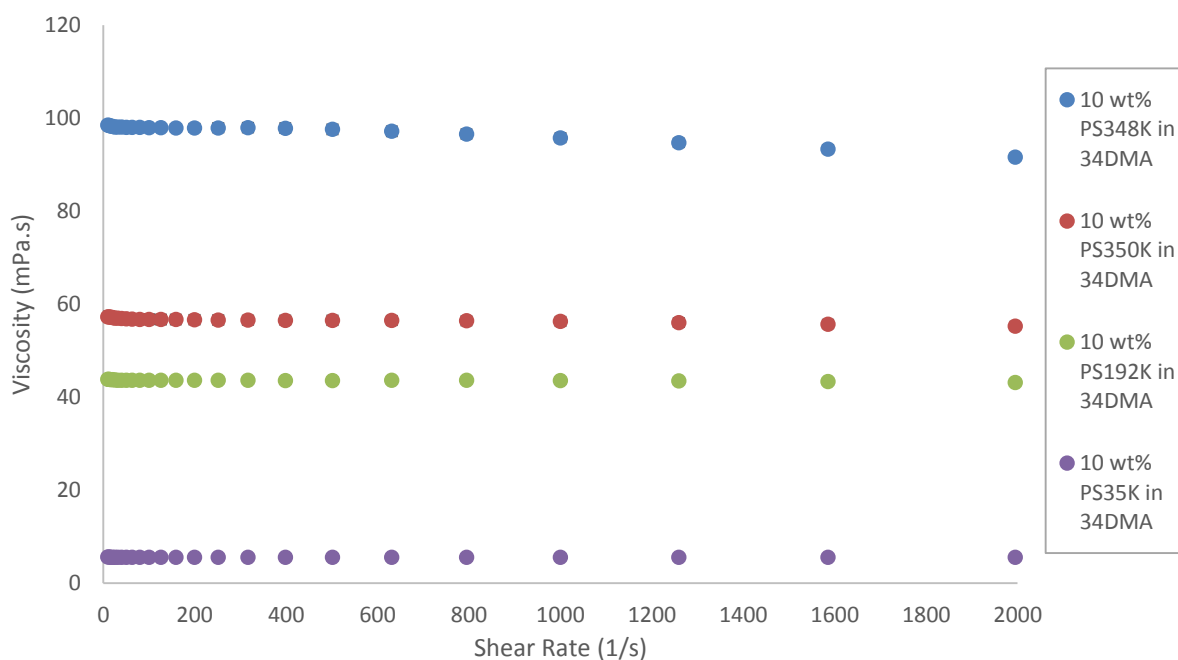
Figure 29: Shear rate dependence of viscosity of readily available polystyrene grades in 3,4-dimethylanisole

There was less of a difference between PS192K and PS350K than expected; higher molecular weight polymer chains usually exhibit a higher degree of entanglement, increasing the viscosity. This was thought to be due to differences in polydispersity indices. The disparity between the viscosity of PS348K and PS350K also suggested the polymers had different molecular weight distributions. Sigma Aldrich was contacted to request more information regarding the polystyrene grades however this information was not available.

PS192K added to 3,4-dimethylanisole at a 10 weight percent (wt%) loading was checked for drawdown coating compatibility using the Wirebar coater. A wirebar yielding 18 µm wet thickness was used as this gave the coating the highest chance of wetting onto the substrate; thicker coatings result in more weight on top of the substrate-formulation interface, minimising potential dewetting. This coating was carried out on a washed piece of 4 inch 0.7 mm corning glass; no surface treatment was applied. A speed setting of 4 (6 being the maximum) was utilised; this has no effect on coating thickness as the speed determined whether lines from the wirebar remained in the coating. The coating was applied and subsequently dried on a hotplate at 130°C for 2 minutes; a complete coating was achieved without any significant visible defects. All work was carried out in a fume cupboard to mitigate safety implications of the solvent.

The same formulation was transferred to the LACE slot die coater, Module A; covers were put in place to prevent the inhalation of solvent vapours. Development was carried out on 8 inch (203.2 mm) corning glass of 0.7 mm thickness; coating issues become more prevalent at a larger scale so it was reasoned that this study would be most valuable at an 8 inch scale. An automated program was setup to move substrates from the substrate rack to the slot die coater, coated substrates were subsequently moved to a hotplate and dried at 130°C for 2 minutes before returning to the substrate rack. The whole process took about 10 minutes per substrate due to aligning steps between each stage. Initial slot die process parameters were selected:

- **Shim thickness** – *100 µm* – this thickness was chosen because lower die-die gaps allow the greatest level of control over the fluid;
- **Plasma treatment** – *no* – the formulation was coated successfully on the wirebar coater without requiring any surface treatment;
- **Slot die selection** – *1* – the slot die head was setup in position 1;
- **Coating width** – *200 mm* – an 8 inch substrate was being used and the corresponding shim width for 8 inch is 200 mm to account for a 1.6 mm gap between the coating and the edge of the substrate;

- **Number of substrate measure points** – *3* – this is the maximum number of points at which the slot die system can check the height of the substrate across the plate ensuring the gap between the die lips and the substrate remains constant;

- **Coating border** – *1 mm* – this is the standard gap left at the start and end of the coating to prevent material from spilling over the substrate;

- **Coating film thickness** – *10 μm* – this was chosen with an aim of depositing 1 μm once the film was dried, the flow rate is controlled by the software in an attempt to uniformly deposit the formulation across the plate;

- **Coating priming gap** – *100 μm* – from past experience this is usually a good starting point and is critical to forming a bead at the start of coating;

- **Coating gap** – *100 μm* – this was kept the same as the priming gap to minimise the number of variables;

- **Coating velocity** – *5 mm/s* – a fairly low speed was chosen to begin with in order to maintain the bead;

- **Coating acceleration** – *10 mm/s* – this was to allow the slot die head to reach its full speed quickly;

- **Material bead volume infuse** – *20 μL* – the aim was to infuse enough material to aid in bead formation without introducing so much material that there would be a thicker start to the coating than required;

- **Material bead flow infuse** – *2,000 μL/min* – this would allow the desired volume to be infused within the first one and a half seconds.

- **Coating start delay** – *6,000 ms* – a longer delay time allows more time for the bead to form; it commonly takes longer for the bead to form with more viscous materials;

- **Pump start offset** – *0 ms* – the was no start offset as there were uncertainties about whether this could have a positive impact on the coating when combined with a relatively low infuse volume;

- **Coating material pump start offset** – *0 mm* – as above, there were uncertainties about the effect of this on the coating;

- **Slot die take-off mode** – *0* – it was decided that it may not be beneficial to begin raising the head before the coating had been completed;

- **Coating material pump stop offset** – *15 mm* – the aim of this was to prevent a build-up of material at the end of the plate;

- **Take-off offset** – *0* – as above, it may not be beneficial to begin raising the head before the coating had been completed;

- **Material bead volume withdraw** – *300 µL* – due to the pump stopping 15 mm from the end it was thought that there wouldn't be a large amount of material remaining at the end of the coating;

- **Material bead flow withdraw** – *30,000 µL/min* – a high flow rate was chosen as there would be limited time to remove material before the head began to raise;

- **Standby gap** – *200 µm* – a larger gap expected to be enough to form a bead in standby position due to a larger amount of material flowing through;

- **Standby bead volume** – *500 µL* – a larger amount of material was infused in the standby position in order to maintain the condition of the lips;

- **Standby bead flow** – *40,000 µL/min* – a high flow rate was selected to allow the bead to form quickly;

- **Standby material flow** – *20 µL/min* – a very low flow rate was selected to prevent the material from blocking the head while not wasting excessive amounts of formulation.

Islands of uncoated areas began to form quickly after coating suggesting dewetting was occurring. This was unexpected as dewetting had not occurred when it was wirebar coated. Plasma treatment and increasing the coating film thickness above 18 µm did little to mitigate this; the effect of plasma treatment on surface energy will be discussed in section 5.b. The difference between the coating success when using the wirebar coater and the LACE slot die coater brought into question the suitability of the wirebar coater as a first step when assessing formulations for slot die coating; the wirebar coater quickly identifies severely incompatible surfaces but it may not be suitable for direct comparison of coating quality.

Stemming from discussions with Professor Tom McLeish, a possible theory for the large disparities between Wirebar coating quality and slot die coating quality could be the high level of shear caused between the wires of the wirebar. When polymers are subjected to high shear the chains are stretched which is an undesirable configuration. When given the chance to relax they expand which could counteract potential dewetting effects.[49] This theory could be tested by using a tapered shim, causing higher shear and potentially stretching the polymers at the bottom of the slot die head i.e. the slot die lips.

Coatings were achieved using the process parameters found in Table 11. The coating priming gap, coating gap, coating velocity and coating acceleration were reduced due to difficulties when forming and maintaining the bead, this may have been in part due to the low shim thickness causing problems when infusing the formulation through the head.

Parameter	Previous value	New value
Coating priming gap (µm)	100	40
Coating gap (µm)	100	40
Coating velocity (mm/s)	5	2
Coating acceleration (mm^2/s)	10	4

Table 11: Changed slot die parameters for best coating of PS192K

Dewetting was thought to be occurring due to the formulation having a concentration too low for chain entanglements to occur suggesting these systems are dilute. This could potentially be overcome either by using a higher loading of PS192K resulting in a semidilute solution, or by substituting for a higher molecular weight polystyrene grade.[50] Entanglement molecular weight will be discussed in section 5.c.i. The LACE line slot die syringe system is limited in relation to maximum viscosity due to the inner diameter of the pipes (3.3 mm) and the pressure limit of the syringe. Though the width of the shim is smaller than the diameter of the pipes, the internal cross-sectional area is larger; area of the shim ranges from 0.01 mm^2 to 0.058 mm^2, internal area of the pipes is 0.0086 mm^2. The highest viscosity formulation successfully used in the LACE line in previous CPI slot die work was ~65 mPa.s. As PS192K was already 45 mPa.s at 10 wt% there was not much freedom to increase the concentration before exceeding the 65 mPa.s limit; PS350K was used for subsequent coatings.

The lack of success due to dewetting when coating 10 wt% PS192K suggested that it would not be possible to coat 10 wt% PS35K using slot die; lower molecular weight polymers become more prone to dewetting due to lower solution viscosity. A new approach was required; the range of concentrations of the highest molecular weight polymer would be used to achieve variations of viscosity, provided there was minimal effect on the surface tension. PS350K was added to 3,4-dimethylanisole in a 1 wt%, 5 wt%, 10 wt% and 15 wt% loading; the effect of this on viscosity, Figure 30, and surface tension, Figure 31, was analysed.
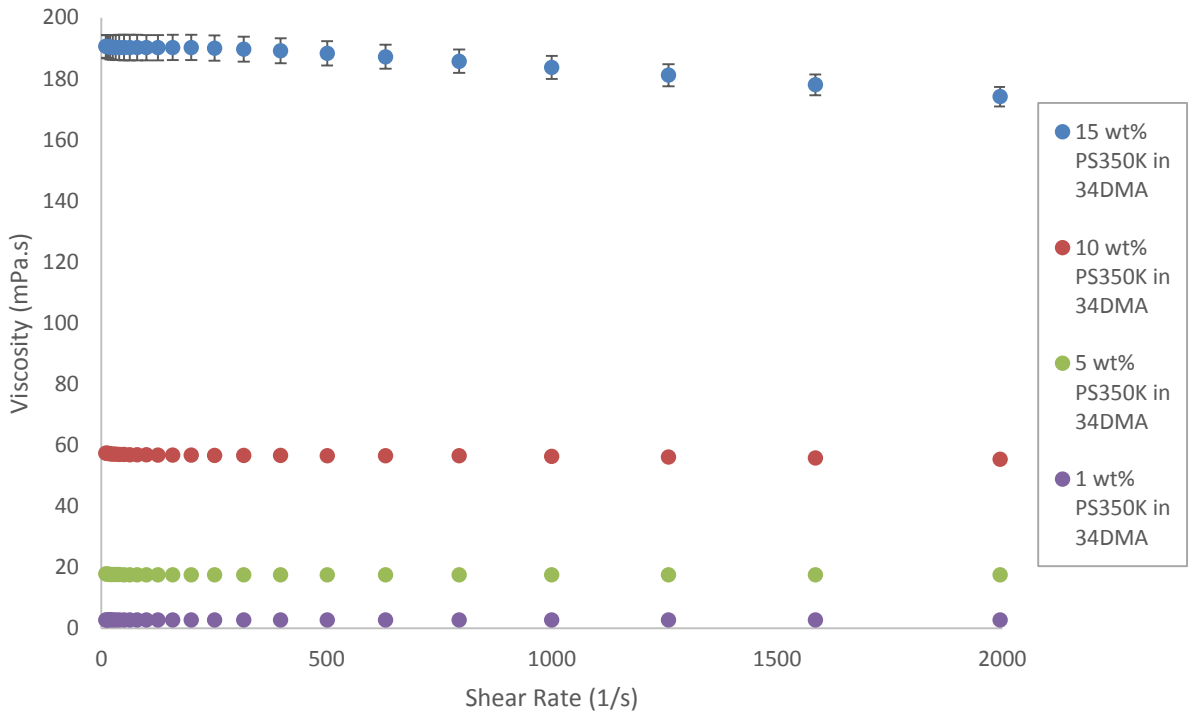
Figure 30: Shear rate dependence of viscosity for PS350K in 34DMA
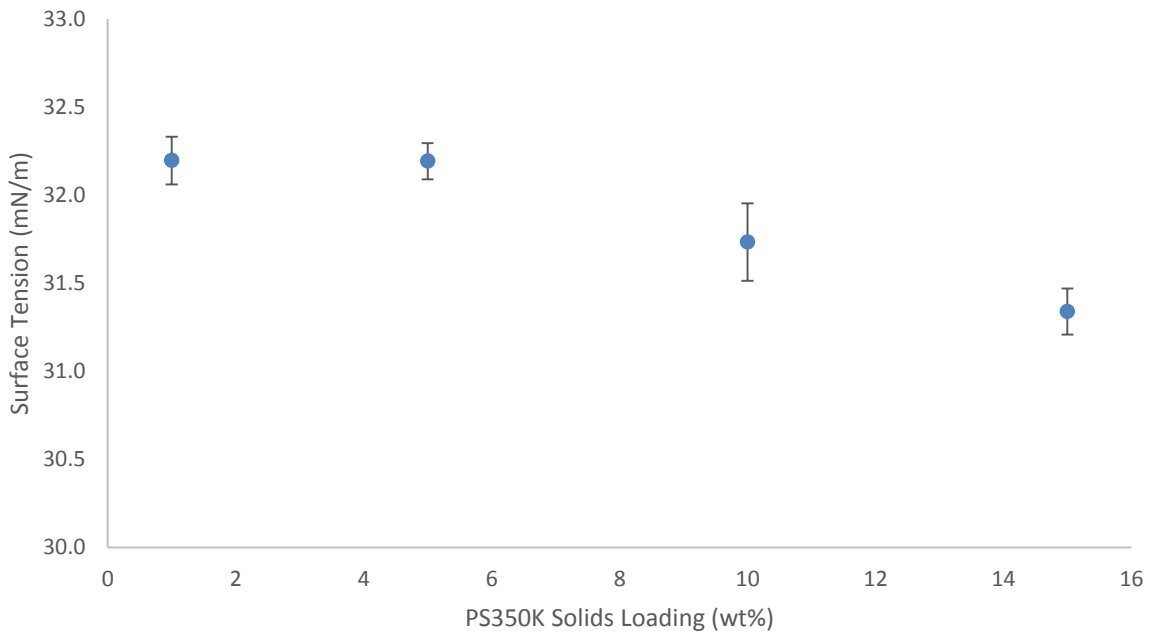
Figure 31: Concentration dependence of surface tension for PS350K in 34DMA

Loadings between 1 and 10 wt% resulted in viscosities within a suitable range for the slot die coater, 15 wt% greatly exceeded the processing limit of the slot die system. Increasing the solids content up to 15 wt% had a minimal effect on the change in surface tension and would not be expected to greatly impact coating as the surface free energy of the stainless steel head and glass substrate are both greater than 35 mN/m.

Slot die coating process development began with 10 wt% PS350K in 3,4-dimethylanisole. The formulation was Wirebar coated using the same settings as the PS192K formulation and this also showed no sign of dewetting. The parameters described in Table 11 were used for the slot die coating of PS350K, though a 150 µm shim was used to minimise the bead issues observed when coating PS192K. Dewetting was again observed. Attempts were made to eliminate this issue by plasma treating and increasing the coating speed, coating gap, coating film thickness; only a small improvement was observed.

The next grade analysed was PS348K; two lower solids content formulations were also analysed with the aim of finding a mixture within the process-able range of the slot die system, Figure 32.
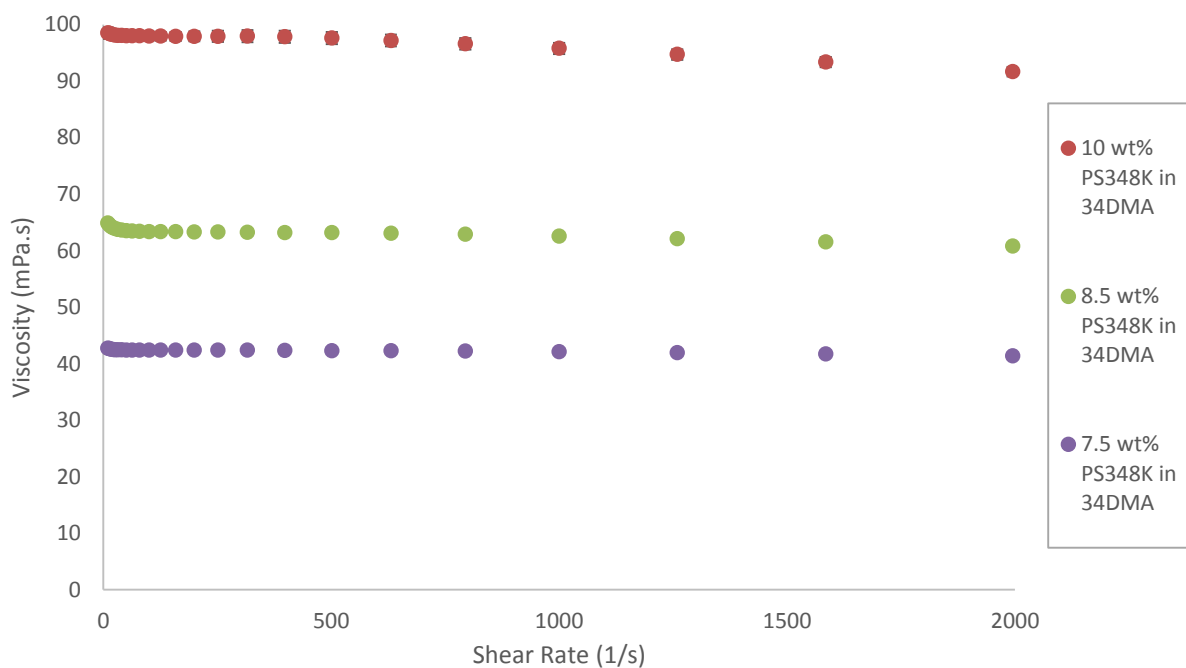
Figure 32: Shear rate dependence of viscosity for PS348K in 34DMA

The formulation containing PS348K added to 3,4-dimethylanisole at an 8.5 wt% loading was slot die coated with similar starting parameters to PS192K and PS350K in 3,4-dimethylanisole, Table 12. A higher coating gap, priming gap, coating speed and coating acceleration and coating film thickness was used to minimise the chances of dewetting.

Parameter	Previous value	New value
Coating film thickness (µm)	10	20
Coating priming gap (µm)	40	80
Coating gap (µm)	40	80
Coating velocity (mm/s)	2	5
Coating acceleration (mm²/s)	4	10

Table 12: Slot die parameters for 8.5 wt% PS348K formulation

Dewetting was observed as with the other polystyrene grades; however the surface of the coatings were visually much rougher. The surface roughness of the coating was analysed using CCI by taking an average of 5 points measured across the plate, the standard deviation of these measurements is also quoted:

- S_a - 33.2 nm ± 12.1 nm
- S_q - 45.2 nm ± 12.8 nm
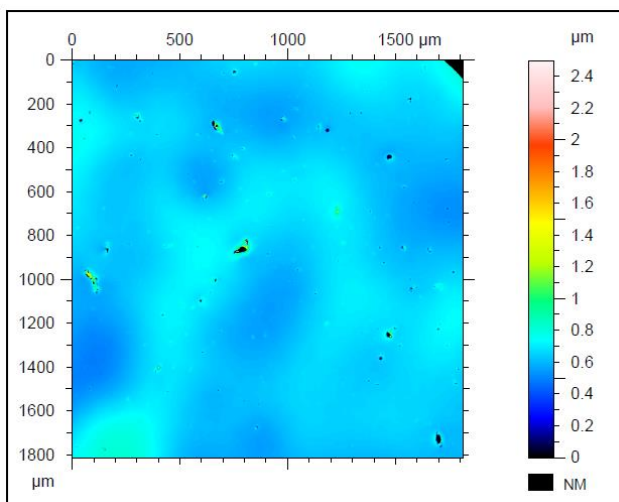
Figure 33: CCI surface map of PS348K coating

Particulates were observed, which were potentially the cause of the dewetting by introducing instability into the wet film. It was unlikely that they were introduced at the formulation stage since the hazy appearance of the coating was not observed with any of the previous polymers, suggesting this grade was contaminated. Increasing the coating speed, coating gap and coating film thickness reduced dewetting but they did not completely eradicate this issue.

Attempts were made to purify the polymer by dissolving it in toluene, centrifuging the mixture at 1000 rpm for 10 minutes and collecting the supernatant; no visible impurities were found in the precipitate. The supernatant was then rotary evaporated at 40°C and 50 mBar, the resulting polymer was dried in an oven at 70°C overnight. An 8.5 wt% formulation in 3,4-dimethylanisole of the purified PS348K polymer was coated using the same parameters as the impure material. The coating visibly looked similar i.e. particles were observed and the surface roughness values were comparable:

- S_a = 29.3 nm ± 12.8 nm

- S_q = 39.6 nm ± 14.8 nm

Polystyrene polymers PS192K, PS350K and PS348K were analysed using the TGA to check for impurities. All polymers exhibited very similar profiles showing a decomposition temperature of 380°C, Figure 34.
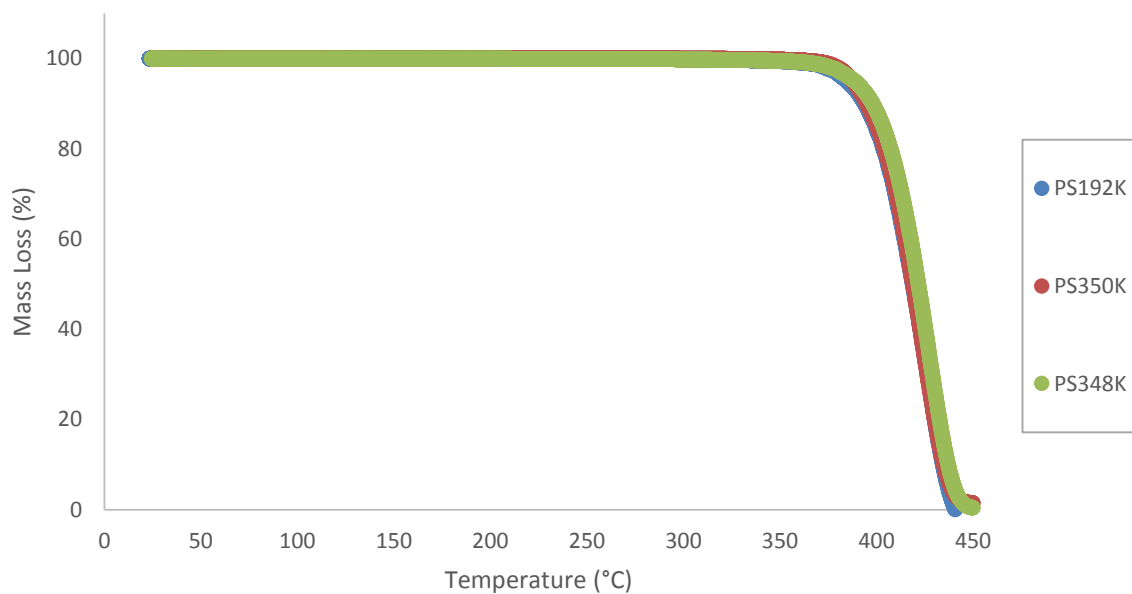
Figure 34: Thermal decomposition of polystyrene grades

Further work would have to go into understanding where the particles were coming from which seemed unnecessary since there were a number of other potentially suitable polymers yet to be trialled. Consequently the processing of this polymer was not continued.

The higher molecular weight polystyrene, PS885K, was added to 3,4-dimethylanisole. There was 1 g of this material provided so the amount of analysis and processing that could be carried out was limited. To conserve material PS885K was added to 3,4-dimethylanisole in a 3 wt% loading which resulted in a viscosity of 34 mPa.s, the formulation exhibited a slightly pseudoplastic profile, Figure 35.
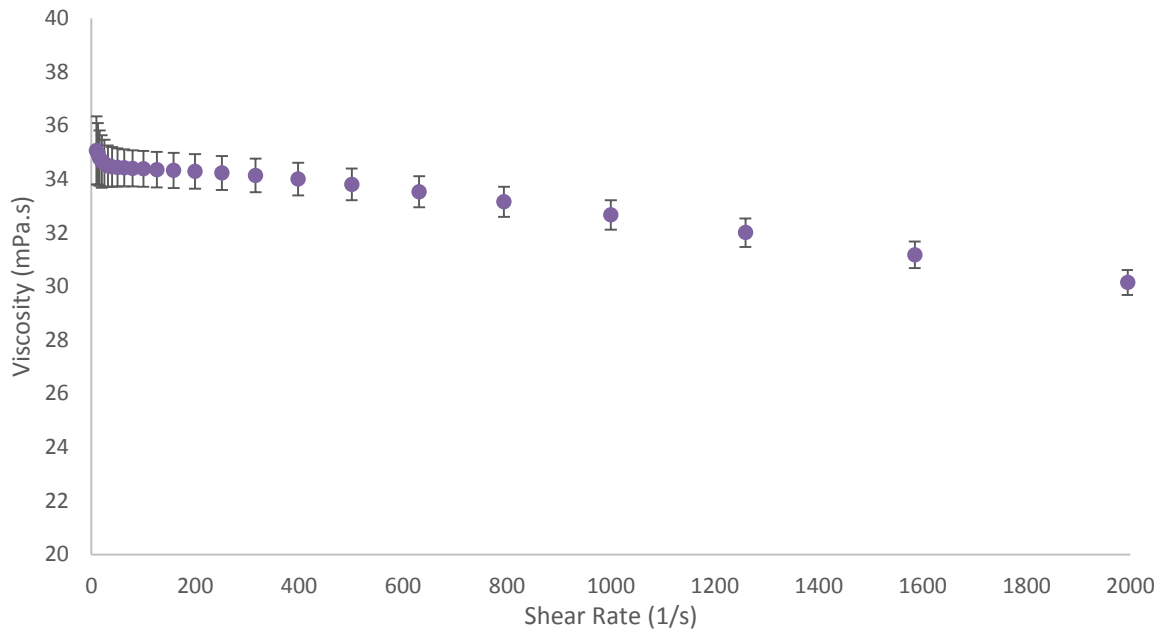
Figure 35: Shear rate dependence of viscosity for 3 wt% PS885K in 34DMA

Dewetting was dramatically reduced without having to increase coating film thickness above 20 μm. Particulates and occasional dewetted areas were observed in the coating which could have been mitigated by filtering the formulation. There was only enough material to carry out one short slot die run so no further development could be carried out.

It became clear that none of the readily available polystyrene grades would be suitable for this study. A larger range of molecular weight polystyrene grades were available from Sigma Aldrich in the form of analytical standards, however since the TGA profiles did not show evidence of any contaminates it would not be reasonable to expect monodisperse systems to yield better results. Other polymers were investigated; polyisobutylene was subsequently assessed.

The work carried out using polystyrene highlighted a key issue when processing polymers using slot die; dewetting was observed during previous projects at CPI and had not been understood. This issue will be further in section 5.c.i.

ii. Polyisobutylene Formulation Development

Five aromatic solvents were chosen from Table 8 on page 63 due to their high boiling points, drop tests were carried out. Dried droplets were inspected visually, Table 13; Tetralin was the only solvent that produced a good coating. Tetralin is classified as potentially carcinogenic so it was undesirable for long term testing, however limited experimentation was carried out to provide a comparison between the coating quality of polyisobutylene with polystyrene.

Solvent number	Solvent name	Drop test quality
2	Mesitylene	3
3	Tetralin (1,2,3,4-Tetrahydronaphthalene)	1
5	4-Methylanisole	4
6	3,4-Dimethylanisole	4
7	Acetophenone	4

Table 13: Polyisobutylene solubility study

PIB500K was added to tetralin in a 1 wt%, 2 wt%, 3 wt%, 4 wt% and 5 wt% loading to determine whether the viscosity could be controlled by modulating the concentration of polymer without introducing more variables; the effect of this on viscosity, Figure 36, and surface tension, Figure 37, was investigated.
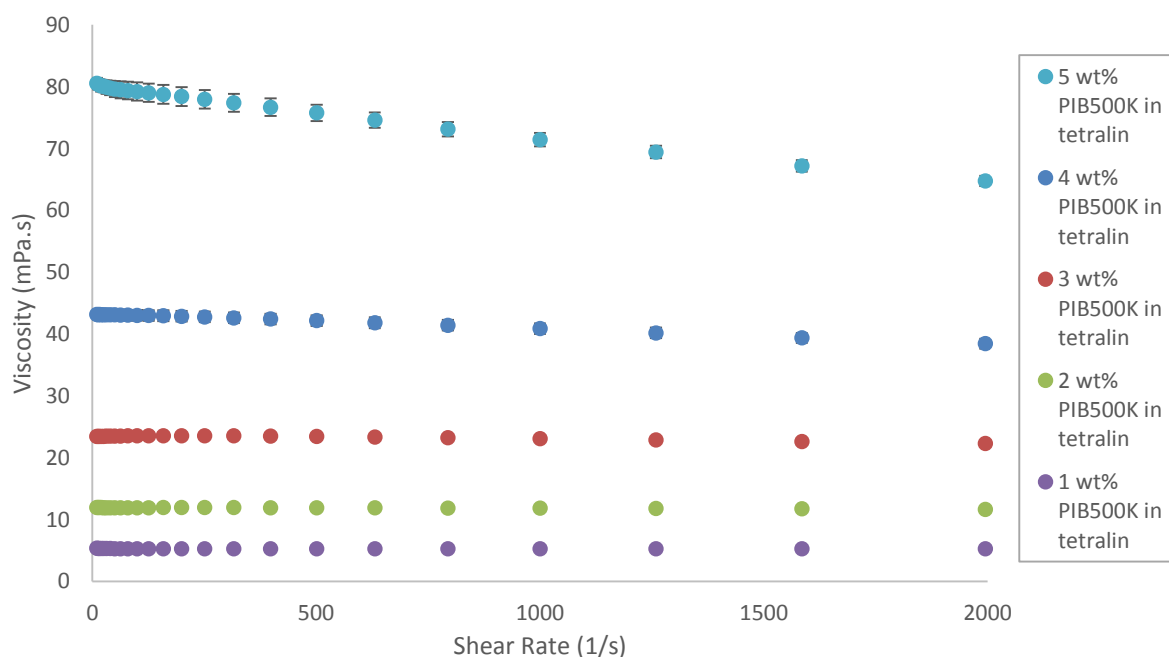
Figure 36: Shear rate dependence of viscosity for PIB500K in tetralin
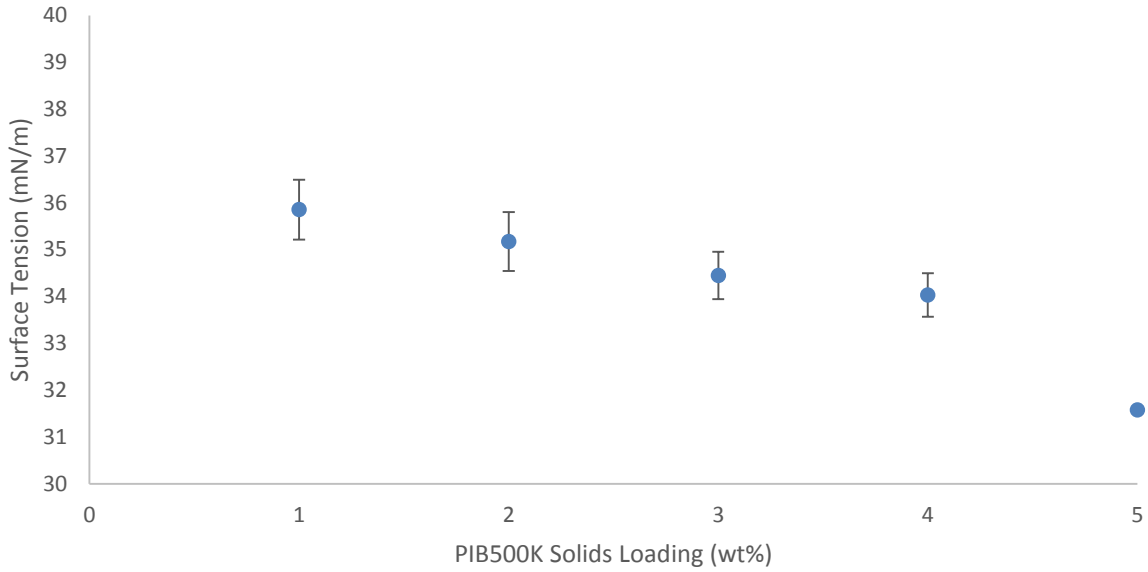
Figure 37: Concentration dependence of surface tension for PIB500K in tetralin

Modulation of solids loading had little impact on the surface tension. A wide range of viscosities were achieved using the selected solids loadings. The 4 wt% formulation was used to check for dewetting issues as this was the highest loading within the viscosity range of the slot die.

PIB500K was added to tetralin at a 4 wt% loading to produce a formulation of 43 mPa.s. It was coated using the starting parameters detailed in Table 14 to produce complete films i.e. no dewetting was observed.

Parameter	Previous value	New value
Coating film thickness (µm)	20	10
Coating priming gap (µm)	80	40
Coating gap (µm)	80	40

Table 14: Slot die parameters for 4 wt% PIB500K in tetralin

The success of PIB coating at a lower loading than polystyrene suggested further investigation was required to understand the degree of entanglement of the polymers. No further slot die coating trials were carried out, due to the previously mentioned safety implications. Polyethylene oxide was the third and final polymer trialled for suitability in this project, outlined in the next section.

iii. **Polyethylene Oxide Formulation Development**

Polyethylene oxide was soluble in water making it a desirable candidate due to the non-hazardous nature of this formulation. In addition to this, slot die processing could be carried out in an identical system located in the ambient module where substrates can be handled manually, allowing for quicker throughput without the requirement for the automated handling system. Water has a high surface tension which would not wet onto glass without the addition of a surfactant. The use of a surfactant provides control over the surface tension therefore this combination of components allows for variation of viscosity and surface tension.

PEO300K was added to water at a 2 wt%, 3 wt% and 5 wt% loading. The mixtures had a hazy appearance; this was due to butylated hydroxyltoluene (BHT) which is insoluble in water. Formulations were centrifuged at 2500 rpm for 10 minutes. A white residue was observed at the bottom of the vials; this was presumed to be BHT. The dissolved PEO in water was collected from the supernatant, the formulation was no longer of cloudy appearance.
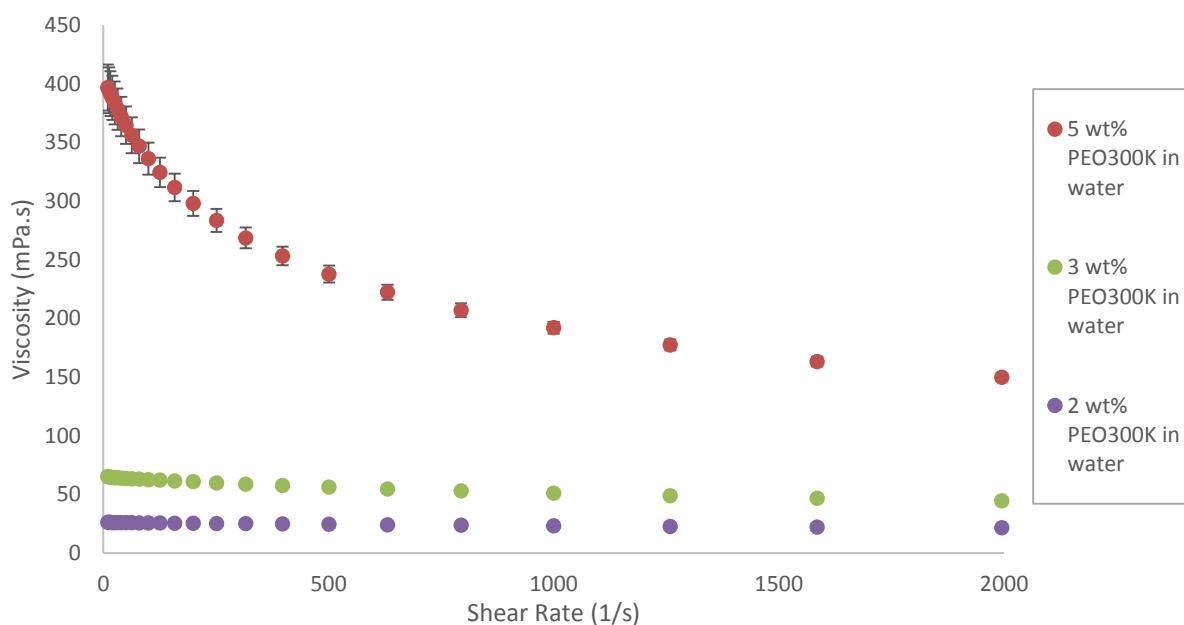
Figure 38: Shear rate dependence of viscosity for PEO300K in water

The 5 wt% formulation was too viscous to be processed by the slot die coater. The 3 wt% PEO300K formulation exhibited signs of pseudoplasticity which could affect uniformity. 2 wt% PEO300K was reasonably Newtonian so it was suitable for slot die coating; this formulation was used to investigate potential surfactants.

In order to control surface tension two non-ionic surfactants were trialled; Triton X-100 and Span 20 as they had previously worked well in water-based systems. The critical micelle concentration for the surfactants was calculated to be approximately 0.01 wt% for Span 20 and 0.011 wt% for Triton X-100. Surfactants were added at a 0.009 wt% loading, to ensure they were below the CMC, to 2 wt% PEO300K in water. Surfactants were kept at concentrations below the CMC to prevent aggregation, maximising surface adsorption. A control containing no surfactant and the two surfactant containing formulations were coated onto cleaned Corning glass using the Wirebar coater incorporating an 18 µm bar. Coatings were dried at 100°C for two minutes and were cooled on a flat metal surface for two minutes. Once the substrates had cooled a crystal structure was observed which is characteristic of polyethylene oxide. No dewetting was observed on the substrates. The coatings were analysed for surface roughness variations, Figure 39. Surfactants are used to increase formulation stability; this can be measured using surface roughness.[51] S_a is the arithmetic mean height, S_q is the root mean square deviation.
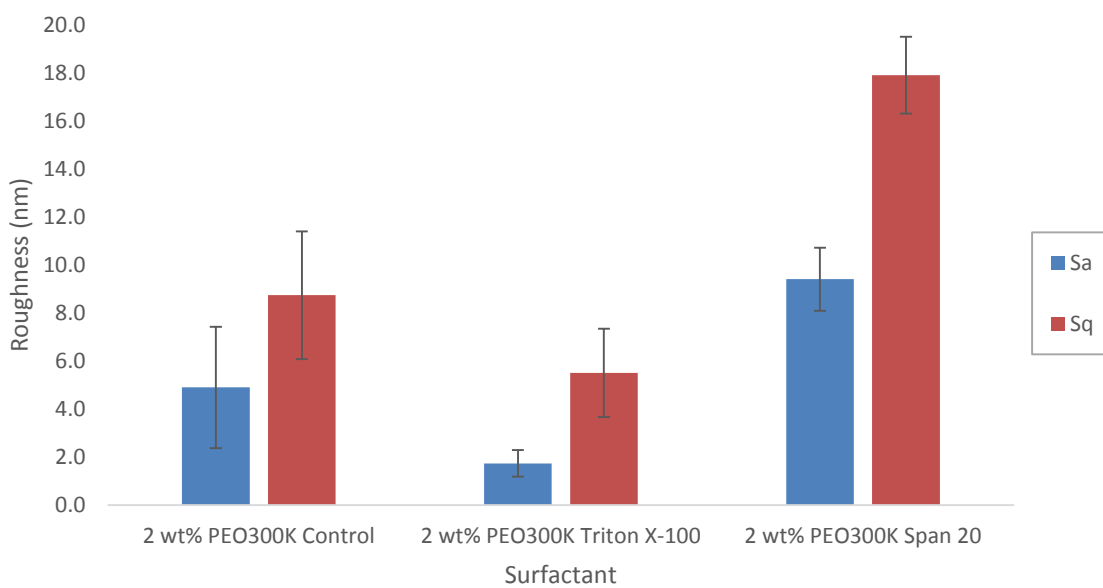
Figure 39: Surfactant dependence of roughness for 2 wt% PEO300K in water

The addition of Triton X-100 resulted in the smoothest surface suggesting it improved mixing between components. Triton X-100 had the highest CMC of the two surfactants so more could be added before exceeding the CMC. Triton X-100 has been used in studies to increase nanoparticle mobility[52] which is advantageous during slot die coating; as the slot die head moves the interface between the lips and the substrate is constantly being replenished so it is beneficial for the surfactant to be able to respond quickly. No information could be found regarding Span 20 mobility.

PEO300K exhibited pseudoplasticity at higher loadings than 2 wt% therefore it would not be possible to develop a formulation above 24 mPa.s. Three lower molecular weight polymers were trialled; PEO37K, PEO100K and PEO200K. Polymers were added to water and 0.01 wt% Triton X-100 at a 5 wt% loading; changes in viscosity was measured, Figure 40.
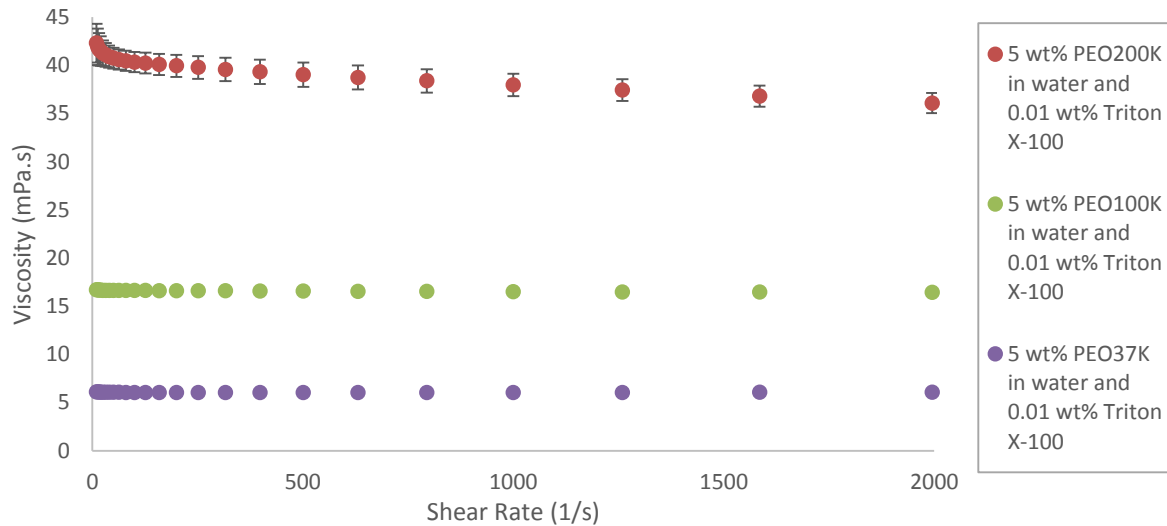
Figure 40: Shear rate dependence of viscosity for PEO in water and 0.01 wt% Triton X-100

The three chosen molecular weights gave a suitable viscosity range exhibiting low levels of pseudoplasticity, this was not expected to have dramatic effects on coating but 5 wt% PEO200K would be monitored for any non-uniformities potentially caused by the rheology.

The effect of surfactant loading on viscosity was found to be less than measurement error, Figure 41; this suggested it was unnecessary to measure formulations containing all concentrations of surfactant. Viscosity measurements were only taken for the formulation with the higher loading of Triton X-100.
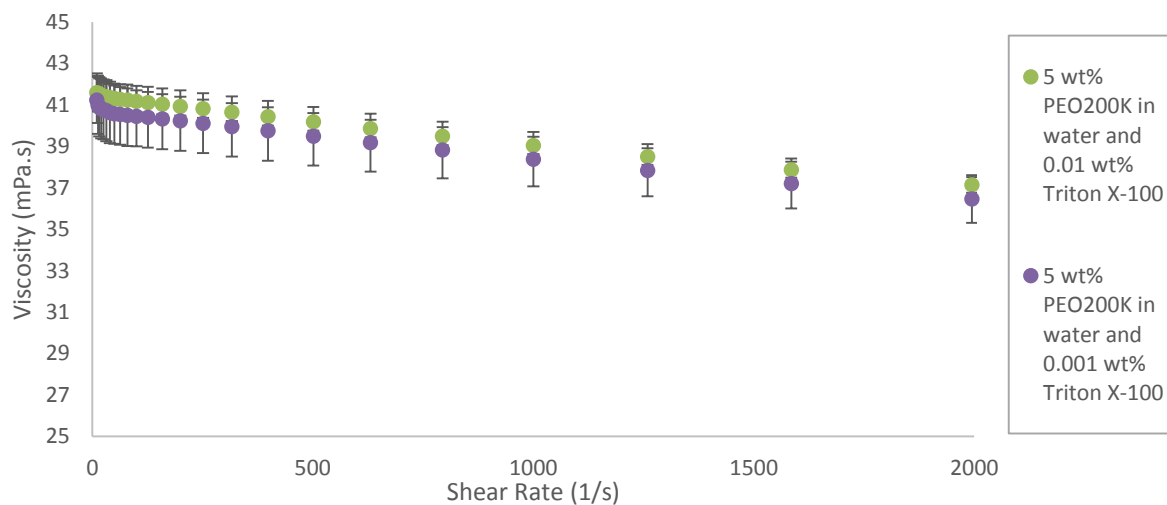
Figure 41: Shear rate dependence of viscosity for PEO200K in water, with 0.001 and 0.01 wt% Triton X-100

The effect of molecular weight on surface tension was analysed for PEO37K and PEO200K combined with two loadings of surfactant; 0.001 wt% and 0.01 wt%. The maximum loading that was within the CMC was 0.01 wt%.
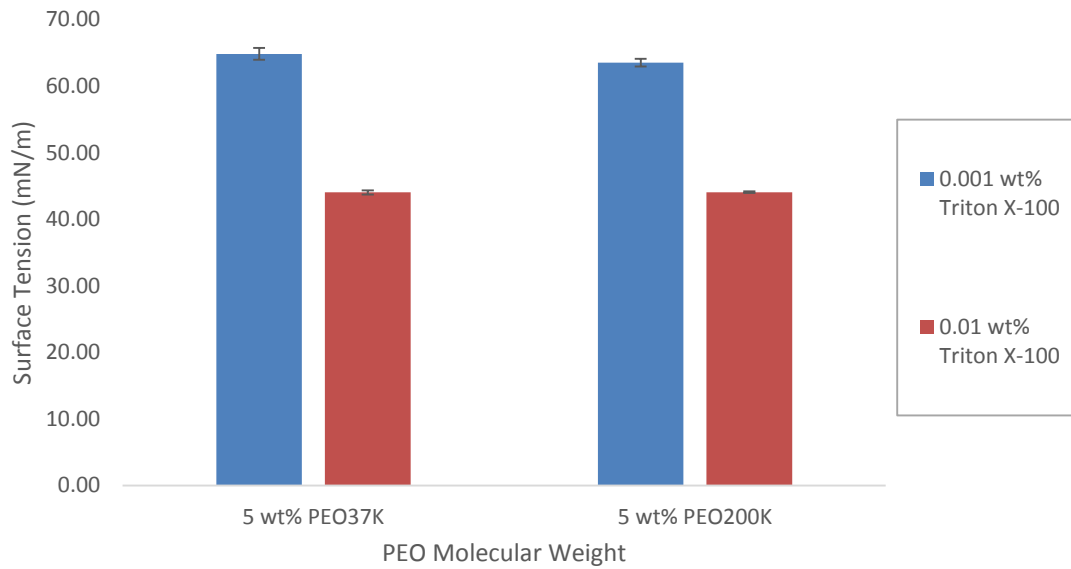
Figure 42: Molecular weight dependence of surface tension for 5 wt% PEO in water

The variation of molecular weight had a minimal effect on the surface tension and was not thought to be significant. The two loadings of surfactant provided a suitable range to allow for assessment of the effects of surface tension without causing dewetting.

This combination of polymer, surfactant and solvent were identified as fulfilling all criteria set out at the start of this section. All further work was carried out using PEO and Triton X-100 surfactant in water. Slot die trials were carried out to identify any potential issues and allow for some initial process development.

b. Initial Slot Die Coating Trials

A Filmetrics method was setup for polyethylene oxide on glass but the refractive index of the polymer was too close to that of glass to obtain a reliable model. Glass substrates were sputter coated with 70 nm of aluminium to achieve an opaque surface to allow for the thickness to be solved for just the top layer i.e. PEO. In addition, aluminium had a vastly different refractive index to the polymer so the interface between the materials would be easily identifiable.

Material	'n' value @ 435.8 nm	'k' value @ 435.8 nm	'n' value @ 632.8 nm	'k' value @ 632.8 nm
Glass	1.5276	0.0000	1.5156	0.0000
Aluminium	0.5795	5.2994	1.3762	7.6162
PEO	1.4288	0.0084	1.4208	0.0078

Table 15: Refractive index of PEO compared with substrate values

The formulation containing PEO37K at a 5 wt% loading and 0.01 wt% Triton X-100 was trialled first. The low viscosity fluid was expected to be the most difficult to coat due to there being the fewest entanglements; the bead would potentially be unstable. The highest amount of surfactant was used to ensure the material would wet sufficiently in these initial trials.

It was coated onto the sputtered aluminium using the Wirebar coater and severe dewetting was observed. The surface free energy (SFE) were of the aluminium surface was measured using water (polar solvent) and diiodomethane (dispersive solvent) contact angles, the SFE was found to be:

- Total – 81.43 mN/m
- Dispersive component - 50.80 mN/m
- Polar component – 30.63 mN/m

The surface was dominated by the dispersive component; water is a polar solvent so the two interfaces were incompatible. The surface was modified using an oxygen plasma treatment to increase the polar component of the surface. It was not possible to measure the SFE after plasma treatment as water droplets wetted completely, however this showed that the polar components now dominated the surface. PEO37K at a 5 wt% loading was coated onto the plasma treated aluminium using the Wirebar coater and no dewetting was observed.

Slot die coating process development began with the process shown in Table 16 onto plasma treated 8 inch aluminium coated glass substrates.

Coating film thickness (µm)	10	Plasma treatment (Y/N)	Y
Coating priming gap (µm)	100	Coating start delay (ms)	3,000
Coating gap (µm)	100	Coating material pump stop offset (mm)	35
Coating velocity (mm/s)	10	Material bead volume withdraw (µL)	1000
Coating acceleration (mm²/s)	20	Standby gap (µm)	100
Material bead volume infuse (µL)	20	Standby bead volume (µL)	1,500

Table 16: Slot die parameters for 5 wt% PEO37k and 0.01 wt% Triton X-100 in water coated onto 8 inch substrates

The resultant coating was analysed with the Filmetrics tool using a method that incorporated an edge exclusion of 15 mm, which was common for 8 inch plates, and 49 measurements were taken across the substrate. The dry coat thickness was calculated to be 1.02 µm ± 0.31 µm, Figure 43, "start" signifies the beginning of the coating, "stop" shows the end.
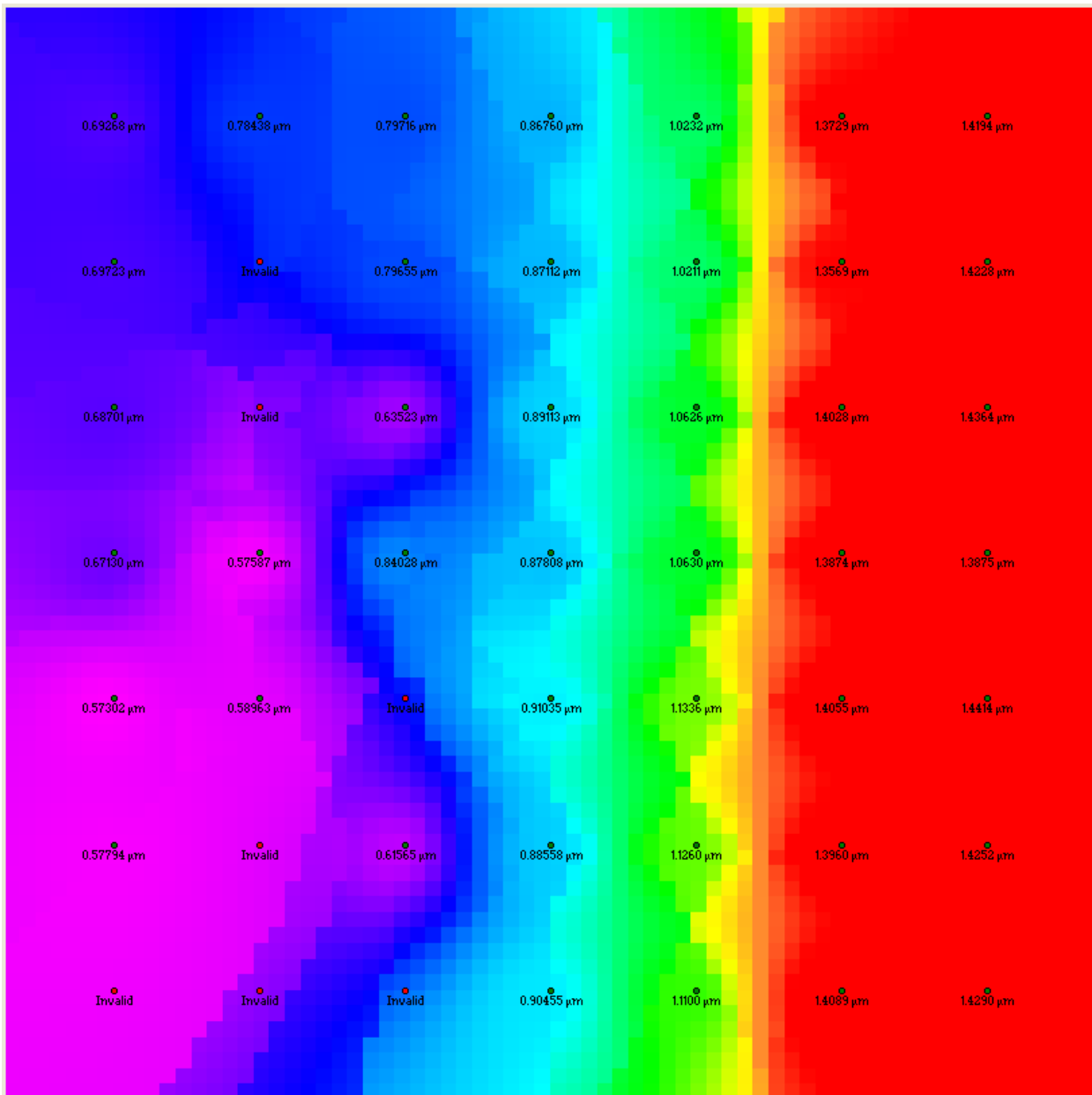
Figure 43: Dry coat thickness map of 5 wt% PEO37k and 0.01 wt% Triton X-100 in water, Run 1

A second plate was coated with the same parameters; the resultant dry coat thickness was measured to be 0.59 µm ± 0.28 µm, Figure 44.
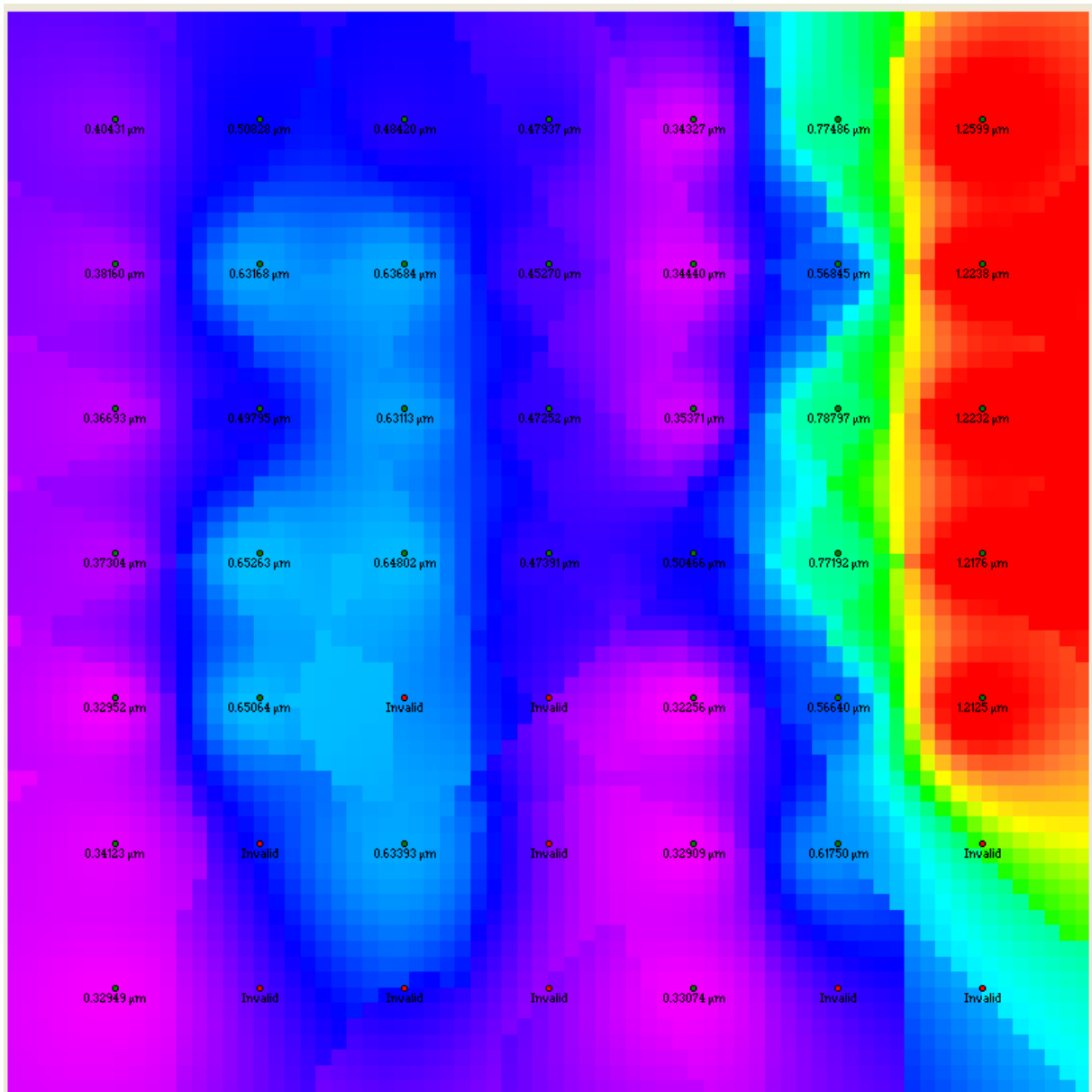
Figure 44: Dry coat thickness map of 5 wt% PEO37k and 0.01 wt% Triton X-100 in water, Run 2

The same parameters were run a third time; dry coat thickness was 0.69 μm ± 0.28 μm, Figure 45.
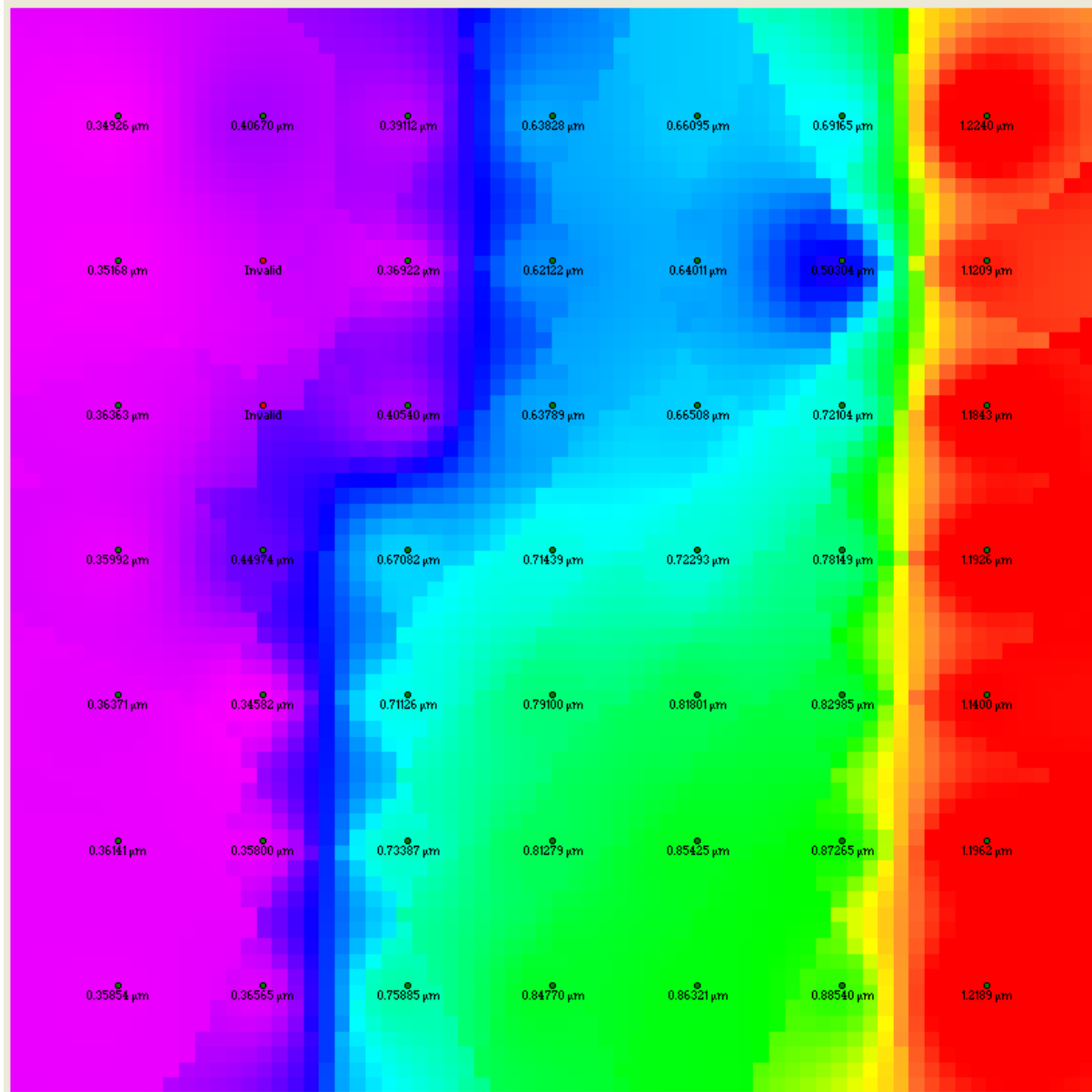
Figure 45: Dry coat thickness map of 5 wt% PEO37k and 0.01 wt% Triton X-100 in water, Run 3

The large variation between the first plate and the following two suggested there was excess material on the lips from the setup process during the first coating. Further coatings showed no improvement so the head was cleaned and the syringe and system was refilled. This was to account for any potential contaminants and bubbles in the system.

Sputtering glass substrates and plasma treating surfaces was time consuming when carried out on 8 inch substrates due to the limitation of the chamber size. A substrate size of 4 inch was sufficient to study coating uniformity issues and would allow for a higher work throughput.

Based on observations from the first coatings the process was altered. Due to the change in substrate size it would not have been possible to directly compare coatings produced using the same process parameters as the first run.

- Coating velocity and acceleration were increased to amplify the flow rate while maintaining the wet coat thickness;
- Material bead volume was reduced to provide less material at the start of the coating;
- Material bead flow infuse was increased resulting in a faster infuse of material;
- The coating material pump stop offset was decreased as the thickness of coatings dramatically reduced for the last two rows of data points;
- Material volume withdraw was increased to account for the decreased coating material pump stop offset as it was expected there would be residual material at the end of coating.

Parameters	Previous value	New value
Coating velocity (mm/s)	10	15
Coating acceleration (mm²/s)	20	30
Coating material pump stop offset (mm)	35	15
Material bead volume infuse (µL)	20	10
Material bead flow infuse (µL/min)	2,000	5,000
Material bead volume withdraw (µL)	1000	1500

Table 17: Slot die parameters for 7.5 wt% PEO100k and 0.01 wt% Triton X-100 in water coated onto 4 inch substrates

This resulted in a dry coat thickness of 0.73 µm ± 0.06 µm, Figure 46, a 10 mm edge exclusion was applied to the Filmetrics method. Uniformity across the substrate had improved.

Stop   Start
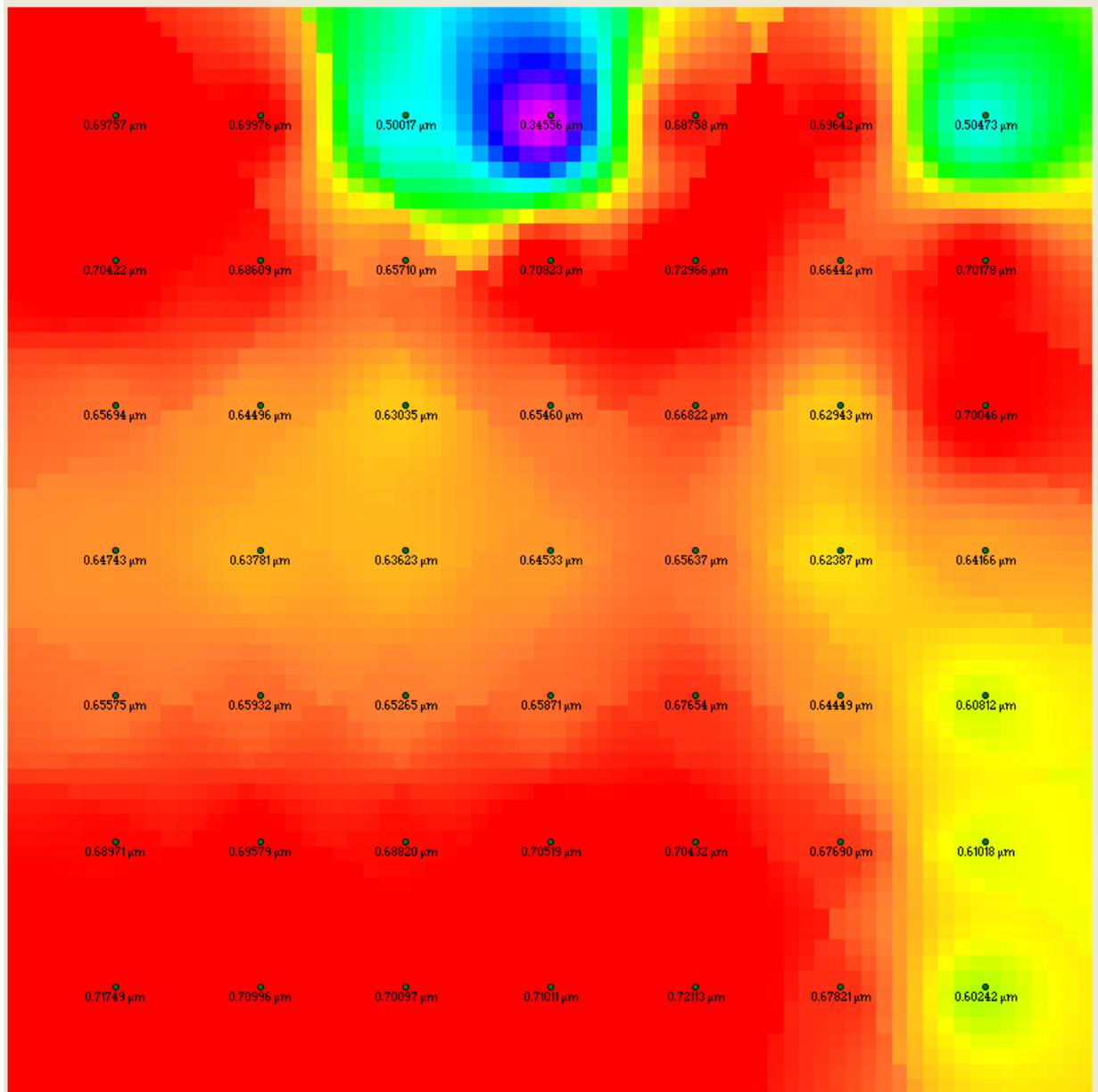
Figure 46: Dry coat thickness map for 5 wt% PEO37k and 0.01 wt% Triton X-100 in water coated onto 4 inch substrates

Subsequent plates were processed but the coatings were incomplete due to the bead not forming on the substrate. Air had been drawn into the lines due to the high withdraw volume which was resulting in the poor coatings. This highlighted the importance of ensuring the lips remain wet at all times.

There were still concerns of contamination due to irregular patterns on coatings; formulations were filtered with a 0.45 µm Millipore syringe filter in addition to centrifugation prior to being loaded into the slot die syringe. Plates were also blown with air to remove any particulates from the surface. All substrates were stored in clean boxes in a class 100 cleanroom. A number of changes were made to the parameters over the course of a number of trials, mainly the end parameters to ensure air was not entrained during future coatings:

- The wet coat thickness was increased to reduce potential dewetting effects;
- Material bead flow infuse was reduced to provide a more gradual infuse of material;
- Coating material pump stop offset was reduced to allow for material to be infused closer to the end of the plate;
- Material bead volume was reduced to prevent air being pulled into the system;
- Material bead flow withdraw was increased to ensure material was withdrawn almost immediately;
- Standby gap was reduced to aid bead formation;
- Standby bead volume was set to 200 µL more than the material bead volume withdraw to prevent the lips from drying without producing too much material at the start of the plate;
- Standby material flow was increased to maintain the condition of the head and lips.

Wet coat thickness (µm)	15		
Material bead flow infuse (µL/min)	500	Standby gap (µm)	70
Coating material pump stop offset (mm)	5	Standby bead volume (µL)	1,200
Material bead volume withdraw (µL)	1,000	Standby bead flow (µL/min)	100,000
Material bead flow withdraw (µL/min)	150,000	Standby material flow (µL/min)	100

Table 18: Slot die parameters for 5 wt% PEO37k and 0.01 wt% Triton X-100 in water coated onto 4 inch substrates run 2

Complete coatings were achieved and the issues of air entrainment was not encountered again. However, lack of repeatability between plates made developing a uniform process difficult; it was difficult to tell whether changes in coating quality were due to a parameter change or tool error.

At this stage it was decided that a more thorough data collection method was required; the development of this process will be described in section 5.d. All previous coatings exhibited dry coat thicknesses of less than 1 μm for the full range of data points; subsequent measurements were carried out in nm units. The variation in results led to a baselining study to determine where the error was coming from; this will be detailed in section 5.e.

The next section incorporates two independent studies, carried out to further understand issues occurring due to formulation issues described in the objectives section.

c. Polymer Investigation

Though polystyrene and polyisobutylene would not be used in slot die coating trials, they could still be used to better understand other coating concerns. Polystyrene was difficult to coat without dewetting being observed, however polyisobutylene had coated without any difficulty. This was investigated using oscillatory rheology to determine the entanglement molecular weight of the polymers in solution.

i. The Effect of Entanglement Molecular Weight On Coating Success

Entanglement molecular weight (M_e) is defined as the molecular weight between entanglements. This can be calculated from an experimental plateau modulus value of a polymer solution. A rationale was employed whereby the presence of a plateau modulus signified some degree of entanglement. This could be used as a way to benchmark whether formulations would be expected to form stable films.

The entanglement molecular weight and plateau modulus (G^0_N) are associated by the following equation[53]:

$$G^0_N = \frac{4}{5}\frac{\rho RT}{M_e}$$

Equation 15: Plateau modulus

where:

- $\rho = Density$
- $R = Ideal\ gas\ constant$
- $T = Temperature$

The plateau modulus can be calculated using oscillatory rheology techniques to determine the crossover modulus. The crossover modulus and plateau modulus are related using the Wu method for polydisperse systems, Equation 16; the model is suitable for polymers with a polydispersity greater than 1 but less than 3.[54]

$$\log\left(\frac{G_N^0}{G_x}\right) = 0.38 + \frac{2.63\log(\frac{M_w}{M_n})}{1 + 2.45\log(\frac{M_w}{M_n})}$$

Equation 16: Finding the plateau modulus using the crossover modulus

where:

- $G_x = Crossover\ modulus$

The crossover modulus is the region where the storage modulus (G': describes elastic behaviour of a polymer) and the loss modulus (G'': describes the viscous behaviour of a polymer) crossover in an oscillatory frequency experiment, Figure 47. It was hoped that a method could be developed to screen materials for potential issues before using 40 mL on the slot die coater.
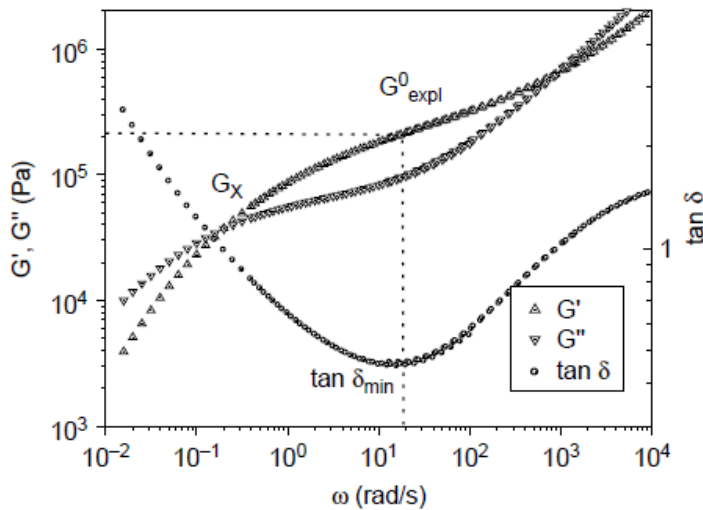
Figure 47: Master curve for polyisobutylene (Mv = 85,000 g/mol, Mv/Mn = 2) [54]

Reprinted with permission from (Liu, C. et al (2006) Evaluation of different methods for the determination of the plateau modulus and the entanglement molecular weight, Polymer, 47: 4461-4479). Copyright (2006) Polymer.

A method was setup using 30 wt% PIB500K in tetralin, a 2 minute equilibration step was carried out at the start of every process;

- Oscillatory strain sweep experiments were run at 20°C:
    - Strain: 0.003 – 3;
    - Angular frequency: 0.6283 and 628.3 rad/s;
    - Log mode, 10 points per decade and a 1 minute equilibration time between readings.
- Oscillatory frequency sweep experiments were run at 20°C:
    - Strain: 0.1 - chosen from within the linear viscoelastic region, determined in the corresponding oscillatory strain sweep experiments;
    - Angular frequency: 0.6283 – 628.3 rad/s;
    - Log mode, 10 points per decade and a 1 minute equilibration time between readings.
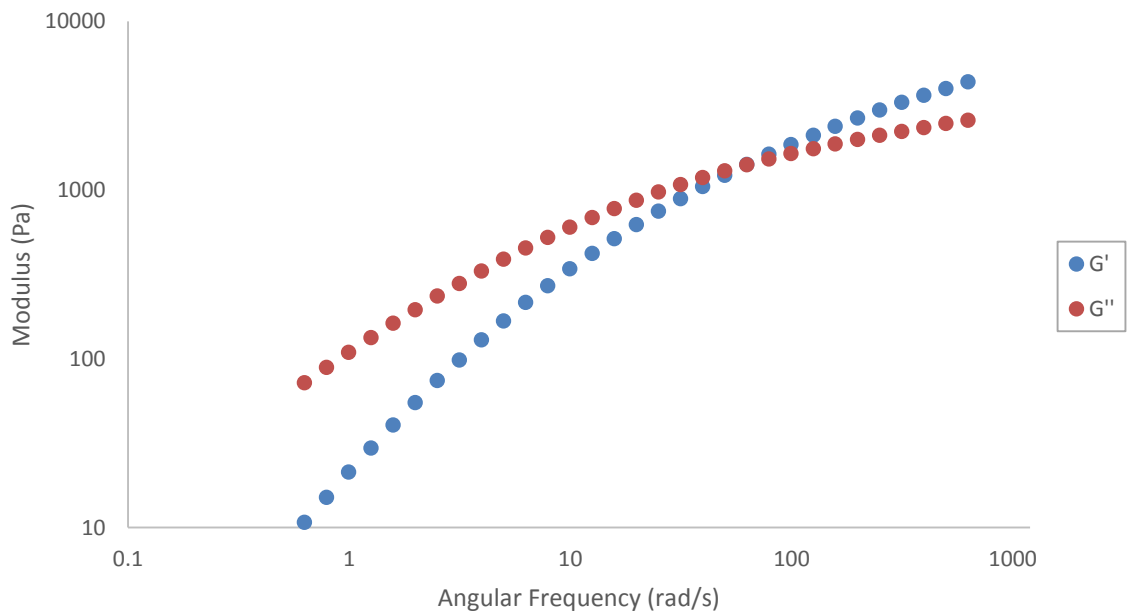
Figure 48: Angular frequency dependence of Modulus for 30 wt% PIB500K in tetralin

G_x = 1440 Pa; $G^0{}_N$ = 11,700 Pa; M_e = 155,000 g/mol

Generally the polymers weight average molecular weight should be approximately three times higher than the entanglement molecular weight before a significant plateau region can be measured. The molecular weight of the polymer did exceed $3M_e$ suggesting entanglement was occurring.

The same process was carried out, at 0.3 strain, using 30 wt% PS350K in 3,4-dimethylanisole however a crossover region was not reached. The process was repeated at 10 - 90°C. Profiles were combined using TTS:

- The 20°C scan was used as the baseline; 20°C is standard processing temperature for slot die coating;
- The Arrhenius model was used.
- Curves were shifted with respect to G".
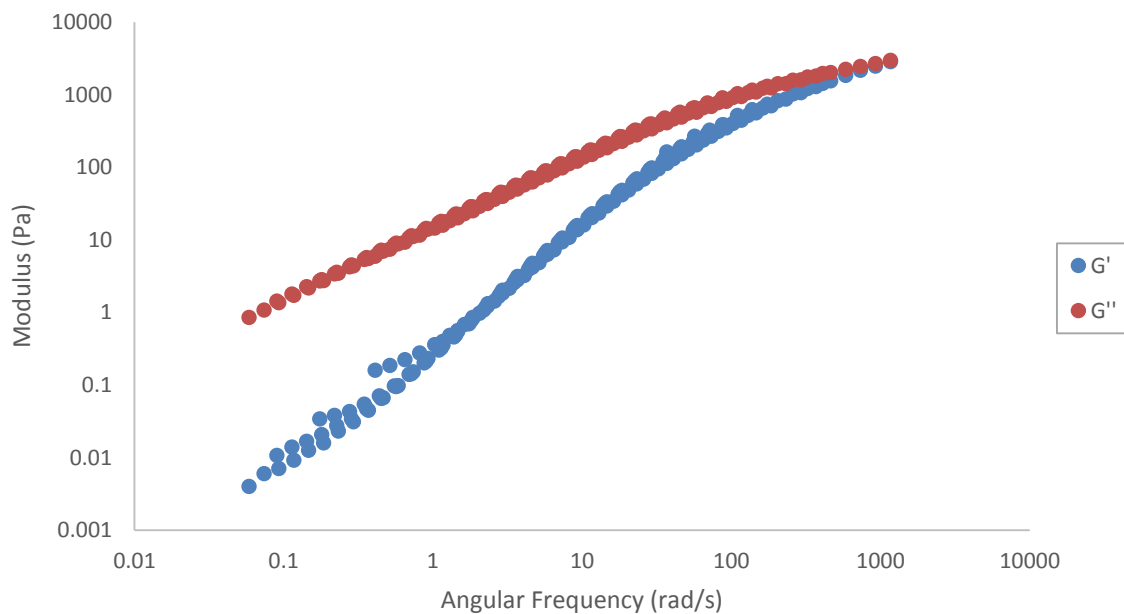
Figure 49: Angular frequency dependence of Modulus for 30 wt% PS350K in 34DMA

The crossover modulus was almost reached; the mean value for the maximum points of G' and G" was taken: G_x= 2920 Pa; $G^0{}_N$ = 20,800 Pa; M_e = 82,200 g/mol

Again the molecular weight of the polymer exceeded $3M_e$ therefore entanglement was thought to be occurring.

Similar processes were carried out for 5 wt% PIB500K in tetralin and 10 wt% PS350K in 3,4-dimethylanisole to ascertain whether dewetting was occurring due to the concentration of the polymer being too low for entanglement to occur. Higher angular frequencies of 10 - 500 rad/s were used with a strain of 0.4. Measurements were only carried out at 20°C.
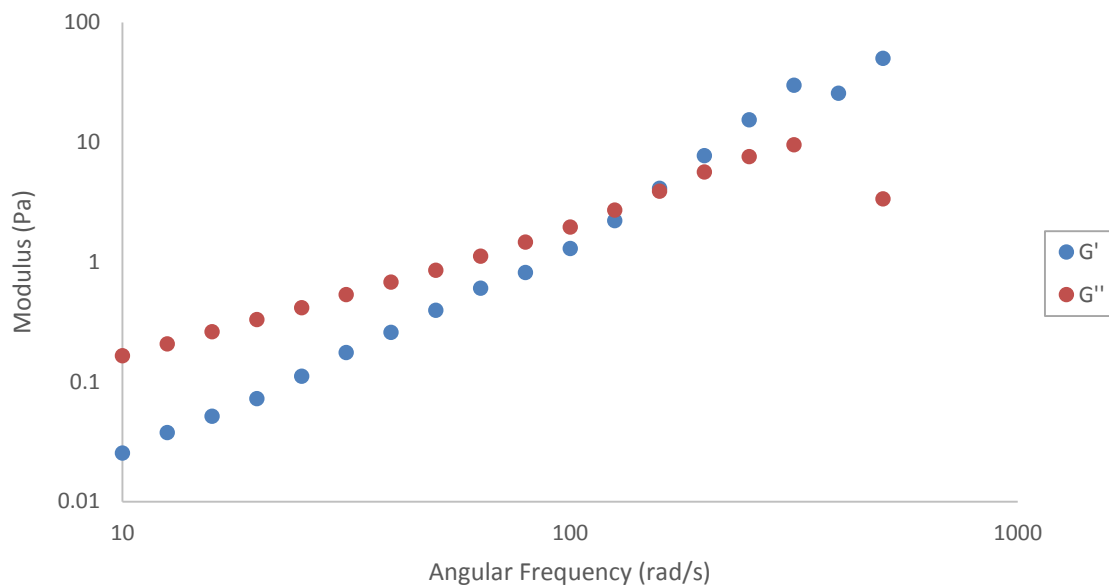
Figure 50: Angular frequency dependence of Modulus for 10 wt% PS350K in 34DMA
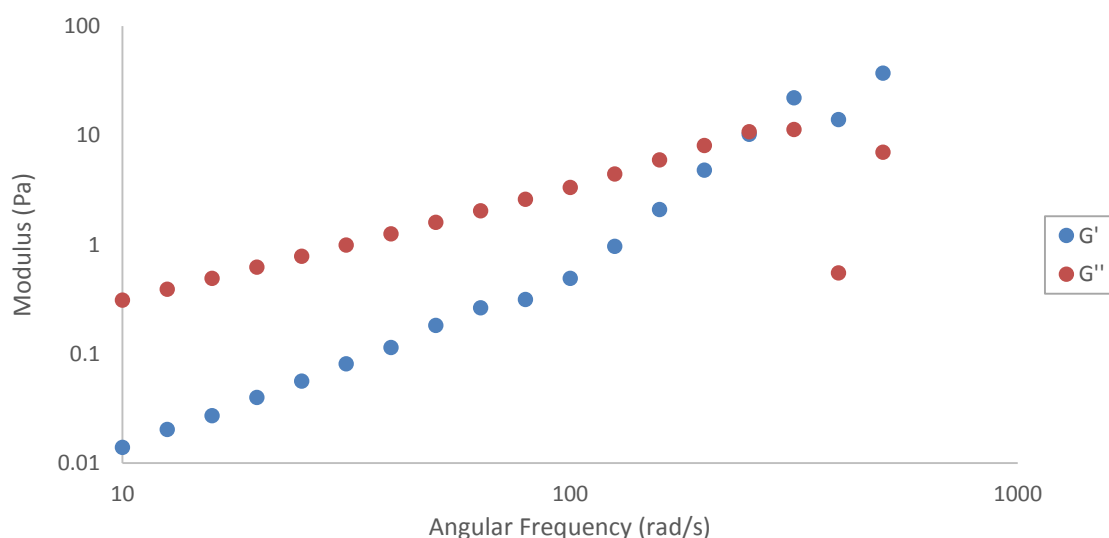
Figure 51: Angular frequency dependence of Modulus for 5 wt% PIB500K in tetralin

A crossover modulus of 3.6 Pa equated to an entanglement molecular weight of 64,500,000 g/mol for 10 wt% PS350k. A crossover modulus of 10.86 Pa resulted in an entanglement molecular weight of 18,500,000 g/mol for 5 wt% PIB500k. Neither value suggested that the solutions contained entangled polymers. Partly as a consequence of this the values are at the limit for which the instrument is reliable, therefore this work was not progressed. The models will also be more reliable when used with higher concentration polymers and polymer melts since there will be a much higher degree of entanglement.

ii. The Impact Of Polydispersity On Coating Quality

The slot die coating of highly polydisperse polymers i.e. >10 polydispersity index is not well documented, however many polymers used in OLED applications are highly polydisperse. One example is a polymer synthesised by Merck Chemicals PDY-132 which emits an orange colour once fabricated into a device and has a polydispersity index of 12.1. It is often used because it costs a third less per gram than the higher purity light emitting polymers, thus reducing the cost to produce devices making them more industrially viable.

The negative aspect of this polymer is once it's been formulated into an ink and slot die coated the resultant dry coatings appear mottled and uneven, Figure 52.
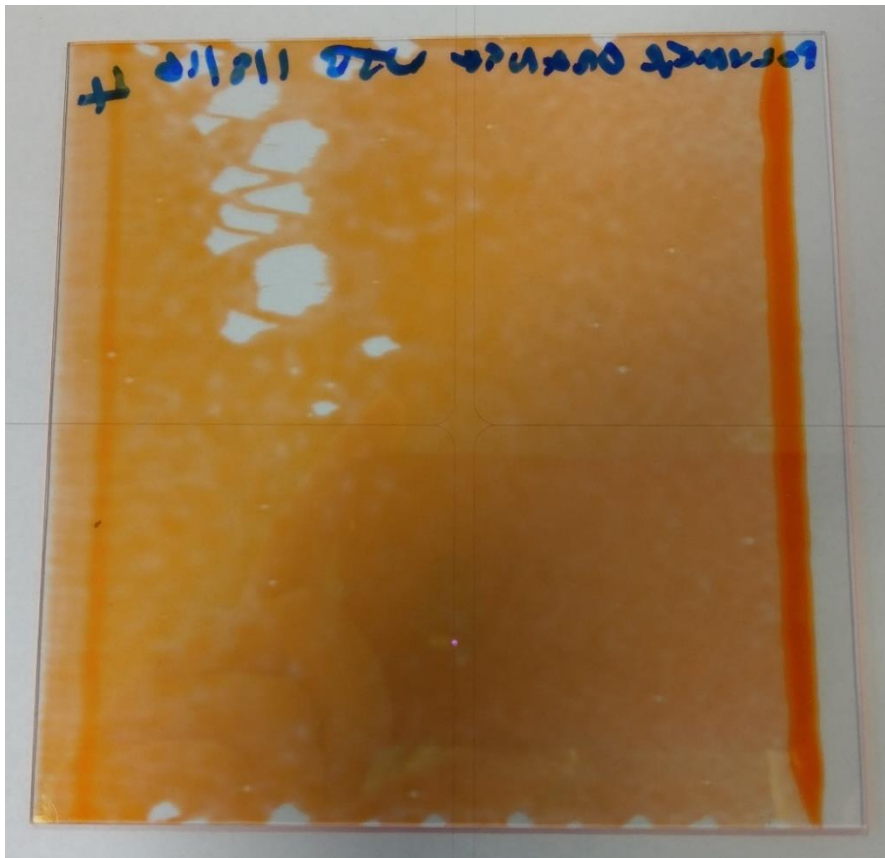
Figure 52: Example of 'mottled' coating effect

Breaking up the polymer chains using a sonic probe has proven to reduce the degree of waviness appearing in PY-132 coatings. Therefore a potential explaination for this phenomenon is that the high level of polydispersity causes instability in the wet coating producing the observed wavy pattern.

A model system was created using polyethylene oxide in water since this system was well understood. A wide range of molecular weights were available from Sigma Aldrich; $100,000 - 8,000,000$ g/mol. The 100K and 8000K grades were chosen due to the order of magnitude difference in molecular weight. The only chemical information that had been obtained by Sigma Aldrich was the viscosity average molecular weight so there was no indication of the polydispersity of these materials, however due to the large difference in molecular weight it was reasoned that any difference in polydispersity would be negligible; a polydispersity index of 1 was assumed.

Effective weight average molecular weight and number average molecular weight were calculated for model systems using the following equations.

$$PDI = \frac{Mw}{Mn}$$

Equation 18: Polydispersity index

$$N_i = \frac{M_i}{M}$$

Equation 17: Number fraction

$$Mn_c = \frac{N_L Mw_L + N_H Mw_H}{N_L + N_H}$$

Equation 20: Calculated number average molecular weight

$$Mw_c = \frac{N_L Mw_L{}^2 + N_H Mw_H{}^2}{N_L Mw_L + N_H Mw_H}$$

Equation 19: Calculated weight average molecular weight

where:

- $PDI = Polydispersity\ index$
- $M = Mass$
- $N = Number\ Fraction$
- $Mn_c = Calculated\ number\ average\ molecular\ weight$
- $Mw_c = Calculated\ weight\ average\ molecular\ weight$
- $N_L = Number\ fraction\ of\ low\ molecular\ weight\ polymer$
- $N_H = Number\ fraction\ of\ high\ molecular\ weight\ polymer$
- $Mw_L = Weight\ average\ molecular\ weight\ of\ low\ molecular\ weight\ polymer$
- $Mw_H = Weight\ averge\ molecular\ weight\ of\ high\ molecular\ weight\ polymer$

Mixtures of a range of polydispersities were calculated with the aim of finding the critical point at which the polydispersity would cause mottling of the film. They are shown in Table 19, mixture 2 was most similar to PDY-132.

Mixture Number	Mass ratio of PEO100K	Mass ratio of PEO8000K	Mn	Mw (g/mol)	PDI
Mix 1	0.75	0.25	132,780	2,075,000	15.63
Mix 2	0.83	0.17	120,174	1,443,000	12.01
Mix 3	0.92	0.08	108,578	732,000	6.74
Mix 4	0.98	0.02	102,015	258,000	2.53

Table 19: Description of polydisperse mixtures

Due to the large variation of molecular weights different concentrations of each mixture would be used; using the same concentration would result in a large range of viscosities which could potentially be outside of the slot die coaters coating capability.

Initial loadings were estimated for each mixture based on previous experience with higher molecular weight polymers. From there, mixtures were diluted to a half and a quarter of the concentration.

Mixture number	Wt% loading of PEO (1L)	Wt% ½ loading (1/2L)	Wt% ¼ loading (1/4L)
Mix 1	2	1	0.5
Mix 2	2.5	1.25	0.625
Mix 3	5	2.5	1.25
Mix 4	10	5	2.5

Table 20: Initial loadings of polydisperse polymer mixtures

Each iteration was tested rheologically and a mean value was taken for shear rates $10 - 1585 \ s^{-1}$ allowing for simpler comparison of results. This was plotted on a scatter graph with a fitted trendline and a loading that would result in a mean viscosity of approximately 30 mPa.s was estimated, Figure **53**. One measurement was taken for each iteration as this would save time; data was to be used as an approximation and the exact viscosity was unimportant for this study.
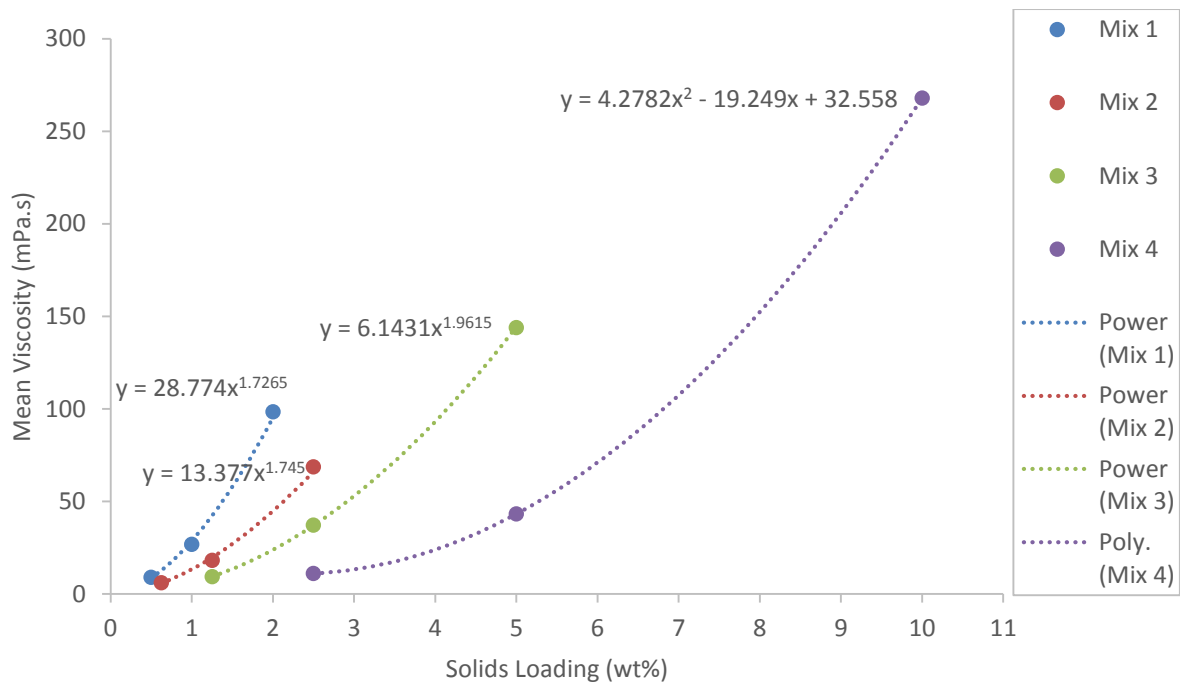
Figure 53: Concentration dependence of viscosity for polydisperse mixtures in 0.01 wt% Triton X-100 and water

Mixture Number	Equation	Proposed Solids Loading (wt%)	Calculated Mean Viscosity (mPa.s)	Measured Mean Viscosity (mPa.s)
1	$y = 28.774x^{1.7265}$	1.1	33.92	23.95
2	$y = 13.377x^{1.745}$	1.6	30.38	25.52
3	$y = 6.1431x^{1.9615}$	2.3	31.47	20.40
4	$y = 4.2782x^2 - 19.249x + 32.558$	4.5	32.57	23.48

Table 21: Calculated PEO solids loadings for polydisperse mixtures

The measured viscosities varied from the calculated values slightly but were well within the slot die coater's viscosity capability. Viscosity variation between mixtures would not affect the study as the coating thickness and uniformity were not being analysed, only the surface quality of the coating was under scrutiny.
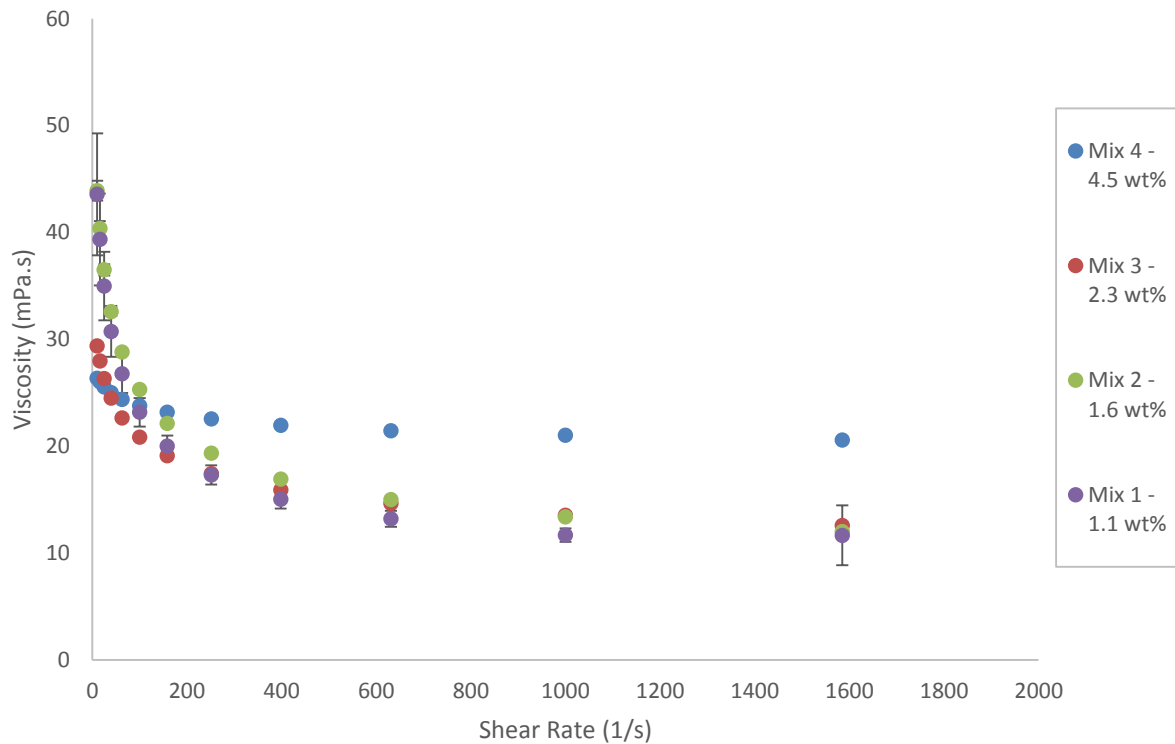
Figure 54: Shear rate dependence of viscosity for polydisperse mixtures in 0.01 wt% Triton X-100 and water

Mix 1 exhibited the greatest degree of measurement variation, this mixture was the most polydisperse suggesting there was some inherent instability.

In addition to the polydisperse mixtures, two 'monodisperse' systems were coated, Figure 55:

- 5 wt% PEO100K – for comparison to a smooth coated surface
- 0.3 wt% PEO8000K – to check whether the mottled effect was being caused by high molecular weight rather than polydispersity.
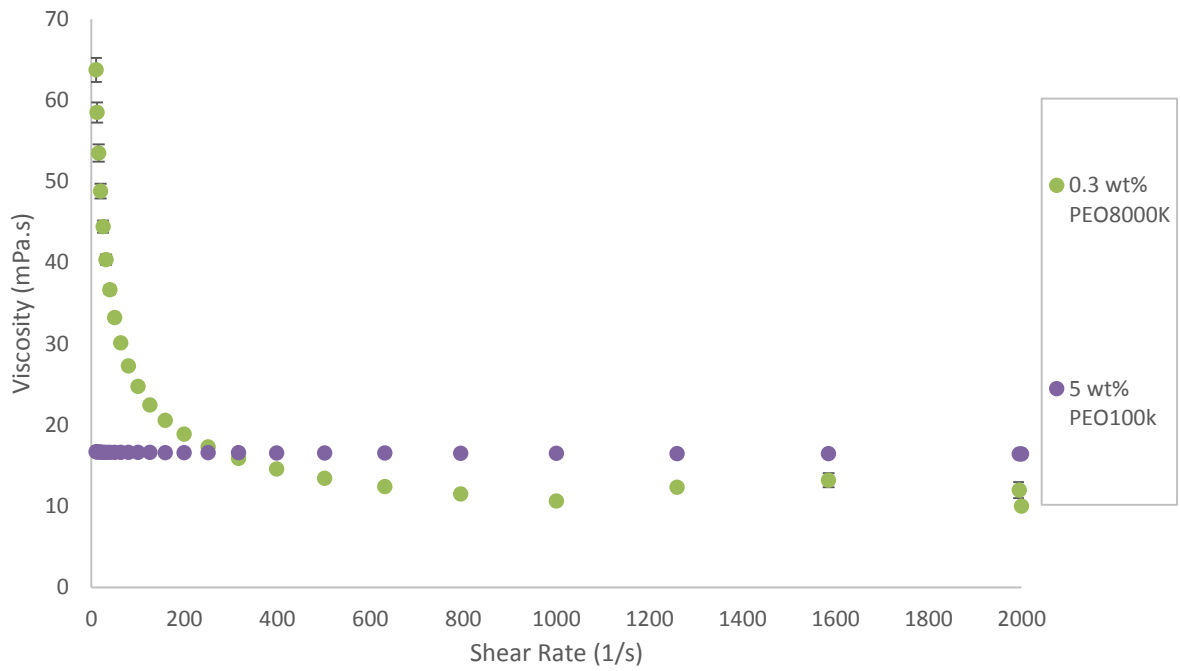
Figure 55: Shear rate dependence of viscosity for 'monodisperse' mixtures

Triton X-100 surfactant was added to the mixtures at a 0.01 wt% loading as this had previously resulted in good wetting onto plasma treated aluminium substrates. It was not possible to find a suitable analysis method; the 1.8 mm viewing window was too small to pick up the wavy patterns, and the subtle colour changes could not be picked up with optical microscopy. Therefore observations were made by eye. Formulations were coated with a process that had exhibited uniform films previously in this project, Table 22.

Shim thickness (µm)	100	Material bead flow infuse (µL/min)	500
Plasma treatment (Y/N)	Y	Coating start delay (ms)	5,000
Slot die selection	1	Pump start offset (ms)	0
Substrate type (inches)	4	Coating material pump start offset (mm)	0
Coating width (mm)	100	Slot die take-off mode	0
Number of substrate measure points	2	Coating material pump stop offset (mm)	10
Coating border (mm)	1	Take-off offset (mm)	0
Coating film thickness (µm)	15	Material bead volume withdraw (µL)	1,000
Coating priming gap (µm)	100	Material bead flow withdraw (µL/min)	150,000
Coating gap (µm)	100	Standby gap (µm)	70
Coating velocity (mm/s)	10	Standby bead volume (µL)	1,200
Coating acceleration (mm²/s)	8	Standby bead flow (µL/min)	100,000
Material bead volume infuse (µL)	20	Standby material flow (µL/min)	100

Table 22: Slot die coater process parameters for polydisperse formulations

The wavy surface quality observed when coating PDY-132 was not observed with the PEO formulations. Usually the wavy pattern can be observed when the coating is still wet and remains in the coating when dry. Although the crystallinity of the PEO coatings made it difficult to observe the pattern once the substrates were dry, it was not seen when the coatings were wet. It was possible that the surfactant was mitigating this issue so the trial was carried out again without adding surfactant to the formulations. Again the wavy surface quality was not observed. This suggested that polydispersity was not the main cause of mottled slot die coatings. It may be that it is a contributing factor but there must be another influencing factor.

The next section describes the method developed to attain detailed thickness data of substrates in the most efficient manner.

d. Analysis Method Development

i. Data Extraction Using Excel 2010

There are no in situ analysis tools on the LACE slot die coater and modifying the system would be a complicated and costly task which could interfere with other CPI work, therefore it was not possible to analyse what was happening to the fluid in real-time. In order to better understand how the material was behaving during coating detailed thickness measurements had to be obtained.

A 361 point scan of a 4 inch substrate took 20 minutes and 25 substrates were generally coated in a day; analysis of each individually would be an inefficient use of time. The Filmetrics tool will not account for multiple substrate analysis at one time, however the large bed allowed for 25 substrates to be placed on at once in a 5 x 5 formation. This led to the development of an excel macro to sort the data from what appeared to be a single 20" x 20" substrate into 25 4" x 4" substrates, allowing for analysis to be carried out overnight.

The software works in mm so inches were converted to mm: 5 x 4" = 5 x 101.6 mm = 508 mm

When creating an analysis design, the software will allow for a number of spots to be radiated from the centre to the outer edge. For example, 4 spots from the centre to outer edge would result in 9 spots in a single line across the plate, 81 spots on the plate in total. Therefore it would only allow for an odd number of analysis points skewing the data on each plate as there should be an even number of points in total in order to distribute them evenly across 5 plates.

The aim was to create a method that would produce thickness measurements at 400 points per plate; 10,000 points in total. The closest method that could be achieved with the software was 51 spots from centre to outer edge, which resulted in 10,201 points across the 25 substrates.

To account for the odd number of results the size of the substrate in the software would have to account for one extra line in the x and y axes, Figure 56. For 10,201 points there would be 101 x 101 points; 1 point in each axis would be discounted therefore 100 points would be within 508 mm. Each point would be 5.08 mm apart from each other so the substrate size would have to be increased by 5.08 mm to account for the additional point.
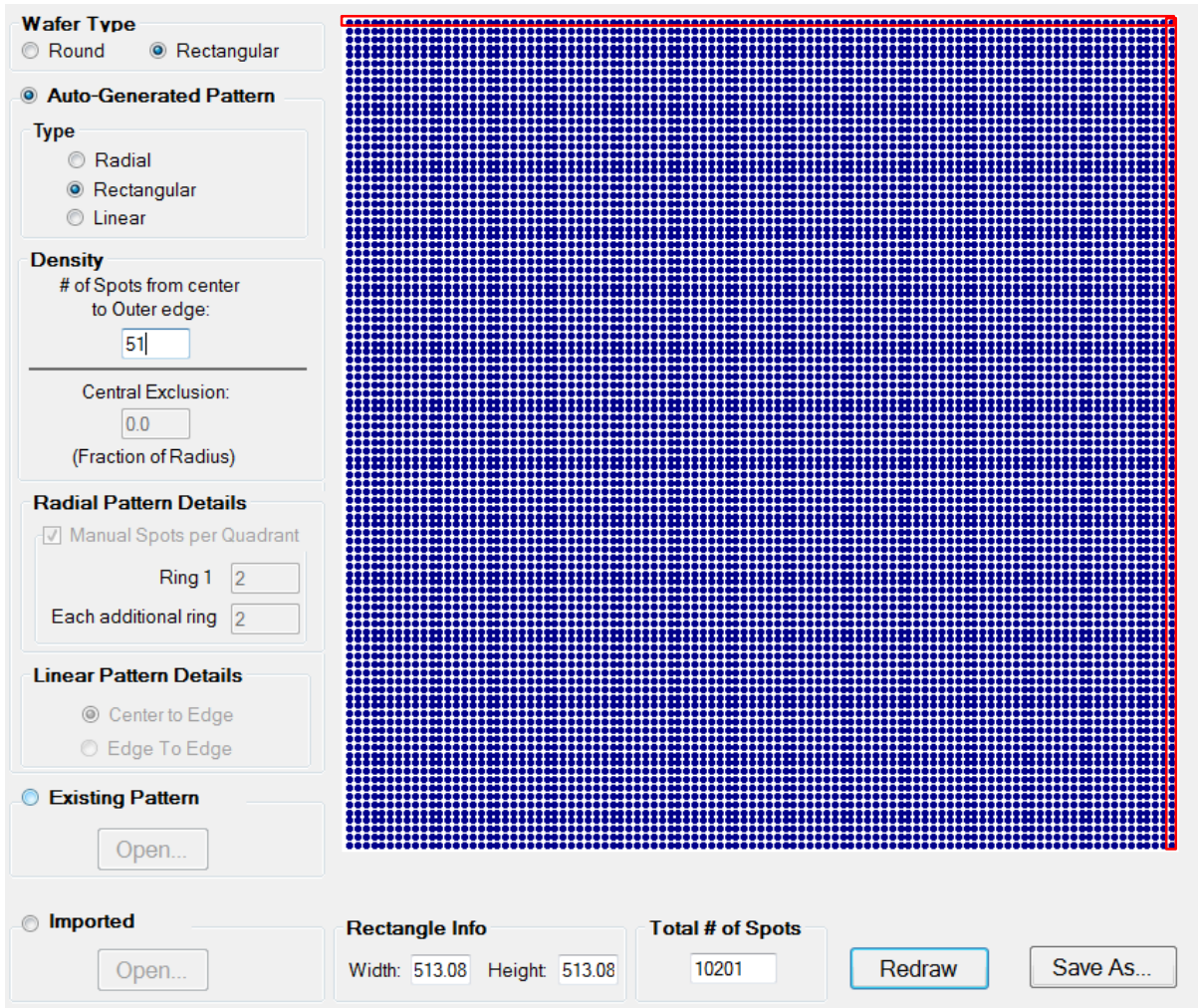
Figure 56: Design of mapping pattern on Filmetrics software

The total size of the analysis area was 513.08 mm x 513.08 mm, when an edge exclusion of 2.54 mm was applied across the whole area the area measured was 508 mm x 508 mm. The gap between each measurement point of 5.08 accounted for a 2.54 edge exclusion on each plate, Figure 57.
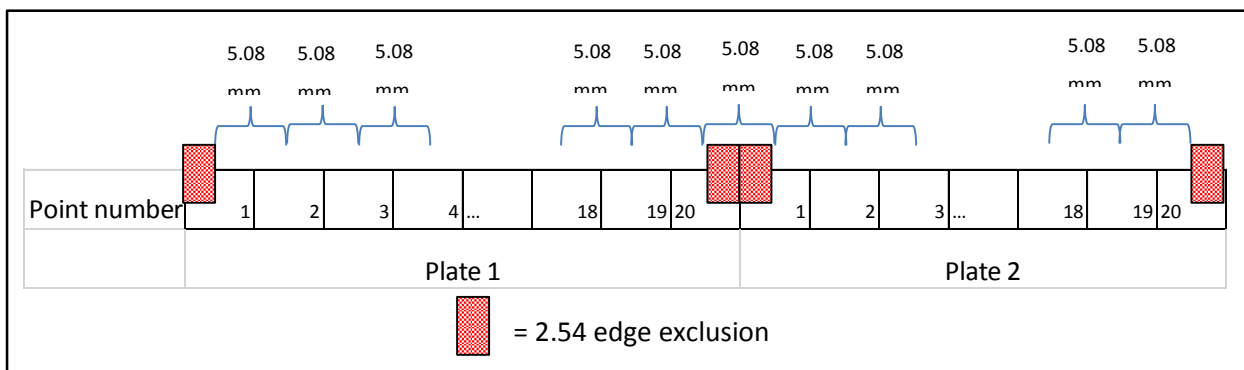
Figure 57: Explanation of edge exclusion

Data was exported as a list of thickness values linked to coordinates that could be separated by a comma i.e. comma separated value file (.csv), Figure 58.

	A	B	C	D	E	F
18	# Measured Die	10201				
19	Edge Exclusion (mm	2.54				
20	Site 1 Layer 1 Thickn	site x (mm)	site y (mm)	Site 1 Layer 1 Thickness Alarm	site x (mm)	site y
21	120	0	0	124	0	
22	Die x (mm)	Die y (mm)	Site 1 Layer 1 Thickness (nm)	Site 1 Layer 1 Thickness Alarm	Site 1 GOF	
23	-254	-254	-1	-1	0.2520651	
24	-248.92	-254	199.4068	0	0.5030585	
25	-243.84	-254	122.8817	0	0.7513154	
26	-238.76	-254	-1	-1	0	
27	-233.68	-254	100.0421	0	0.8531031	
28	-228.6	-254	297.2034	0	0.6809684	
29	-223.52	-254	307.1989	0	0.7059698	
30	-218.44	-254	305.3654	0	0.7317781	
31	-213.36	-254	305.2399	0	0.6620855	
32	-208.28	-254	298.4366	0	0.6981804	

Figure 58: Example output Filmetrics mapping data

A macro was recorded to copy and paste each row to create a spreadsheet pictorial representation of data, the code is shown and explained below.

```
Sheets("Data Import").Select
```

The sheet containing the data to sort is selected.

```
Range("C23:C123").Select
```

The range to be copied is selected, this is one full row of data.

```
Selection.Copy
```

The selected range is copied.

```
Sheets("5x5").Select
```

The sheet that the raw data is being moved to for sorting is selected.

```
Range("B102").Select
```

The first cell in the row where that data will be copied to is selected.

```
Selection.PasteSpecial Paste:=xlPasteAll, Operation:=xlNone, SkipBlanks:= _
    False, Transpose:=True
```

Raw data is recorded in columns where thickness values are associated with x coordinate values, this has to be transposed and pasted into a row to reflect the location of the values as seen in reality.

This was repeated 101 times until all data had been reformatted, Figure 59.
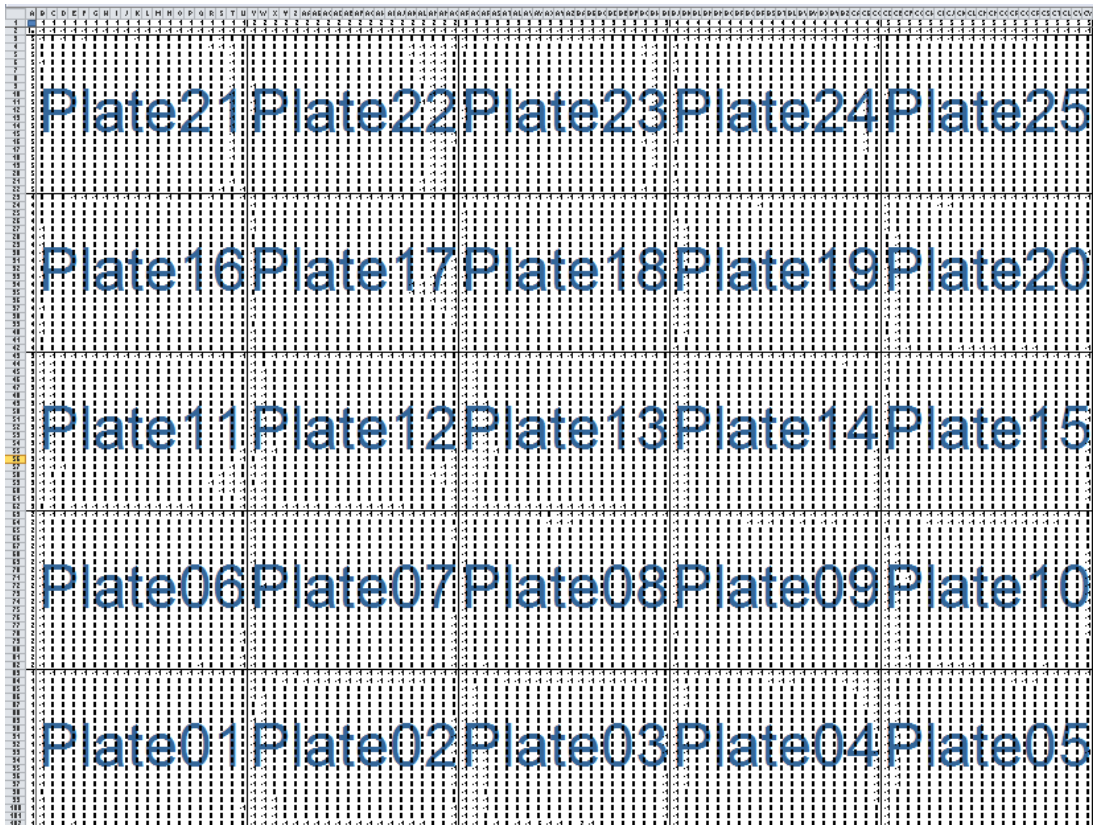
Figure 59: Five by five substrate layout

On a separate sheet, the data is reformatted again to separate each plate, removing the "-1" values by incorporating the appropriate cell into an IF statement. This will be further explained in the next section. For example:

$$\text{Cell value} = IF('5x5'!AH65 < 0, "", '5x5'!AH65)$$

Equation 21: Data reformatting to individual substrate plot

Sheet reference

Cell reference

The data was subjected to conditional formatting whereby a 2-colour scale was employed:

- Lowest value – 1 – light blue
- Highest value – 800 – dark blue

Stop / Start

	97.5	92.5	87.5	82.5	77.5	72.5	67.5	62.5	57.5	52.5	47.5	42.5	37.5	32.5	27.5	22.5	17.5	12.5	7.5	2.5	
2.5		300.7	221.73	218.22	230.28	193.23	204.43	165	159.43	156.78	134.03	159.63	155.6259	129.41	141.28	141.4	131.6	141.49	136.8	128.61	2.5
7.5		193.39	250.41	217.41	214.95	211.11	205.75	200.79	187.36	176.7	153.84	158.79	154.6607	144.92	134.07	130.02	128.81	125.74	130.29	129.72	7.5
12.5			282.34	211.79	205.58	202.32	193.81	187.22	172.02	164.14	153.55	155.36	151.2981	145.11	137.45	132	128.69	125.39	125.61	152.21	12.5
17.5			306.51	216.3	209.53	207.21	202.59	194.95	184.74	170.09	161.72	159.59	154.3802	147.01	139.98	135.51	130.27	126.34	129.37	214.39	17.5
22.5			305.72	221.58	212.19	209.86	208.21	202.3	193.22	178.84	168.58	163.78	157.586	144.5	142.55	138.63	133.18	128.38	131.66	187.27	22.5
27.5			317.1	228.16	210.83	212.11	206.84	206.36	201.43	186.41	174.41	166.72	160.2403	152.07	143.83	140.41	134.53	129.71	127.33	133.27	27.5
32.5	135.991		317.41	227.06	211.07	211.78	201.39	206.56	188.17	186.72	176.2	169.89	162.4785	150.85	148.61	136.18	139.4	132.38	139.2	134.75	32.5
37.5	134.441		325.44	222.95	212.8	210.74	209.92	203.82	196.97	183.46	173.64	167.04	161.9781	153.59	146.82	142.64	138.25	132.33	132.19	148.67	37.5
42.5	134.039		306.57	206.59	194.84	190.45	182.47	174.74	165.88	158.83	153.09	148.08	144.5735	139.79	133.57	133.39	129.77	127.23	123.37	142.85	42.5
47.5	123.415		288.58	176.97	155.64	156.96	154.27	151.06	144.85	140.25	138.22	137.07	134.5153	132.03	129.24	128.21	125.94	121.19	120.29	127.82	47.5
52.5	204.263		151.58	211.77	154.53	152.76	153.33	151.62	140.87	134.26	130.93	129.26	127.5346	125.53	123.27	123.41	123.01	118.72	109.16	118.04	52.5
57.5	492.005		676.19	224.74	157.21	152.98	154.4	145.22	127.65	137.91	132.19	129.57	127.1623	125.87	124.04	119.05	118.36	113.24	117.16	221.28	57.5
62.5	167.496		209.09	234	177.65	166.54	155.6	159.7	152.62	148.45	141.07	137.09	133.8303	129.94	127.9	125.34	121.86	116.14	122.38	287.61	62.5
67.5	119.211		264.25	189.29	160.24	157.29	157.82	155.13	148.23	139.73	135.48	132.13	128.7853	127.69	125.2	123.59	119.46	116.08	123.29	287.34	67.5
72.5	102.046		248.29	164.43	152.85	147.87	145.75	142.42	139.85	135.05	132.61	129.83	127.5019	125.2	123	119.7	114.79	111.19	118.47	220.88	72.5
77.5	446.26		206.5	157.56	147.51	142.86	139.66	138.75	138.05	135.25	131.99	131.39	127.0227	125.05	122.62	119.25	115.25	111.78	115.21	212.02	77.5
82.5	304.61		181.71	143.23	125.08	137.99	134.51	134.49	134.71	132.98	131.01	128.68	126.4914	124.78	121.01	120.19	116.61	114.96	114.27	301.65	82.5
87.5	134.24		164.22	146.05	137.06	134.65	130.46	131.7	131.73	130.3	128.33	126.82	125.4866	122.2	118.03	113.59	123.97	108.3	121.84	120.89	87.5
92.5	335.95		170.45	149.4	144.59	137.19	133.63	133.54	133.25	132.5	130.59	128.58	125.9483	122.06	117.31	113.09	109.49	109.04	125.41	303.33	92.5
97.5	131.02		145.19	151.25	153.2	143.82	145.59	139.24	134.46	134.13	131.85	129.73	128.1314	125.52	121.41	125.79	123.89	122.1	110.07	204.84	97.5
	97.5	92.5	87.5	82.5	77.5	72.5	67.5	62.5	57.5	52.5	47.5	42.5	37.5	32.5	27.5	22.5	17.5	12.5	7.5	2.5	

Figure 60: Example sorted and formatted FIlmetrics data

A cross-sectional view of the coatings in the direction of coating was created by taking a mean of each column and plotting it on a scatter graph.
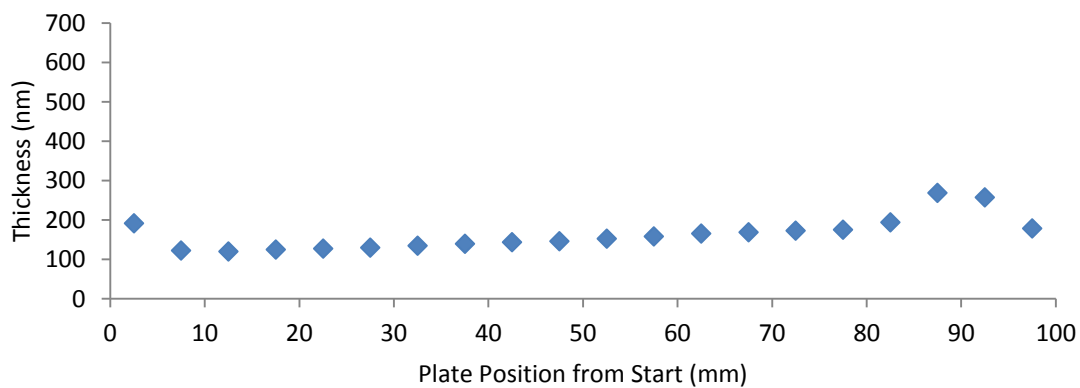
Figure 61: Example cross-section thickness data

ii. Data Manipulation of Measured Data

Once data was efficiently being imported into Excel more detailed data manipulation could be carried out. This section will describe a number of equations that were used to calculate some of the important properties that were described in section 1.c.

A smaller number of data points were used to demonstrate the effect of these equations on measured values. An edge exclusion of 1 mm had been applied to this data and 49 points were measured across the substrate.

Stop							Start	
	99	83	66	50	34	17	1	
1	382.54	677.74	773.15	566.47	758.31	-1	790.42	1
17	-1	785.27	791.98	808.72	859.71	866.64	660.47	17
34	-1	795.28	792.89	814.81	874.96	867.38	497.6	34
50	-1	787.27	797.51	799.43	860.44	843.65	661.99	50
66	-1	816.88	803.36	808.34	861.88	838.24	663.5	66
83	-1	839.56	811.15	809.4	879.82	840.78	652.42	83
99	-1	829.67	810.04	804.61	815.07	653.49	606.69	99
	99	83	66	50	34	17	1	

Figure 62: Example dry coat thickness (nm) i.e. measured data

From the dry coat thickness data, a number of parameters were calculated for the thickness stated at each measured point (coloured values); units were taken into consideration. The numbers around the edge of the data signified the distance from the edge of the coating. The '-1' values signified a point where a thickness value could not be measured, the removal of these invalid points will be described.

Two excel functions were used in this section to filter and combine sections of data; 'IF' and 'VLOOKUP' statements.

IF function: *checks whether a condition is met and returns one value if true and another value if false.*
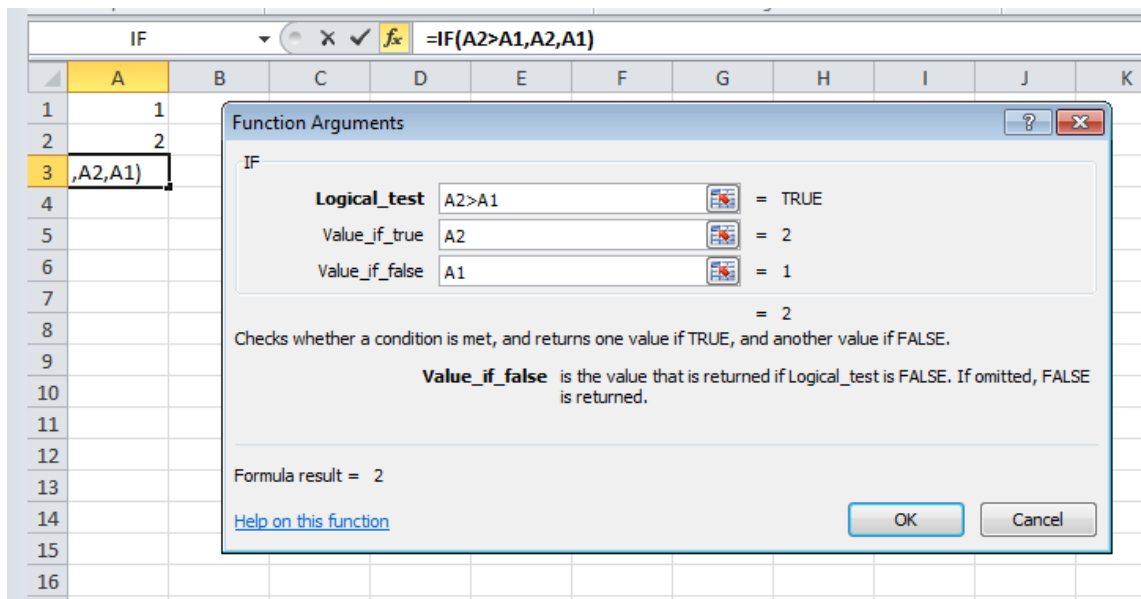
Figure 63: Example of a use of the 'IF' function in Excel 2010

VLOOKUP function: *Looks for a value in the leftmost column of a table and then returns a value in the same row from a specified column.*
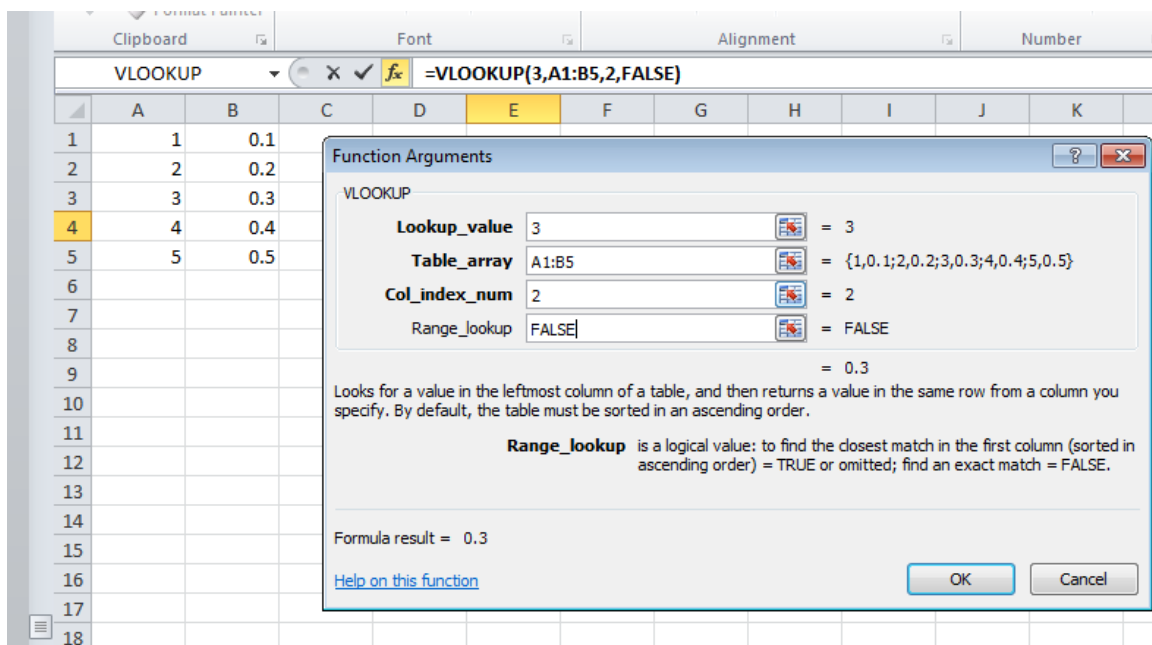
Figure 64: Example of a use of the 'VLOOKUP' function in Excel 2010

First the theoretical wet coat thickness was calculated using the volume weight percent:

$$H_w = \frac{H_d}{v\%} \times 100$$

Equation 22: Calculation of the theoretical wet coat thickness

where:

- $H_d = Dry\ coat\ thickness$

- $H_w = Wet\ coat\ thickness$

- $v\% = Volume\ percent\ of\ solids$

The density of PEO37K was not available from Sigma Aldrich but it was found to be 1.2 g/cm3 at two sources.[55] [56] This value was used to calculate the volume percent loading of the 5 wt% PEO37K formulation.

Stop						Start	
	99	83	66	50	34	17	1	
1	9.1809	16.266	18.556	13.595	18.199	-0.024	18.97	1
17	-0.024	18.846	19.007	19.409	20.633	20.799	15.851	17
34	-0.024	19.087	19.029	19.555	20.999	20.817	11.942	34
50	-0.024	18.895	19.14	19.186	20.651	20.248	15.888	50
66	-0.024	19.605	19.281	19.4	20.685	20.118	15.924	66
83	-0.024	20.15	19.468	19.426	21.116	20.179	15.658	83
99	-0.024	19.912	19.441	19.311	19.562	15.684	14.561	99
	99	83	66	50	34	17	1	

Figure 65: Theoretical wet coat thickness (um) calculated for example data

An 'IF' statement was used to remove invalid points on measured data:

$$H_w = IF\left[(\frac{H_d}{v\%} \times 100) < 0, "\ ", (\frac{H_d}{v\%} \times 100)\right]$$

Equation 23: Modification of theoretical wet coat thickness calculation to account for invalid readings

i.e. if the calculated value is less than zero the cell will be left blank, if the calculated value is not less than zero then the calculated value will be input to the cell, Figure 66.

	Stop						Start	
	99	83	66	50	34	17	1	
1	9.1809	16.266	18.556	13.595	18.199		18.97	1
17		18.846	19.007	19.409	20.633	20.799	15.851	17
34		19.087	19.029	19.555	20.999	20.817	11.942	34
50		18.895	19.14	19.186	20.651	20.248	15.888	50
66		19.605	19.281	19.4	20.685	20.118	15.924	66
83		20.15	19.468	19.426	21.116	20.179	15.658	83
99		19.912	19.441	19.311	19.562	15.684	14.561	99
	99	83	66	50	34	17	1	

Figure 66: Example theoretical wet coat thickness (um) data incorporating 'IF' function

The speed of coating was represented in the same format, accounting for acceleration using:

$$v = IF\left[\sqrt{2aS} > v, v, \sqrt{2aS}\right]$$

Equation 24: Calculation of speed with respect to acceleration

Where:

- $v = Velocity$

- $S = Distance\ from\ the\ start\ of\ the\ coating$

- $a = Acceleration$

Which denotes: if the calculated velocity is greater than the stated coating velocity, the value shown should be the coating velocity, if not then the value shown should be the calculated velocity.

Figure 67: Example data showing changing speed with acceleration

Now that the data had been formatted, Equation 6 could be used to calculate the flow rate at different points on the plate.

Figure 68: Calculated flow rate (uL/min) values for example data

Further analysis could be carried out using Equation 5 to estimate the shear rate in the head at various points across the plate.

Stop						Start
99	83	66	50	34	17	1

1	55.031	97.496	111.22	81.491	109.09		88.077	1
17		112.97	113.93	116.34	123.67	124.67	73.596	17
34		114.41	114.06	117.22	125.87	124.78	55.448	34
50		113.25	114.73	115	123.78	121.36	73.765	50
66		117.51	115.57	116.28	123.99	120.59	73.935	66
83		120.78	116.69	116.44	126.57	120.95	72.699	83
99		119.35	116.53	115.75	117.25	94.008	67.604	99

| | 99 | 83 | 66 | 50 | 34 | 17 | 1 | |

Figure 69: Shear rate (1/s) in the head calculated for example data

Using rheology data obtained earlier the viscosity at each point was deduced using the calculated shear rate:

$$\eta = VLOOKUP[IF(\dot{\gamma}_L < \dot{\gamma}_{min}, \dot{\gamma}_{min}, \dot{\gamma}_L)], TABLE_{\dot{\gamma}\eta}, 2, TRUE$$

Equation 25: Calculation to lookup viscosity values from measured data

Where:

- $\dot{\gamma}_L = Shear\ rate\ in\ lips$

- $\dot{\gamma}_{min} = Lowest\ experimental\ shear\ rate\ value$

- $TABLE_{\dot{\gamma}\eta} = Results\ table, shear\ rate\ v.s.viscosity$

- $TRUE = Find\ closest\ match$

Look up value (if shear rate in lips value is less than the lowest measured shear rate, use the lowest shear rate value, if not use shear rate in lips value) in shear rate column, return viscosity data and find the closest match.

Stop							Start	
	99	83	66	50	34	17	1	
1	5.737	5.731	5.731	5.731	5.731		5.731	1
17		5.731	5.731	5.731	5.731	5.731	5.732	17
34		5.731	5.731	5.731	5.731	5.731	5.737	34
50		5.731	5.731	5.731	5.731	5.731	5.732	50
66		5.731	5.731	5.731	5.731	5.731	5.732	66
83		5.731	5.731	5.731	5.731	5.731	5.732	83
99		5.731	5.731	5.731	5.731	5.731	5.732	99
	99	83	66	50	34	17	1	

Figure 70: Measured viscosity (mPa.s) data related to calculated shear rates for example data

The calculated information provided useful data as it showed that the changes in shear rate were not large enough to affect the viscosity suggesting this was not the cause of non-uniformity and lack of repeatability for the 5 wt% PEO37K formulation. This will be used later in this study to assess the effect of pseudoplasticity on some of the higher molecular weight formulations.

The next section describes the baselining study carried out to identify sources of error, dictating the maximum uniformity possible with this combination of materials and equipment.

e. Baselining: Locating The Source Of Error

Variation between results was being observed suggesting there was a source of error at some stage in the process. A number of avenues were explored.

i. Formulation Preparation

Formulations were prepared in a non-cleanroom environment so there was potential for particulates to be introduced into the mixture. However all formulations were centrifuged to remove any contaminants making this issue a lower risk. Ideally all formulations would be filtered using a syringe filter prior to each run but this was not feasible due to the higher viscosity materials.

The possibility of instability within the formulation was unlikely as all mixtures had been rheologically tested. No phase separation was observed when subjected to high shear and standard deviation was low.

As a final check, 5 wt% PEO37K was spin coated at 1000 rpm for 1 minute and dried at 100°C. This was carried out on three oxygen plasma treated aluminium substrates.
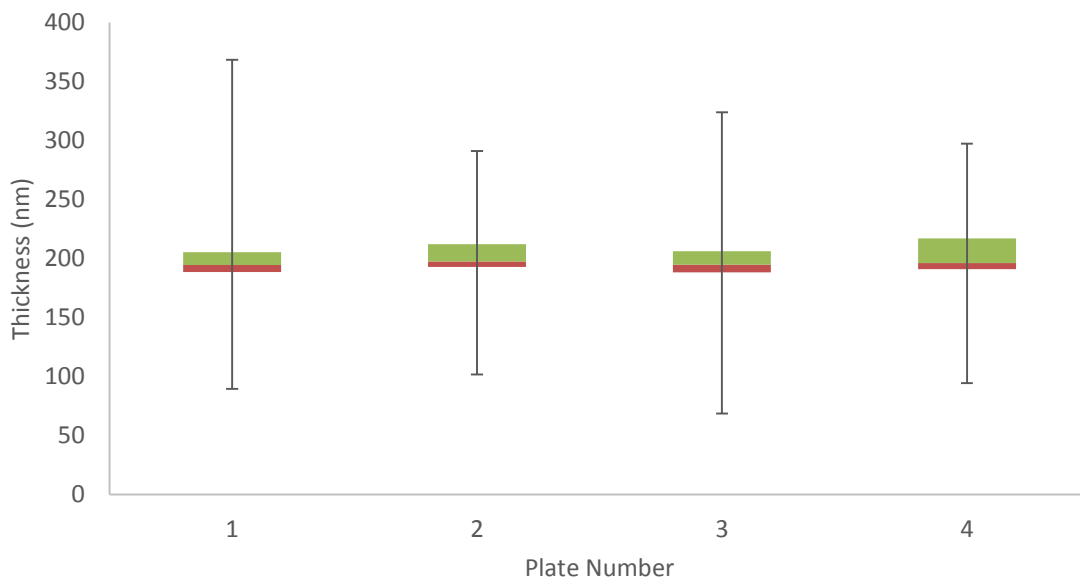
Figure 71: Repeatability of spin coated plates

There were a number of defects on the coating as the formulations were not developed for spin coating, this resulted in variable max and min values. However the box regions of the data were uniform. This was sufficient to remove any suspicions of error being caused by the materials.

ii. Substrate Preparation

The aluminium substrate was checked for thickness and roughness repeatability.

- Thickness - 68.2 nm ± 1.5 nm
- Roughness (Sa) 0.59 nm ± 0.05 nm
- Roughness (Sq) 0.75 nm ± 0.07 nm

The thickness variation was too low to have any effect on coating uniformity. Roughness was extremely low and again would not be expected to have any effect on coating uniformity of a 600 nm coating.

The effect of the surface treatment across the substrate was checked using diiodomethane contact angles; five measurements were taken across the plate: 31.76 mN/m ± 0.85 mN/m. The variation was ± 2.8% which is within acceptable error and was potentially due to measurement error, therefore the plasma treatment was uniform across the substrate.

iii. Filmetrics Analysis Repeatability

The analysis method was checked for degree of error by analysing the same plate twice.
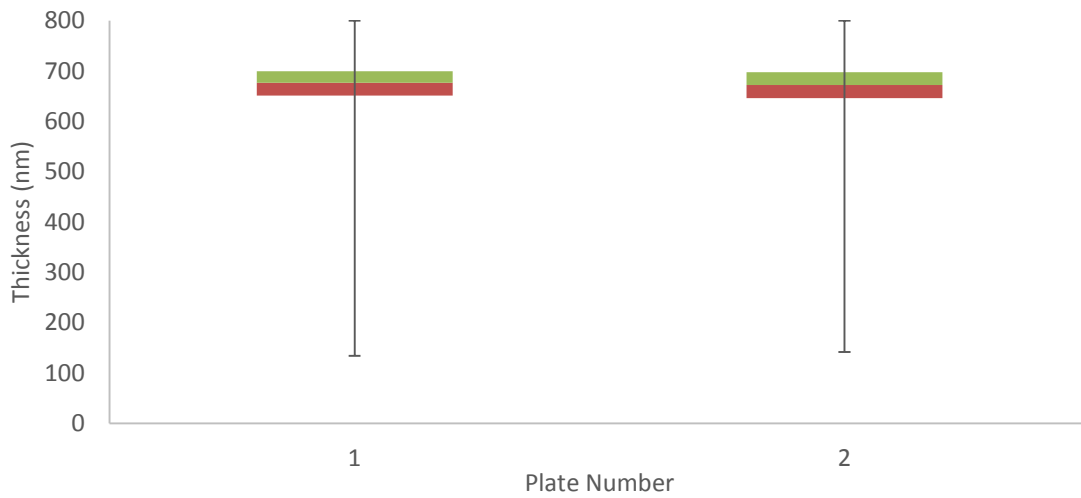
Figure 72: Repeatability of Filmetrics - 1 plate measured twice

Results were highly repeatable. The Filmetrics method was then analysed by measuring the same plate at 3 different orientations.
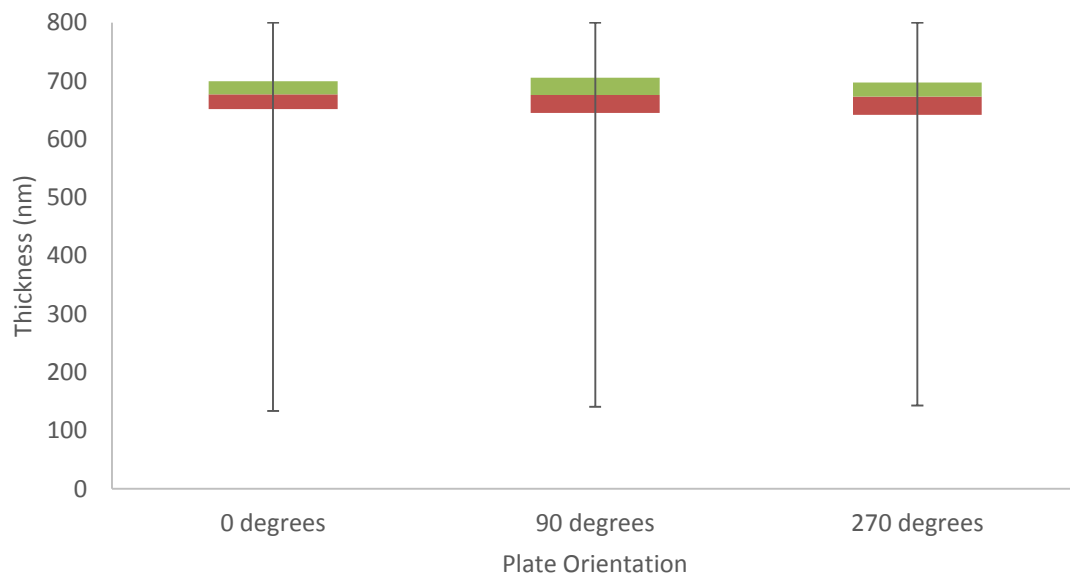
Figure 73: Repeatability of Filmetrics - 1 plate measured at three orientations

Again the results were repeatable, there was a small difference between the 0 degree plate when compared with the 90 and 270 degree orientated plates. This suggested that the orientation of the PEO crystals was having a small effect on the results but this was not enough to cause concern.

iv. Slot Die Coating Repeatability

There were a number of areas of the slot die process where error could potentially be introduced:

- Head setup
- Syringe loading
- Coating
- Substrate drying

Slot die heads are dismantled and cleaned after every use. When reassembled the setup is carried out in the same manner everytime; the shim and heads can only sit in the correct place due to the location of the screw holes therefore it is highly unlikely that the head was being setup incorrectly. The head is calibrated during every setup; inbuilt sensors on the slot die housing measure the height of the head to ensure the coating gap is consistent.

There were a two slot die heads that could be used with a number of shim thicknesses; during setup the inernal face of one of the heads became scratched. The depth of the largest scratch was measured with the CCI across a number of regions; it was 12.88 µm at it's deepest point which was significant when compared with the Sa roughness value of 28.9 nm stated in section 1.a. The affect of this on coating repeatability was analysed. The same coating process was carried out on five 8 inch plates for the damaged head and an undamaged head. Eight inch substrates were used to check the uniformity across the whole of the slot die head. Coatings were measured across 81 points, 15 mm around the edge of the coating was excluded.
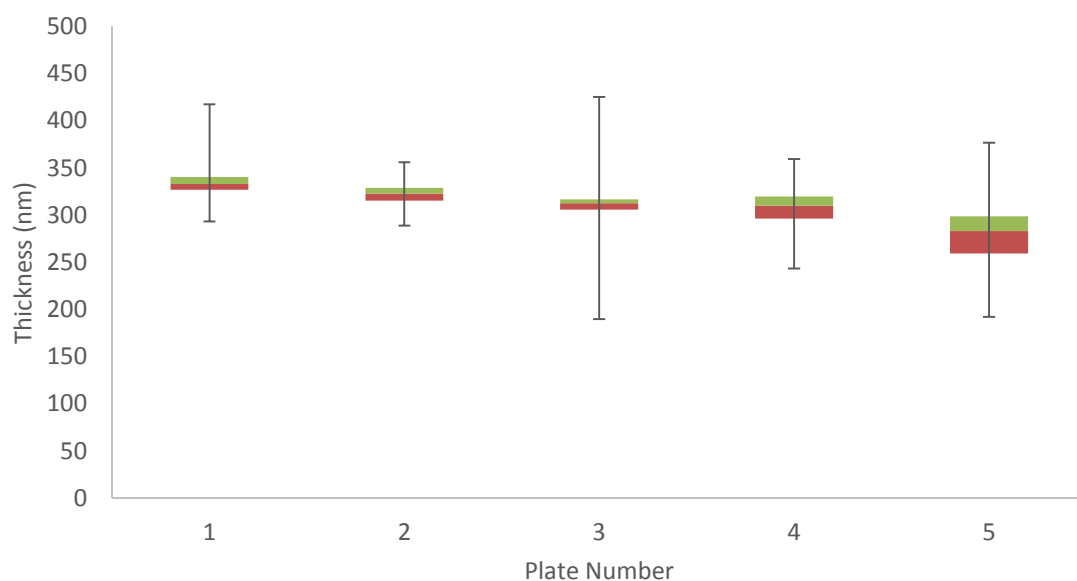
Figure 74: Box plot showing plate variation using the damaged head

The same process was carried out using the second head that had no visible scratches, setup with the same shim thickness, Figure 75.
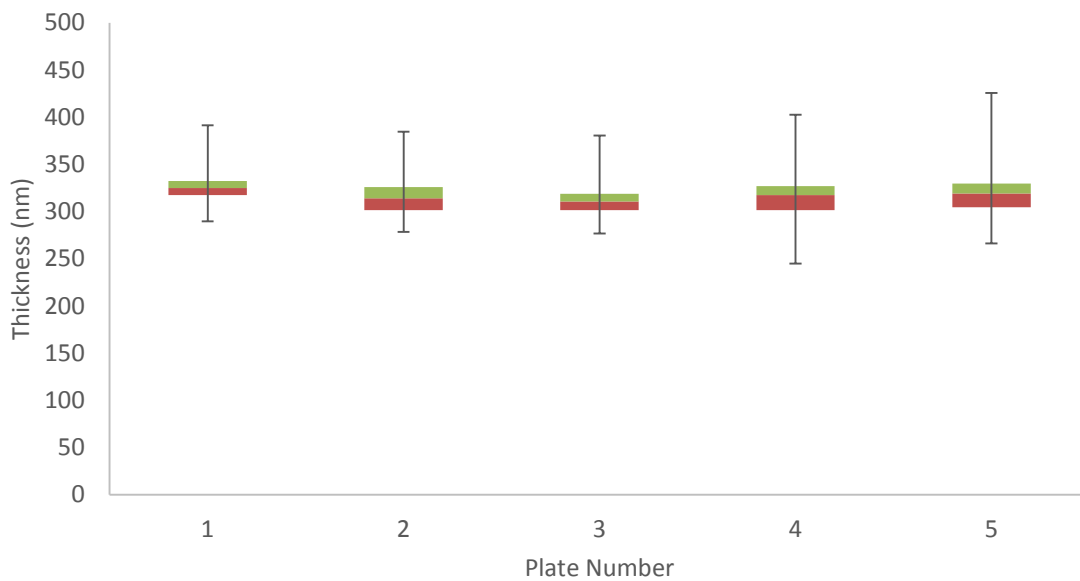
Figure 75: Box plot showing plate variation using an undamaged head

There was a noticeable improvement in repeatability when using the undamaged head for coating; the damaged head was not used for any further trials and the internal faces were regularly checked for scratches. There was still variation between plates suggesting this was not the only source of error.

The process of filling the syringe with fluid and loading it into the housing is a common source of air entrapment. All formulations were degassed and left to settle once loaded into the syringe. At the start of the syringe setup 2 mL is fed into the waste line to remove any potential trapped air. It is also easy to see when air has been trapped in the lines and this has not been observed since the degassing and loading precautions have been introduced.

Air can also be introduced at the last step of coating; the fluid withdraw into the slot die head. If the end parameters are incorrectly optimised then air may be sitting at the bottom of the slot die head. Parameters have been selected so that enough fluid remains at the end of the plate to avoid air entrainment while preventing the excess from affecting coating uniformity. In addition to this 1.2 mL is purged out of the head in the standby position to account for the 1 mL that is withdrawn from the plate, keeping the lips in good condition.

Issues can also arise if the substrate is not dried quickly enough. Due to coating being carried out manually, the substrate can be moved to a hotplate immediately. However the thin wet coat often begins to dry in air while the slot die platen is still in motion, before it can be moved to the hotplate.

This can bring about issues such as the film withdrawing from the edges of the plate and areas of the plate drying at different rates. This was overcome by increasing the wet coat thickness of coatings from 8 μm to 15 μm which did result in slower film drying.

At this stage it was becoming likely that the coating variation was inherent to the equipment and it may not be possible to overcome. Alterations were made to the analysis of the data to minimise the effects of the observed error so that overall trends could be used to carry out a design of experiments study.

The same process was ran 10 times and the results were plotted in a series of box plots.
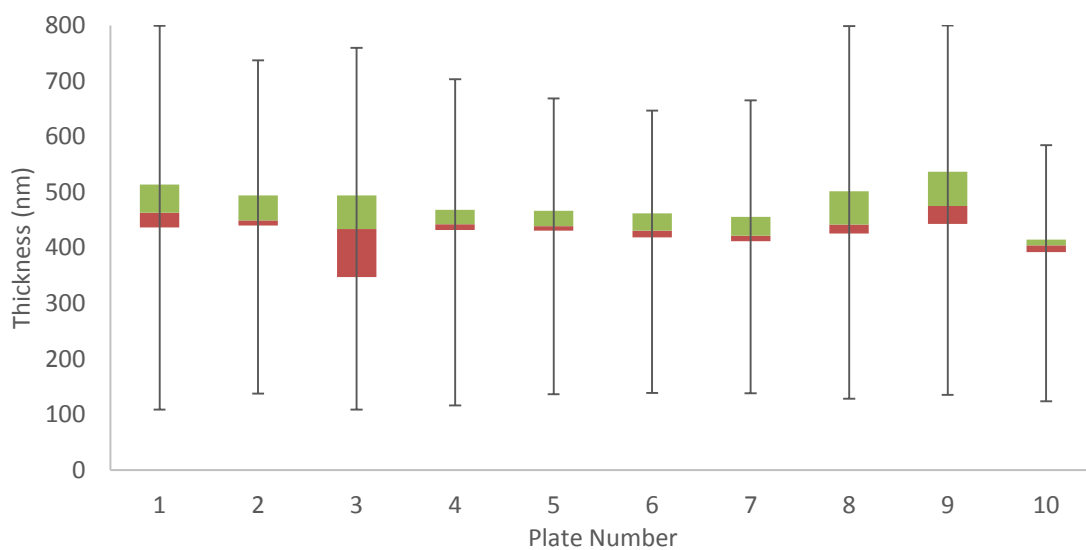
Figure 76: Box plots showing plate variability across 10 plates

	Mean Thickness (nm)
Standard Deviation of mean thickness (nm)	26.19
Uniformity of mean thickness (%)	5.89

	Standard Deviation of thickness across substrate (nm)
Min (nm)	57.26
Max (nm)	115.14
Range (nm)	57.88

Table 23: Mean and standard deviation values showing variability across 10 plates

All changes to coating parameters affect the coating thickness in the coating direction, Figure 77, any error in the head direction cannot be controlled by changes parameters. Therefore the cross-section data was used for subsequent analysis to minimise the effects of any uncontrollable errors.
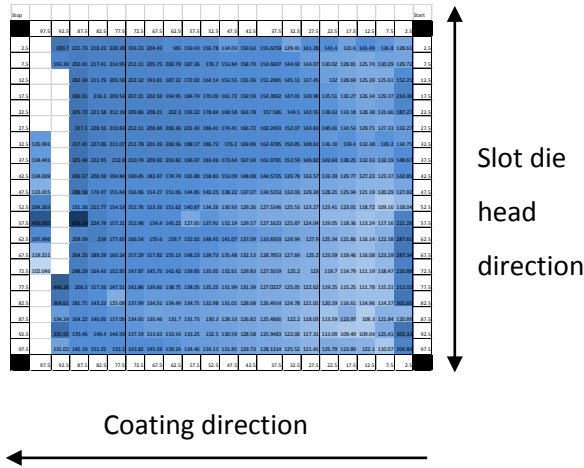
Figure 77: Explaination of coating direction and head direction on a substrate

It was also clear that the start and the stop regions created the greatest degree of variation. These regions were analysed separately to the middle section, which was also advantageous because different parameters affected different regions e.g. volume infuse was expected to affect the start region, the effects should be negligible for the stop region.
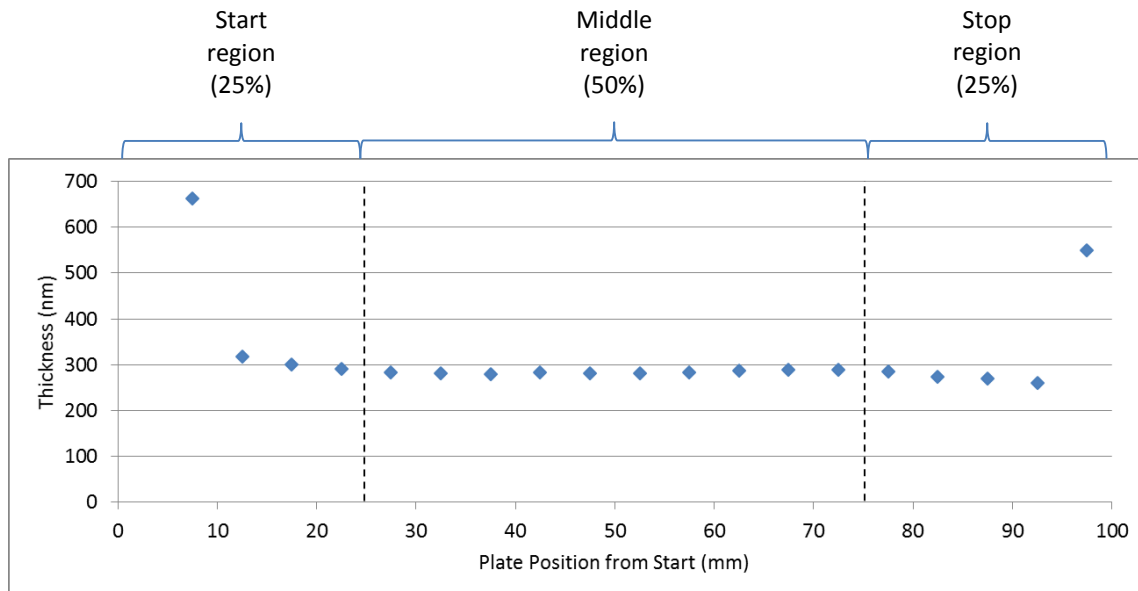
Figure 78: Explanation of start, middle and stop regions

Each region was checked individually for repeatability, Figure 79.
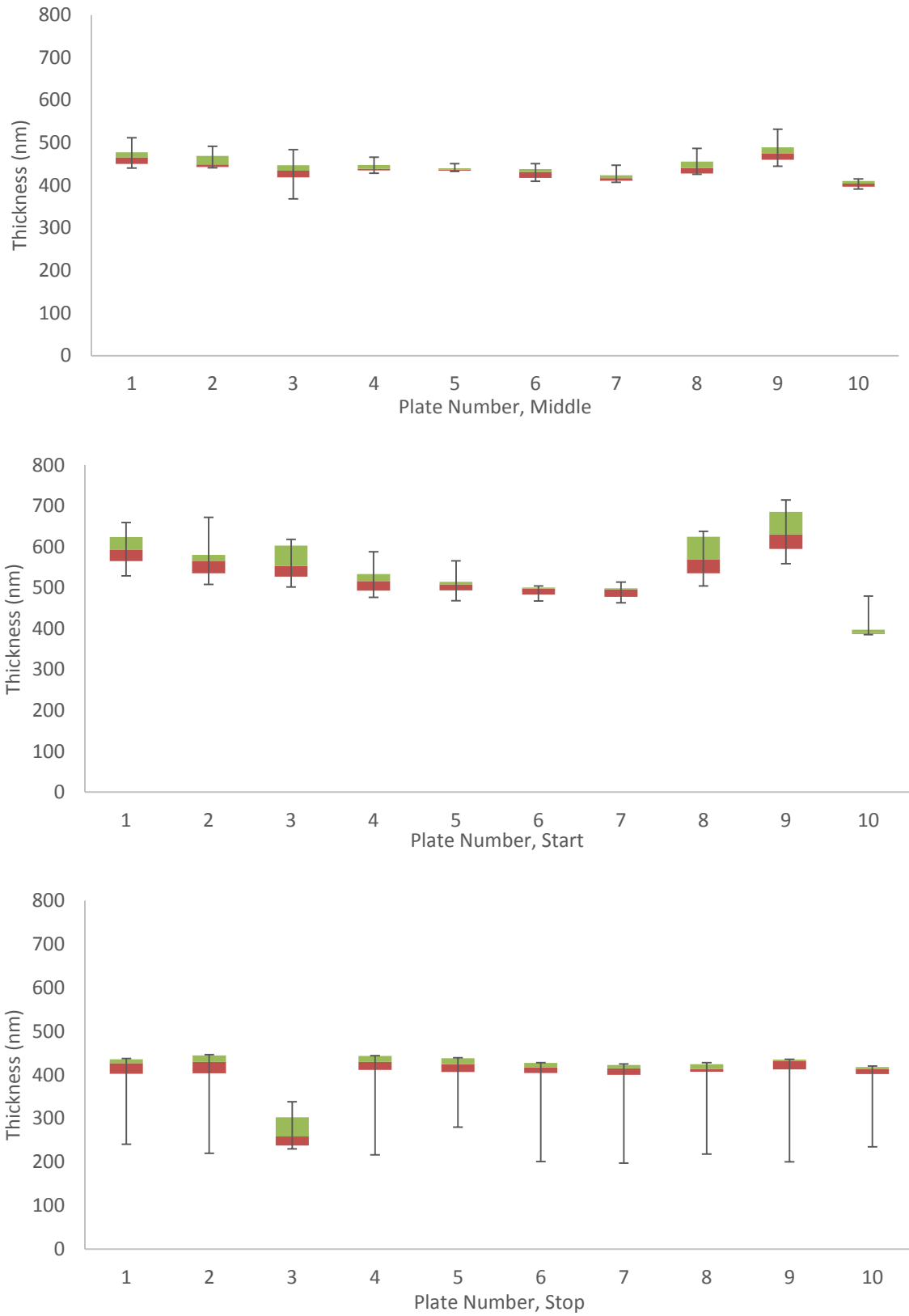
Figure 79: Box plots for cross-section data of the middle, start and stop regions of 10 plate repeats

Plate number	Middle Cross-Section Mean (nm)	Start Cross-Section Mean (nm)	Stop Cross-Section Mean (nm)	Plate number	Middle Cross-Section Standard Deviation (nm)
Standard Deviation of mean thickness (nm)	22.28	65.43	35.62	Min (nm)	5.39
Uniformity of mean thickness (%)	5.05	12.21	9.57	Max (nm)	32.82
				Range (nm)	27.43

Table 24: Mean and standard deviation values for cross-section data of the middle, start and stop regions of 10 plate repeats

With the exception of plate 3, the stop region yielded the most uniform results. If plate 3 was considered an outlier and was removed from the analysis then the resultant uniformity of mean thickness dropped to 2.14%. The start region yielded the least uniform results suggesting the source of coating thickness variation was being introduced at the start of the plate; this could impact on the middle region but should be negligible by the end of the plate. The cause of this could be due to residual material from when the head was in standby position. Fluid flows through the head to prevent polymer drying on the lips, the head will remain in this position for slightly variable amounts of time therefore different volumes of material may have collected on the lips. Further work would focus on the middle section. Since the deviations of the middle section followed the same trend as the start, analysis the start region would be carried out in relation to the middle section. Responses will be defined further in section 5.f.i.

The inherent error of each process had been quantified, the error was thought to be sufficiently low to allow for the design of experiments trials to progress. Repeatability would be checked at each stage to ensure result deviations were caused by factor changes.

f. Design of Experiments

Design of experiments (DOE) is a statistical technique used to better understand relationships between experimental factors. Most process development is carried out by changing one variable at a time (OVAT), allowing the researcher to understand how each factor affects the outcome. However, if there is a relationship between factors then the optimum value for said factors may never be found using standard OVAT methods.

Often a screening study is carried out with a number of selected factors with a high value and a low value chosen for each. From there a more in depth study can be carried out to provide detailed analysis of potential relationships. The requirements for this study are to determine whether there is a relationship between the parameters and material properties and to quantify their effect on coating uniformity.

Factor high and low values were determined using the parameters in Table 25 as a starting point, which resulted in complete coatings for all formulations shown in Figure 40. Parameters not included in the design of experiments study remained as shown in Table 26.

Coating gap (μm)	120	Material bead volume infuse (μL)	20
Coatig velocity (mm/s)	10	Material bead flow infuse (μL/min)	500
Coating acceleration (mm²/s)	8		

Table 25: Starting parameters for DOE design

Slot die selection	1	Slot die take-off mode	0
Substrate type (inches)	4	Coating material pump stop offset (mm)	10
Coating width (mm)	100	Take-off offset (mm)	0
Number of substrate measure points	2	Material bead volume withdraw (μL)	100
Coating border (mm)	1	Material bead flow withdraw (μL/min)	150,000
Coating film thickness (μm)	15	Standby gap (μm)	70
Coating start delay (ms)	5,000	Standby bead volume (μL)	1200
Pump start offset (ms)	0	Standby bead flow (μL/min)	100,000
Coating material pump start offset (mm)	0	Standby material flow (μL/min)	100

Table 26: Parameters unchanged during DOE design

i. Factorial Screening

A number of factors were highlighted to potentially be having an effect on coating uniformity that was not yet understood:

- Coating gap
- Coating velocity
- Coating acceleration
- Material bead volume infuse i.e. Volume infuse
- Material bead flow infuse i.e. Flow infuse

In particular, the relationships between coating velocity and coating gap as well as volume infuse and flow infuse needed to be defined. Many of the other parameters had effects that could be explained e.g. material bead stop offset controlled how much material remained at the end of the plate and therefore affected the thickness of the coating at the end of the plate.

Viscosity and surface tension were investigated by using the formulation know-how attained in section 5.a.iii. Formulations were developed to incorporate both factors to ascertain whether they affected one another. Experiments were grouped by which formulation was used as changing the coating fluid required a full clean up and setup; viscosity and surface tension were categorised as the hard-to-change (HTC) factors.

Due to the high number of factors, a screening study was carried out using only high and low values in a quarter factorial, i.e. a 2-level fractional factorial. Fractional factorials are designs where only a fraction of the possible experimental combinations are carried out, in this case a quarter of the trials were completed[57]. Factor 'highs' and 'lows' were chosen within a range that was expected to produce complete coatings. Due to the issue of repeatability each parameter combination was repeated twice i.e. ran a total of three times.

Initial trials were carried out using the formulations shown in Figure 42; it became apparent that the low molecular weight polymer (5 wt% PEO37K) and the lowest loading of surfactant (0.001 wt%) resulted in dewetting. Higher molecular weight polymers were incorporated at lower loadings (2.5 wt%) and a slightly higher loading of surfactant was utilised (0.003 wt%).
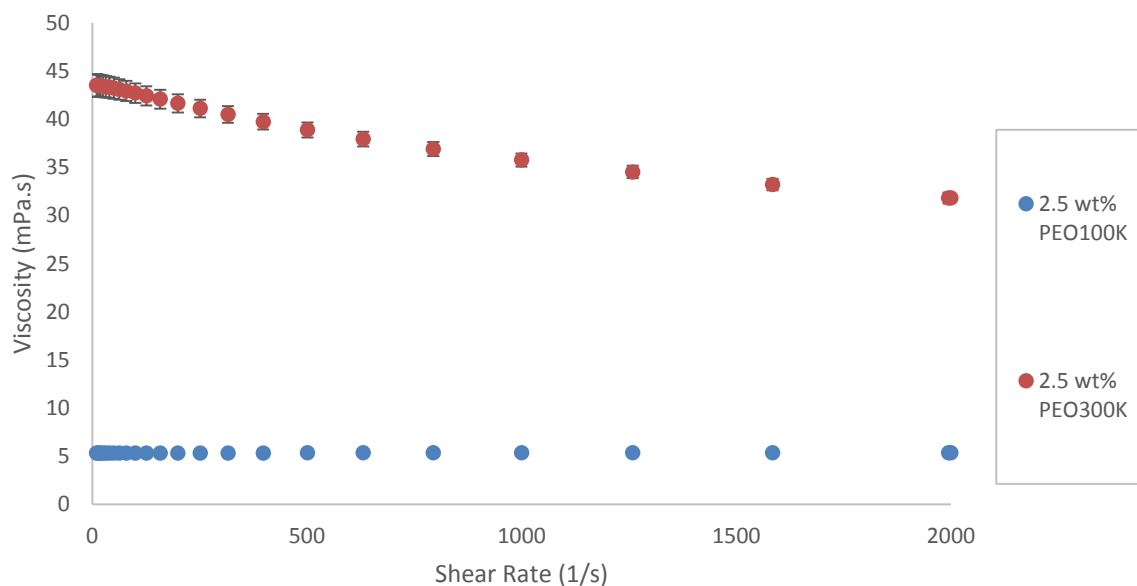
Figure 80: Shear rate dependence of viscosity for 2.5wt% PEO in water

The resultant formulations used to test the high and low data points of viscosity and surface tension are shown in Table 27.

Polymer	Triton X-100	Mean Viscosity 10 – 1500 1/s (mPa.s)	Surface Tension (mN/m)
2.5 wt% PEO100K	0.003 wt%	5.3	61.11
2.5 wt% PEO100K	0.01 wt%	5.3	44.84
2.5 wt% PEO300K	0.003 wt%	40.9	62.56
2.5 wt% PEO300K	0.01 wt%	40.9	44.39

Table 27: Formulations used for quarter factorial trial 1

Due to the requirement for a full clean up and setup when changing materials, the trial was carried out in 4 batches of testing each comprising 24 runs. Mean values were taken for the surface tension of PEO100K and PEO300K. Parameters were selected following initial trials to determine the operating window for all materials whereby a complete coating was achieved.

Mean viscosity (mPa.s)	Mean Surface Tension (mN/m)	Coating Gap (μm)	Coating Velocity (mm/s)	Coating Acceleration (mm²/s)	Volume Infuse (μL)	Flow Infuse (μL/min)
5.3	44.62	70	2	0.5	10	50
40.9	61.83	150	12	450	30	500

Table 28: Slot die parameters used for quarter factorial trial 1

The responses used for this factorial analysis were calculated from the cross-section data, see Figure 78 for graphical representation of values:

- 'Middle mean' = mean of cross-section data for the middle 50% of data
- 'Middle SD' = standard deviation of cross-section data for the middle 50% of data
- 'Start difference' = mean of cross-section data for the start region minus middle mean
- 'Stop difference' = mean of cross-section data for the stop region minus middle mean

Each region of coating was analysed independently as different parameters were expected to affect different areas, as discussed in section 5.e.iv. The middle mean was the region least affected by outliers so it would give the most accurate representation of the mean value. There was a noticeable difference in thickness values between plates so this could be most effectively compared using the middle mean. The start difference and stop difference allowed for comparison of the outer regions with the middle region; a positive value signified a thicker region when compared with the middle region, a negative value represented a thinner region.

An updated Excel 2010 template was created to allow for efficient collection and storage of data. Data was to be imported from the raw data using the method described in section 5.d.i. From sheet '5x5' each plate was automatically transferred into the 'Plates' sheet using Equation 21 for correlating cells to provide data in the format of Figure 60 and Figure 61. Here the data was manipulated to provide the responses, which were referenced in the 'Comparison' sheet where data was stored in a format that could be copied directly into MiniTab for analysis, Figure 81.

	A	B	C	D	E	F	G	H	I	N	O	Y
1	Plate	Viscosity (mPa.s)	Surface tension (mN/m)	Coating Gap (um)	Coating Velocity (mm/s)	Coating Acelleration (mm/s2)	Volume Infuse (uL)	Flow Infuse (uL/min)	Cross-section, Middle Mean (nm)	Start Difference (nm)	Stop Difference (nm)	Cross-section, Middle SD (nm)
2	1	37	52	200	1	450	1	500	=Plates!Z20	=Plates!AE20	=Plates!AF20	=Plates!AF23
3	=A2+1	37	52	70	1	450	30	50	=Plates!Z47	=Plates!AE47	=Plates!AF47	=Plates!AF50
4	=A3+1	37	52	70	1	450	30	50	=Plates!Z74	=Plates!AE74	=Plates!AF74	=Plates!AF77
5	=A4+1	37	52	200	30	0.5	30	50	=Plates!Z101	=Plates!AE101	=Plates!AF101	=Plates!AF104
6	=A5+1	37	52	200	30	450	30	500	=Plates!Z128	=Plates!AE128	=Plates!AF128	=Plates!AF131
7	=A6+1	37	52	200	30	450	30	500	=Plates!Z155	=Plates!AE155	=Plates!AF155	=Plates!AF158
8	=A7+1	37	52	200	1	0.5	1	50	=Plates!Z182	=Plates!AE182	=Plates!AF182	=Plates!AF185
9	=A8+1	37	52	70	30	0.5	1	500	=Plates!Z209	=Plates!AE209	=Plates!AF209	=Plates!AF212
10	=A9+1	37	52	70	1	0.5	30	500	=Plates!Z236	=Plates!AE236	=Plates!AF236	=Plates!AF239
11	=A10+1	37	52	200	1	0.5	1	50	=Plates!Z263	=Plates!AE263	=Plates!AF263	=Plates!AF266
12	=A11+1	37	52	70	30	450	1	50	=Plates!Z290	=Plates!AE290	=Plates!AF290	=Plates!AF293
13	=A12+1	37	52	70	30	450	1	50	=Plates!Z317	=Plates!AE317	=Plates!AF317	=Plates!AF320
14	=A13+1	37	52	70	1	0.5	30	500	=Plates!Z344	=Plates!AE344	=Plates!AF344	=Plates!AF347
15	=A14+1	37	52	70	1	450	30	50	=Plates!Z371	=Plates!AE371	=Plates!AF371	=Plates!AF374
16	=A15+1	37	52	200	30	0.5	30	50	=Plates!Z398	=Plates!AE398	=Plates!AF398	=Plates!AF401

Comparison | Plates | 5x5 | Data Import | ⊕

Figure 81: Storage of data for DOE with cell references

The first block of the trial was carried out using PEO300K and 0.003 wt% Triton X-100, parameters are shown in Table 29; the colour coordination signifies repeats of the same parameter combinations. Plate 1 was a dummy plate which was coated to remove any excess material remaining on the lips after the setup routine.

Plate Number	2	3	4	5	6	7	8	9	10	11	12	13	14	15	16	17	18	19	20	21	22	23	24	25
Coating gap (μm)	150	70	70	150	150	150	150	70	70	150	70	70	70	70	150	70	150	70	70	150	150	150	150	70
Coating velocity (mm/s)	2	2	2	12	12	12	2	12	2	2	12	12	2	2	12	12	2	12	2	12	12	2	2	12
Coating acceleration (mm²/s)	450	450	450	0.5	450	450	0.5	0.5	0.5	0.5	450	450	0.5	450	0.5	0.5	450	0.5	0.5	0.5	450	450	0.5	450
Material bead volume infuse (μl)	10	30	30	30	30	30	10	10	30	10	10	10	30	30	30	10	10	10	30	30	30	10	10	10
Material bead flow infuse (μl/min)	500	50	50	50	500	500	50	500	500	50	50	50	500	50	50	500	500	500	500	50	500	500	50	50

Table 29: First part of factorial experiment incorporating three non-consecutive repeats

When the resultant coatings were analysed it became apparent that plates coated with the same parameters were very different. The exceptions were plates that were carried out in sequence i.e. plates 3 and 4, 6 and 7, 12 and 13. Some examples are shown below in the form of box plots. Cross-section profiles are shown in Figure 83. There were a small number of invalid points on each of the plates but they were not extreme enough to account for the large disparities between results.
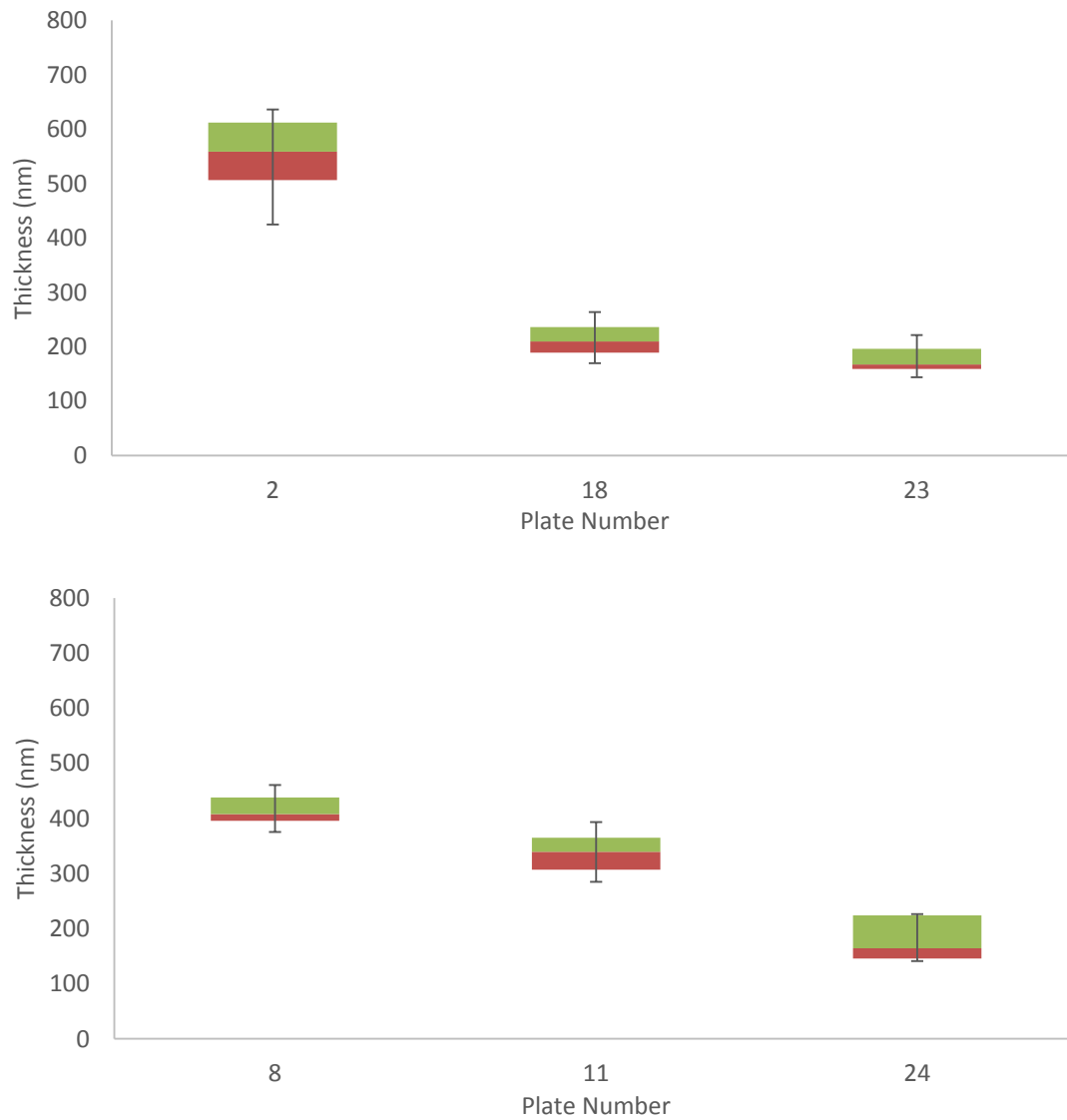
Figure 82: Box plots for plates coated non-consecutively with the same parameters
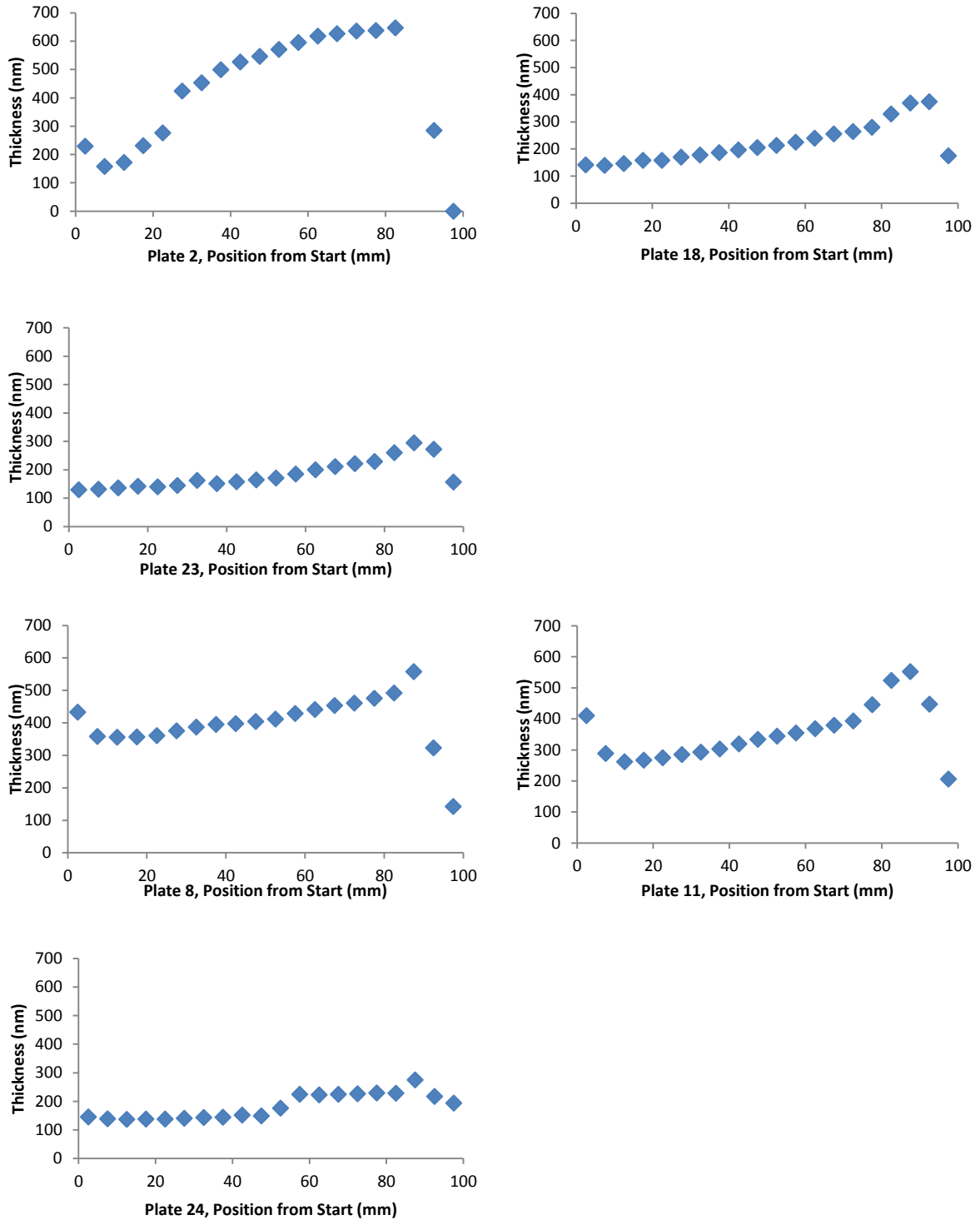
Figure 83: Thickness variations between plates coated non-consecutively with the same parameters

Plates that were closer in the coating schedule i.e. plates 18 and 23, plates 8 and 11, exhibited similar thickness profiles. Plates coated subsequently but with different parameters also showed some similarities, box plots and cross-section profiles shown in Figure 84 and Figure 85.
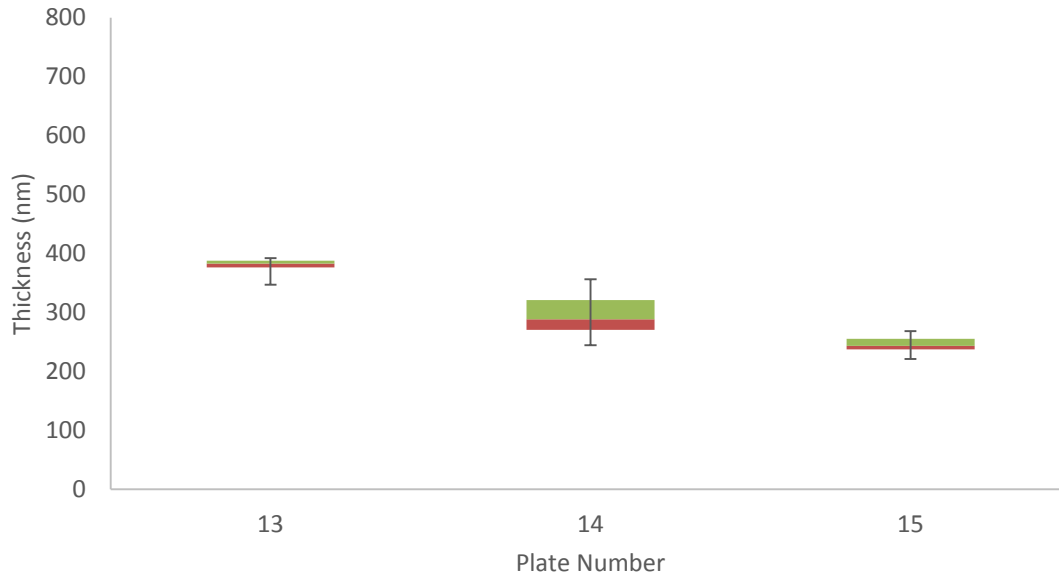
Figure 84: Box plots for plates coated consecutively with the different parameters
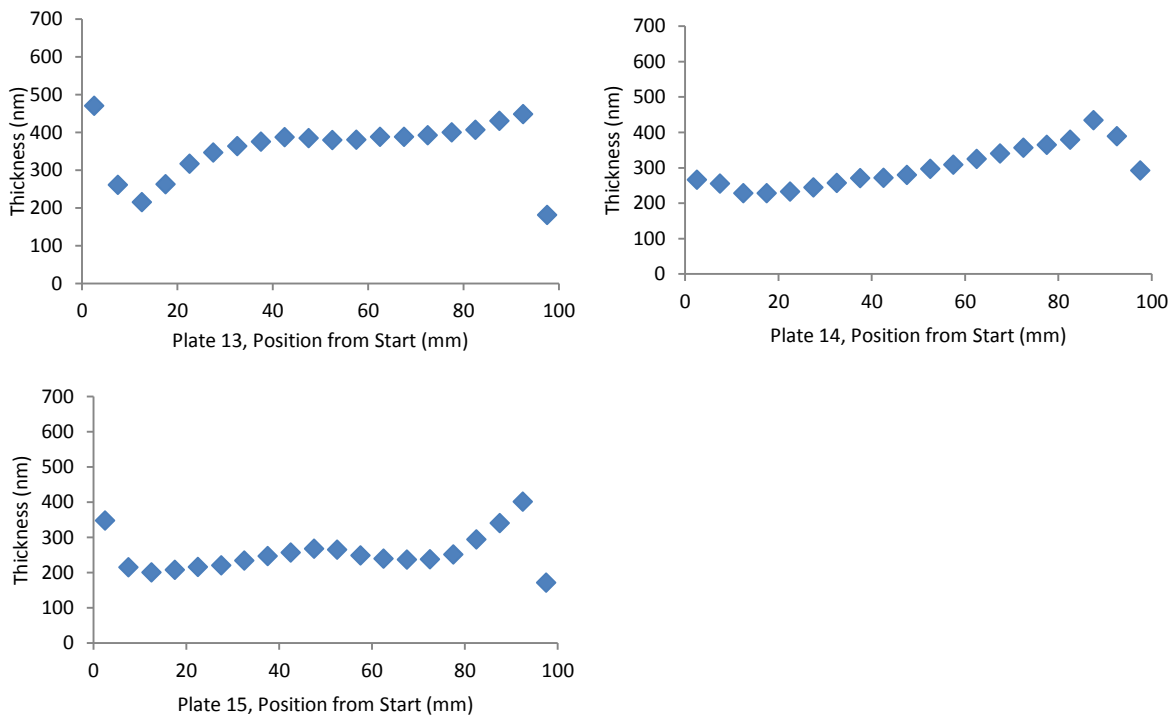
Figure 85: Thickness variations between plates coated non-consecutively with the same parameters

This suggested that there was a residual effect of the previous parameters on each plate. This variation was expected to greatly skew results; therefore in place of running three repeats, 1 or 2 dummy plates would be ran prior to running one plate for each combination.

To determine how many dummy plates were required two processes were ran 5 times. The standard deviation of Middle Mean values were compared for three subsequent plates to ascertain whether coatings were becoming more repeatable. In both cases the largest reduction in standard deviation was observed for plates 3, 4 and 5. The DOE was carried out by running two dummy plates prior to coating one measurable plate; incorporating additional measured parameter repeats would drastically increase the number of coating iterations. Box plots of all five plates for both trials are shown in Figure 86 and Figure 87.

Plate	Trial 1 Cross-Section Middle Mean (nm)	Trial 2 Cross-Section Middle Mean (nm)
1	467.31	296.80
2	457.33	262.80
3	431.60	255.85
4	442.37	241.28
5	438.15	251.66

	Trial 1 (nm)	Trial 2 (nm)
Standard Deviation of Plate 1, 2 and 3	18.42	21.91
Standard Deviation of Plate 2, 3 and 4	12.92	10.98
Standard Deviation of Plate 3, 4 and 5	5.43	7.50

Table 30: Analysis of improving coating repeatability with increasing number of repeats
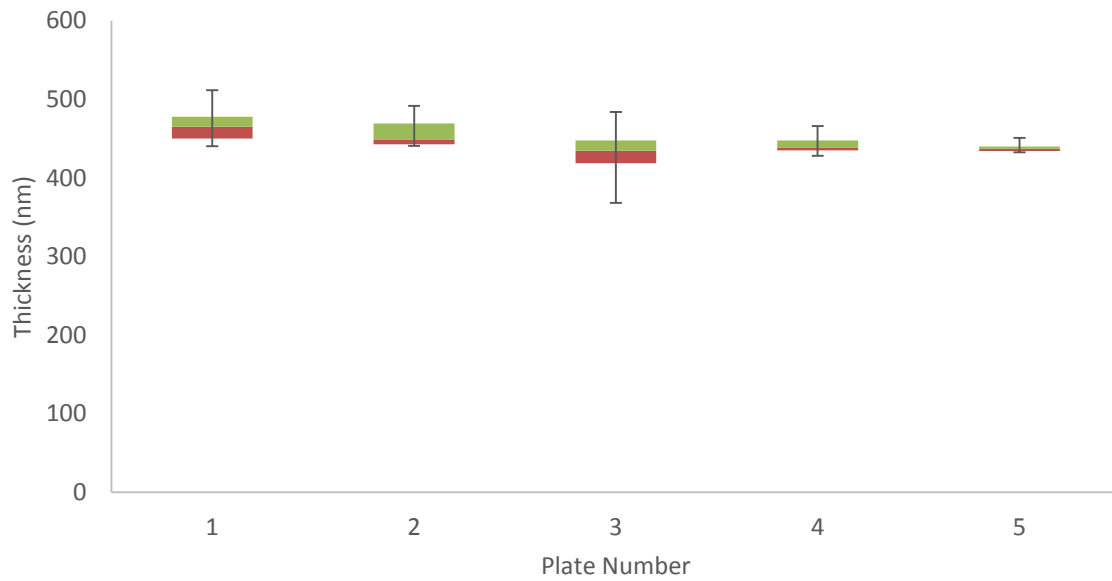
Figure 86: Box plots showing improving coating repeatability with increasing number of repeats, trial 1
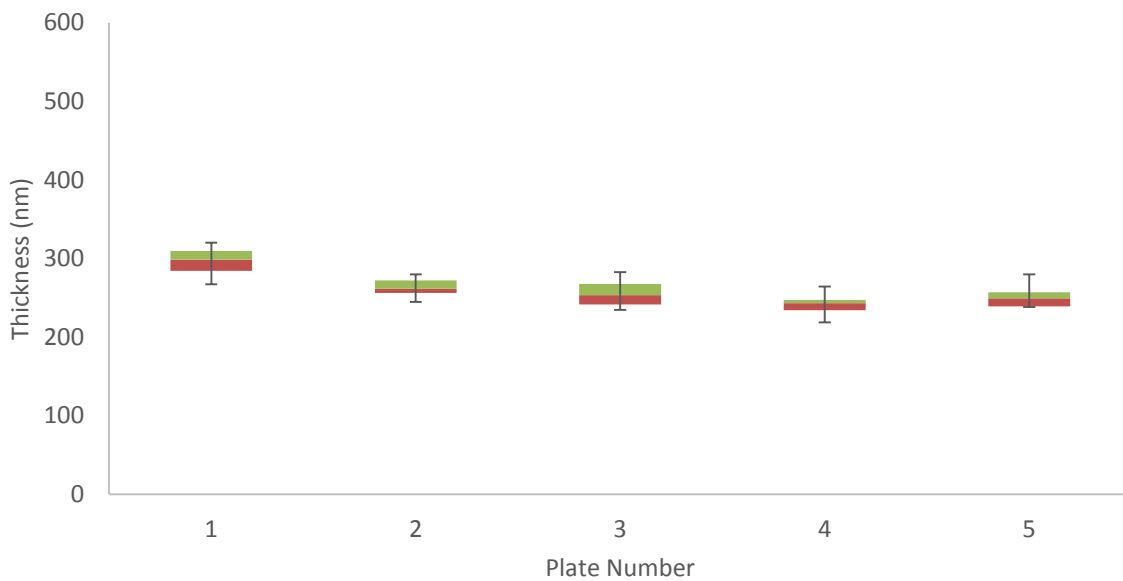
Figure 87: Box plots showing improving coating repeatability with increasing number of repeats, trial 2

In future all parameter sets would be ran with two dummy plates before attaining one final coating which would be measured. The further modified study incorporated 4 batches of coating and 24 runs per batch, of which 8 per batch would be measured. No further repeats could be incorporated as this would dramatically increase the size of the screening study.

The quarter factorial results were analysed using MiniTab 17 and Pareto charts were created for each response. A Pareto chart is a bar chart that displays factors and factor combinations in order of the statistical significance of their impact on the response. It works on the basis of the 80/20 rule that 80% of effects are a result of 20% of causes, also known as the Pareto Principle. The standard effects were calculated by dividing each factor's coefficient by the standard error. Anything above 0.05 degrees of freedom was considered significant[58].

There were no factors highlighted that affected Middle SD and Start Difference, but there were a number of variables that affected Middle Mean and Stop Difference, Figure 88. Any factors that resulted in a value greater than 74.9 for Middle Mean and 18.88 for Stop Different had a statistically significant effect on the response, they are listed below.
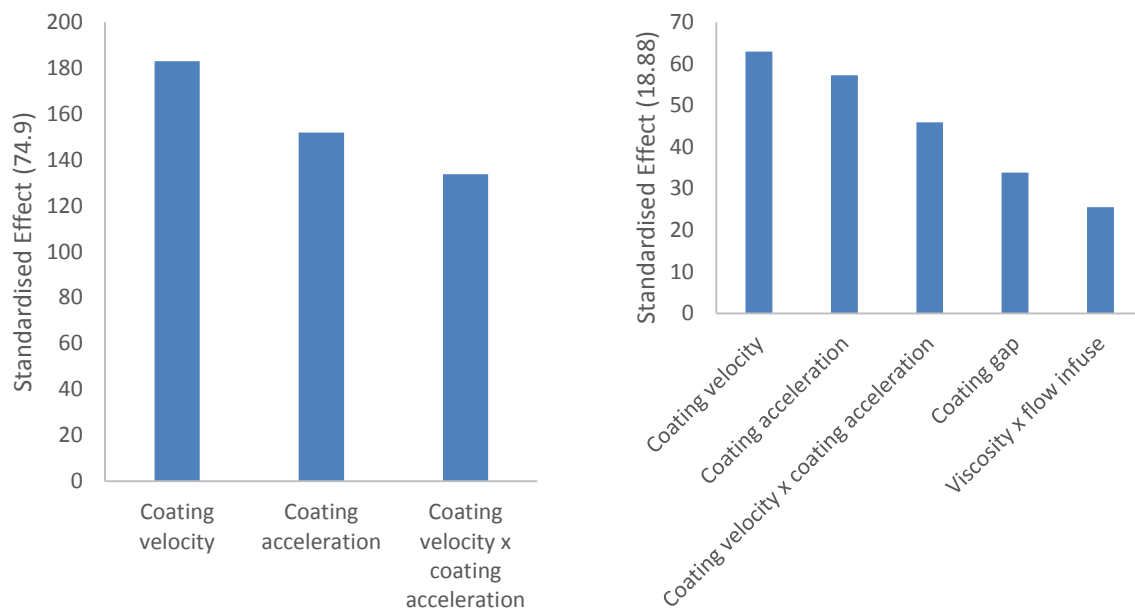
Figure 88: Pareto charts of standardised effects for Middle Mean (left) and Stop Difference (right)

It was unexpected that the coating velocity and acceleration had such a great effect on the coating thickness which suggested that the flow rate of the syringe and the slot die parameters were not synchronised. It was also unanticipated that the coating acceleration was having such a notable effect on the end of the coating since the slot die head should be up to full speed by the end of the plate, so the largest effect should occur at the start of the coating. However, when parameters were checked the acceleration was too low for the slot die to reach full speed by the end of the plate, Figure 89. Therefore the 'high speed low acceleration' iteration effectively analysed a lower speed with a maximum of 9.87 mm/s.

Stop																				Start
	9.87	9.62	9.35	9.08	8.80	8.51	8.22	7.91	7.58	7.25	6.89	6.52	6.12	5.70	5.24	4.74	4.18	3.54	2.74	1.58
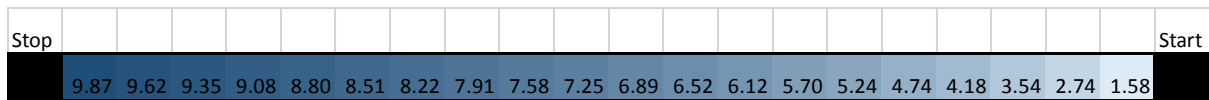
Figure 89: Diagram showing changing speed with acceleration across the cross-section of a 4 inch substrate

The effect of coating gap, viscosity and flow infuse on the Stop Difference could be reasoned. The end of the coating is highly dependent on the success of the material withdraw. A higher coating gap will require the fluid to be drawn further to reach the head. The lower viscosity fluids will be less structured so it will be more difficult for the slot die to exhibit control over the fluid. It was observed during experimentation that coating the low viscosity fluid resulted in larger puddles of material remaining at the stop region. Incorrect coating gap and flow infuse values could result in a build-up of material on the lips which would be intermittently deposited during the coating, resulting in unexpected changes to the coating thickness.

Due to the oversight of the low acceleration value not being suitable, half of the experiments were repeated using 2 mm/s^2 which would result in the slot die being up to full speed after 37.5 mm of the plate. It also seemed reasonable to add more iterations to the next batch of coating to upgrade the study to a half factorial, providing more reliable information. The same high and low values were used for all factors except acceleration but they were incorporated into different combinations.

The results of the half factorial were standardised across the responses; anything above 2.037 was considered to have an effect on the response, Figure 90.
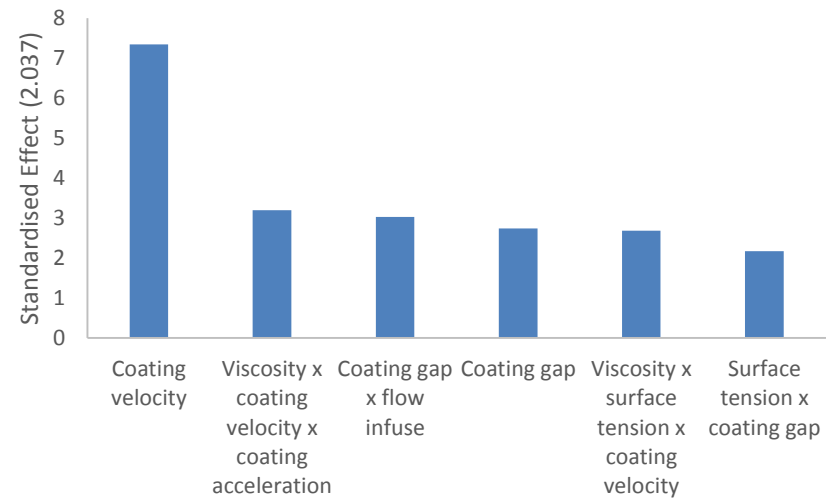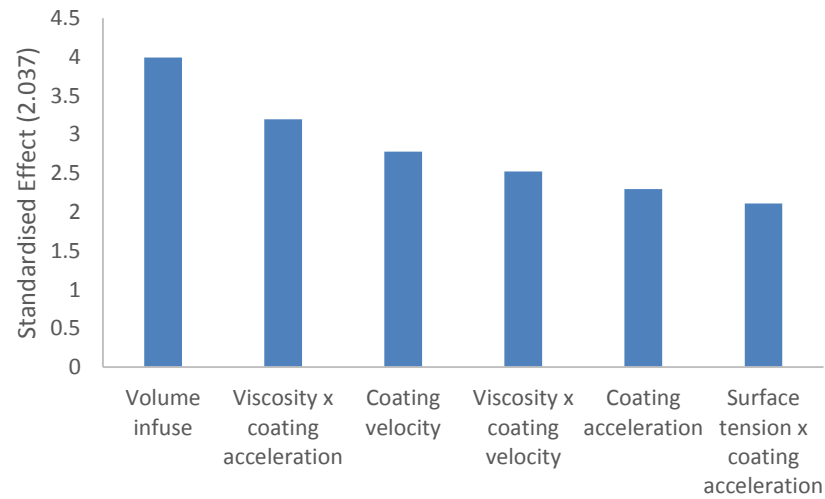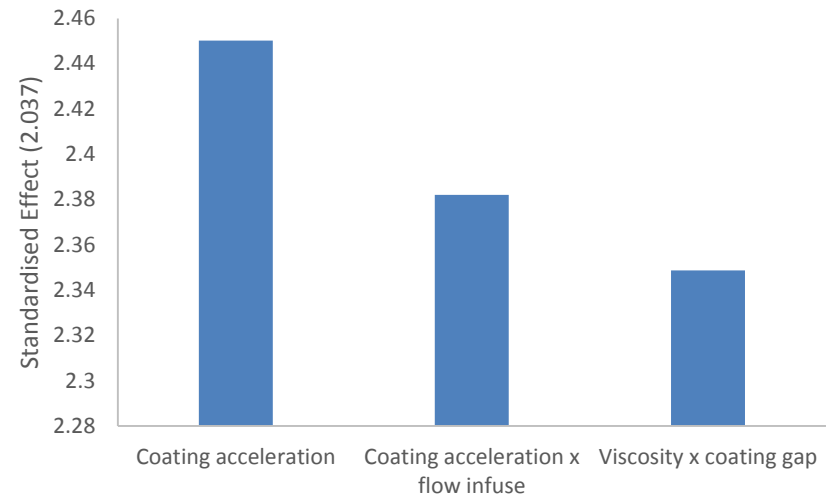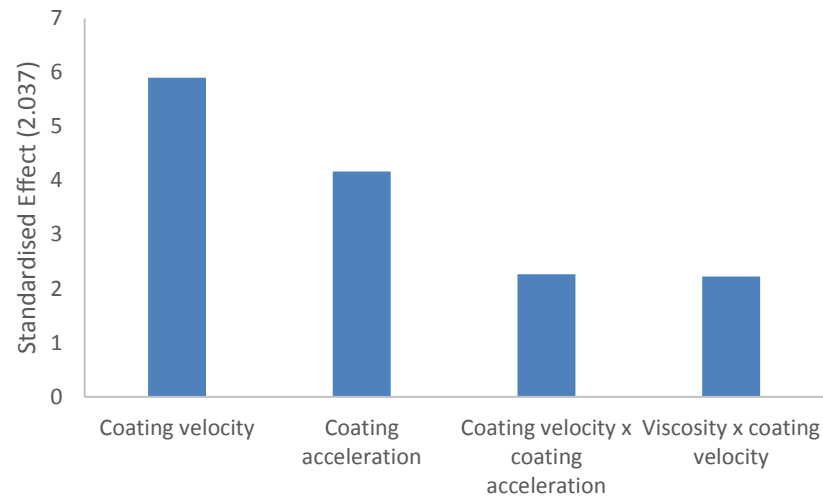
Figure 90: Pareto charts of standardised effects for half factorial experiment; Middle mean (top left), Middle SD (top right), Start difference (bottom left), Stop difference (bottom right)

The middle mean i.e. the dry coat thickness was strongly affected by the coating velocity and acceleration. It had been assumed that the flow rate was automatically adjusted by the Harvard syringe units to account for changes in coating speeds; the half factorial data suggested that this was not the case. Middle mean was only affected by viscosity when the effects are coupled with that of the coating velocity. This again suggested the issue was related to the system's calculation of the flow rate. These parameters were investigated in three response surface experiments; achieving the correct coating thickness is crucial for the success of making devices. The response surface studies should locate a region within the operating window where the expected coating thickness could be achieved.

Following on from the discovery of flow rate inconsistencies, it is not unexpected that coating acceleration should have an effect on standard deviation; low accelerations will cause a thickness gradient. It could be included in a response surface study to investigate whether it could be used to counteract issues occurring in the start region. The influence of coating gap could be resulting in one of two things; if the gap is too low then material builds up on the lips and is deposited in an uncontrolled manner later on the plate. The second outcome is that if the gap is too high then the meniscus is not completely stable resulting in non-uniform deposition. The flow infuse will influence how stable the bead is right at the start of the plate, so an unfavourable flow rate at infuse resulting in an imperfect meniscus could potentially impact the rest of the plate, and combined with coating gap issues would result in non-uniformity.

The surface tension was found to be having a minimal effect on the chosen responses; it had a small effect on the start and stop regions when combined with the effects of other parameters. This could be due to the small range of surface tension values studied. It was difficult to find a wide range of surface tensions without causing dewetting of the formulation while not exceeding the CMC. However this data does suggest that within this operating window surface tension has a negligible effect on coating uniformity.

The start and stop regions were also affected by the coating velocity and coating acceleration, adding to the suspicion of flow rate inconsistencies. Volume infuse only affected the start region; it had been included in the study to check for a relationship with the flow infuse. Variation of the volume infuse expectedly modified the amount of material at the start of the plate, but no relationship with the flow infuse was observed. The effect of viscosity on the start region was suspected to be linked to meniscus stability. The stop region was affected by the coating gap; higher gaps result in further for the fluid to travel to the head during withdraw. The effect of flow infuse was unexpected, this may be a residual effect of bead instability.

To ensure the effect of viscosity was not caused by pseudoplasticity, a coating of the higher viscosity formulation (2.5 wt% PEO300K) was checked using the data manipulation methods in section 5.d.ii. The parameters that had been used for the coating were:

- Coating gap – 70 µm
- Coating velocity – 12 mm/s
- Coating acceleration – 2 mm^2/s
- Material bead volume infuse – 10 µl
- Material bead flow infuse – 50 µl/min

The range of shear rate values was not large enough to cause large viscosity deviations across the plate, Figure 91; the calculated viscosity values were 42.4 – 43.5 mPa.s. Therefore the effects of viscosity were not caused by pseudoplasticity.

Stop	97.5	92.5	87.5	82.5	77.5	72.5	67.5	62.5	57.5	52.5	47.5	42.5	37.5	32.5	27.5	22.5	17.5	12.5	7.5	2.5	Start
2.5	34.196	72.197	74.542	89.003	88.735	87.734	61.932	87.975	62.193	70.766	73.083	75.977	75.964	81.258	80.148	77.854	77.688	72.779	61.5	35.36	2.5
7.5	83.491	52.99	59.583	58.271	57.387	57.312	57.464	59.104	60.617	62.044	63.483	65.953	71.757	72.501	71.658	69.432	67.774	57.491	57.505	31.937	7.5
12.5	109.62	51.656	57.876	56.296	55.869	55.681	56.471	58.718	60.602	62.001	63.541	65.851	71.591	72.154	71.437	68.899	66.945	55.442	52.032	29.486	12.5
17.5	125.43	50.218	57.881	56.386	56.03	55.906	56.46	58.637	60.221	61.622	63.1	65.657	71.286	72.028	71.141	68.816	65.788	54.557	50.552	27.883	17.5
22.5	135.96	49.22	57.524	56.258	56.254	56.19	56.7	58.802	60.399	61.766	63.021	65.668	71.384	72.17	71.289	68.673	64.805	53.791	49.284	27.773	22.5
27.5	153.96	48.373	56.692	55.385	54.968	54.926	55.188	57.775	60.53	63.612	65.685	69.348	73.576	74.055	73.873	70.728	68.213	56.852	51.936	25.332	27.5
32.5	82.686	48.488	56.708	55.375	55.182	55.187	55.389	58.485	61.139	64.185	66.165	69.83	73.843	74.501	73.936	70.454	67.932	56.95	52.051	25.702	32.5
37.5	114.27	48.823	56.649	55.328	55.362	55.267	55.226	57.923	60.711	64.096	65.829	69.552	73.49	73.992	73.518	70.214	68.064	56.565	52.707	24.719	37.5
42.5	108.3	50.311	57.984	56.767	56.913	57.424	57.835	59.766	61.716	63.152	64.219	67.194	72.565	73.221	71.986	69.23	65.671	53.968	52.103	27.25	42.5
47.5	107.92	50.8	58.342	56.719	57.239	57.834	58.334	59.886	61.522	62.673	63.769	66.07	71.585	72.095	70.893	68.737	66.123	55.621	54.535	28.46	47.5
52.5	20.902	50.554	58.113	56.227	56.74	56.854	57.468	59.561	61.48	63.042	63.541	65.964	71.571	72.271	71.221	68.973	65.63	54.705	53.803	28.542	52.5
57.5	35.573	50.031	57.8	56.006	55.59	55.517	56.008	58.65	60.982	63.293	64.599	67.537	72.695	73.452	73.054	70.178	68.083	56.883	53.569	24.82	57.5
62.5	59.599	50.428	58.815	58.054	57.648	57.564	57.531	59.174	60.703	62.004	63.064	66.418	72.373	73.197	72.01	69.151	65.789	54.866	51.739	28.47	62.5
67.5	59.194	49.892	58.796	57.803	57.51	57.344	57.689	58.878	60.61	62.143	63.504	67.098	72.889	73.598	72.927	70.031	67.075	53.766	48.707	27.405	67.5
72.5	20.945	48.511	57.133	55.621	54.679	54.708	54.618	57.688	59.824	62.697	65.488	70.526	74.646	75.353	74.554	71.859	70.064	58.389	53.563	22.767	72.5
77.5	99.549	49.233	57.154	55.704	55.027	54.889	55.502	58.442	60.948	63.346	65.043	68.903	73.572	74.339	73.335	70.56	68.046	56.019	50.355	24.893	77.5
82.5	46.813	48.911	57.481	55.587	55.26	55.104	55.533	58.331	60.698	63.091	64.753	68.165	72.975	73.549	73.158	70.481	68.638	56.623	50.185	24.616	82.5
87.5	20.67	49.713	57.692	55.909	55.397	55.061	55.75	58.367	60.468	62.278	63.862	66.767	72.208	73.112	72.757	70.59	68.59	57.514	48.625	26.45	87.5
92.5	87.384	51.158	58.018	55.903	55.158	54.667	55.492	56.486	60.206	62.096	63.368	65.988	71.872	72.738	72.546	70.307	68.969	58.415	48.937	25.539	92.5
97.5	20.775	57.085	59.294	57.354	56.742	57.06	57.963	59.633	61.007	62.066	62.822	65.05	70.693	71.917	70.212	68.402	66.529	56.659	47.719	25.368	97.5
	97.5	92.5	87.5	82.5	77.5	72.5	67.5	62.5	57.5	52.5	47.5	42.5	37.5	32.5	27.5	22.5	17.5	12.5	7.5	2.5	

Figure 91: Calculated shear rate for 2.5 wt% PEO300K and 0.01 wt% Triton X-100 in water

There was not enough time remaining to study the start and stop regions in detail. However assessing the uniformity of the middle region was expected to provide some insight to the coating success of the outer regions. Response surface studies were carried out for the middle mean and middle SD responses.

ii. Response Surface Studies

A full response surface was designed for the Middle SD and Middle Mean for associated variables. Response surface studies 1, 2 and 3 were carried out simultaneously due to time constraints; trials were grouped by formulation and therefore shim thickness due to the time required to setup the head with a different shim thickness. Response surface 4 was designed as a result of the findings in studies 1-3. Results will be grouped and presented by response surface number.

A central composite design was used for up to 4 continuous and categorical factors. Central composite response surface designs are effectively extended factorial designs which include 3 further factor levels within the high and low values, allowing for the estimation of curvature.[59] As with the factorial experiment, two dummy plates were ran prior to one measured plate for each iteration; there were no repeats. Coating velocity, coating acceleration, coating gap and flow infuse could easily be altered using the software, however modifying the viscosity required some formulation development.

To produce a variety of viscosities at a consistent solids loading two stock solutions were produced; 2.5 wt% PEO100K (abbreviated to 2.5-100K) and 2.5 wt% PEO300K (2.5-300K). They would be mixed at varying ratios to achieve a range of viscosities. Since surface tension was shown to have no effect on the Middle Mean or Middle SD both formulations contained 0.01 wt% Triton-X100 to ensure the highest degree of wetting onto substrates. A number of iterations were formulated to be used to create a viscosity curve, Table 31.

Ratio of 2.5-100K: 2.5-300K	wt% 2.5-100k	wt% 2.5-300K
1:0	100.00	0.00
1:1	50.00	50.00
1:2	33.33	66.67
1:5	16.67	83.33
1:10	9.09	90.91
1:20	4.76	95.24

Table 31: Table of viscosity iterations to produce viscosity curve of 2.5-100K: 2.5-300K combinations

The rheology was measured once as results were used as an estimation, mean values were taken between 10 and 1585 s-1 shear rates. Values were correlated using an exponential fit trendline, Figure 92.
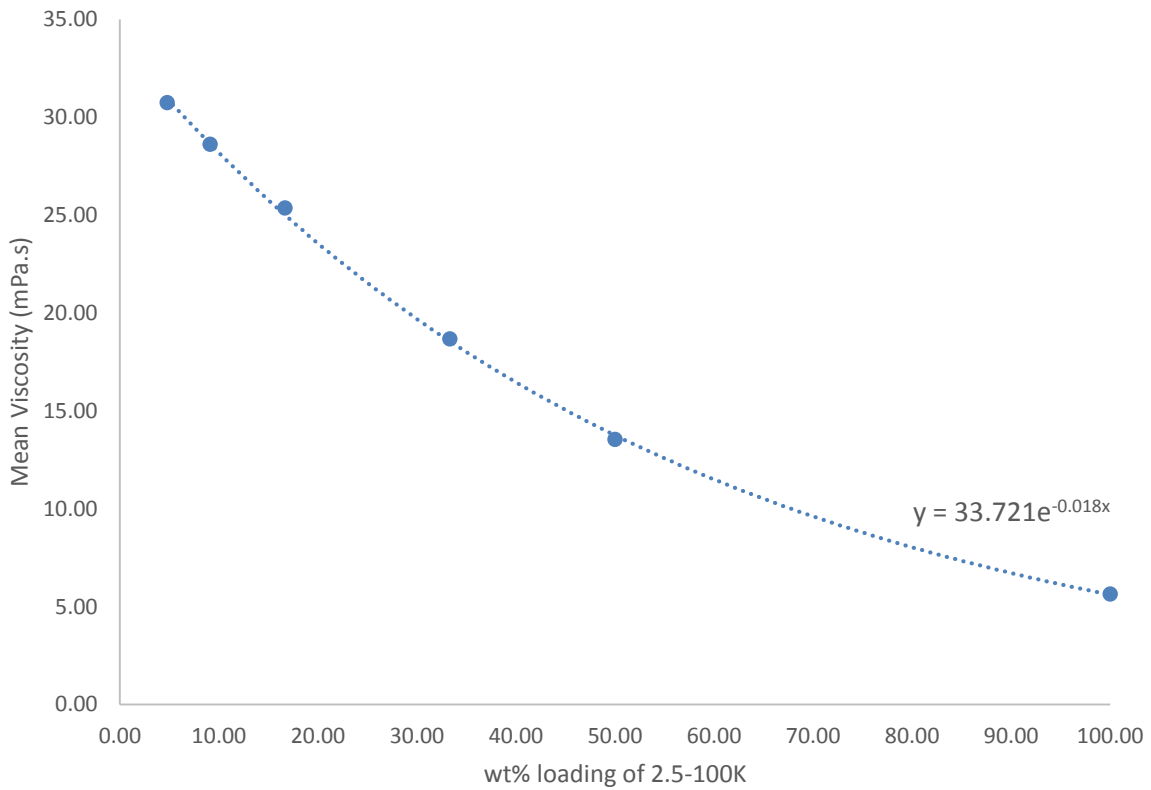

Figure 92: Mean viscosity values for 2.5-100K: 2.5-300K mixtures

The trendline equation was used to estimate the required loading of 2.5-100K for 12.5 mPa.s, 22 mPa.s and 31.5 mPa.s formulations. Resultant formulations were rheologically analysed and mean values recorded.

Formulation Name	Expected Viscosity (mPa.s)	wt% 2.5-100k	wt% 2.5-300K	Measured Viscosity (mPa.s)
Low	N/A	100	0	5.3
Low/Mid	12.5	55.1	44.9	14.0
Mid	22.0	23.7	76.3	26.1
Mid/High	31.5	3.8	96.2	37.6
High	N/A	0	100	40.9

Table 32: Expected and measured viscosities based on trendline equation

The measured viscosities did not fully match up, the 'Low/Mid' and 'Mid' formulations were close enough but the 'Mid/High' was too close to the highest viscosity to provide meaningful data. The loading of 2.5-100K was increased to reduce the viscosity further, Table 33.

Formulation Name	wt% 2.5-100k	wt% 2.5-300K	Measured Viscosity (mPa.s)
Mid/High	12.5	87.5	34.1

Table 33: Adjusted 'Mid/High' formulation viscosity data

A graph of the final viscosity profiles to be used in the response surface study are shown below.
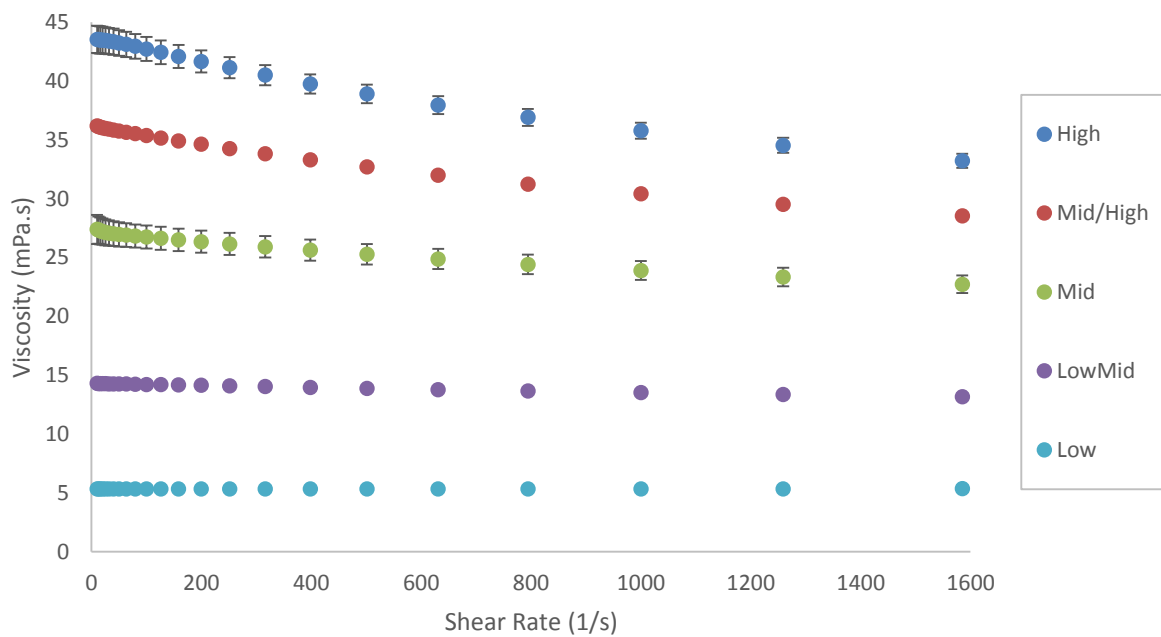
Figure 93: Viscosity traces for response surface formulations

Response surfaces 1, 2 and 3 were carried out simultaneously to make this study more time-efficient; trials were carried out in batches dependant on which shim thickness they required. Response surface 4 was carried out as a result of the findings in the first three studies.

a. Response Surface 1

The first response surface carried out was for the response 'Middle SD' and associated factors. The high and low values were input to a MiniTab response surface wizard; a Central composite design incorporating 4 continuous factors was created. Coating acceleration, flow infuse and coating gap were automatically calculated by MiniTab, viscosity was manually input based on the formulation work that had been carried out, Table 34. See appendix 5 for the full list of parameter combinations.

Viscosity (mPa.s)	Coating Acceleration (mm/s²)	Flow Infuse (uL/min)	Coating Gap (um)
5.3	3.0	50	70
14.0	93.6	163	90
26.1	226.5	275	110
34.1	359.4	388	130
40.9	450.0	500	150

Table 34: Factor levels selected for response surface 1

Parameters not investigated in this study were set to the following:

- Triton X-100 loading – 0.01 wt%
- Coating speed – 12 mm/s
- Volume infuse – 20 uL

Mean densities were calculated for each polymer combination using the ratios stated in Table 32 and Table 33 and the pure polymer densities stated in Table 6. Equation 26 was used to calculate the volume percent loading of PEO based on the calculated densities. From there Equation 22 was used to calculate the expected dry coat thickness based on a wet coat thickness of 15 μm.

$$v\% = \frac{wt\%}{\rho_R}$$

Equation 26: Calculation of volume percent solids loading

where:

- $\rho_R = Density\ relative\ to\ water$

Formulation Name	Relative density	Volume %	Estimated Thickness (nm)
Low	1.13	2.21	332
Low/Mid	1.17	2.14	322
Mid	1.19	2.10	315
Mid/High	1.2	2.08	313
High	1.21	2.07	310

Table 35: Calculated relative polymer densities

The range of thickness values was 310 nm – 332 nm. An acceptable degree of error is ±5%; the highest thickness (formulation 'Low') resulted in the highest 5% uniformity of 16.6 nm standard deviation. Contour plot results were blocked by <5%, 10% and >15% thickness uniformity with respect to the calculated film thickness for all combinations, the colour key is shown in Figure 94.
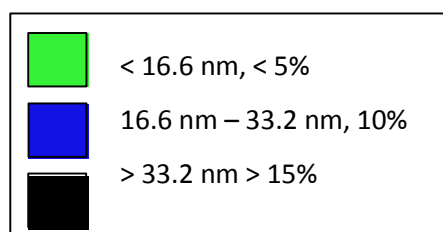
Figure 94: Colour key for thickness (nm) of response surface 1 results
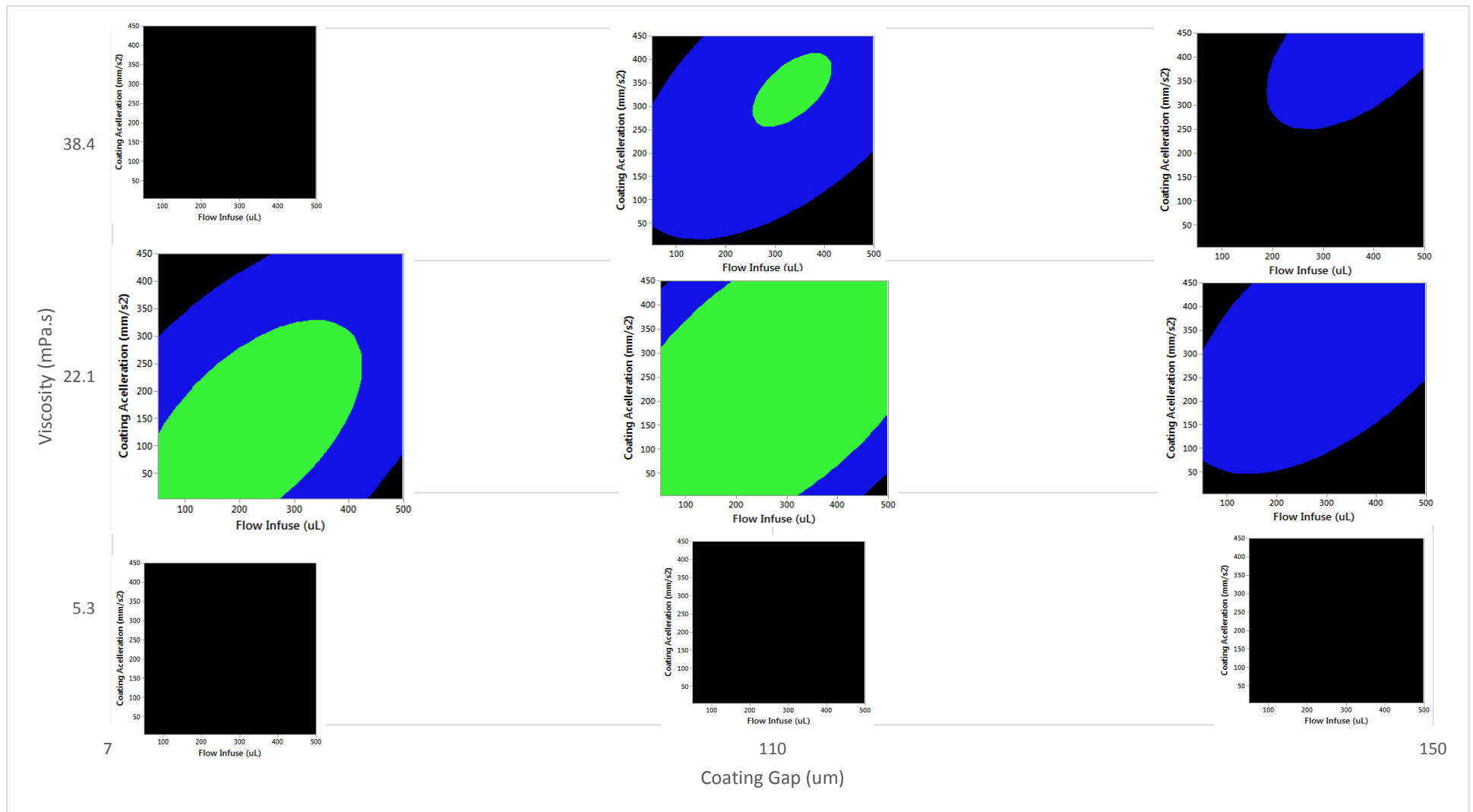
Figure 95: Response surface 1 contour plot results grouped by viscosity and coating gap
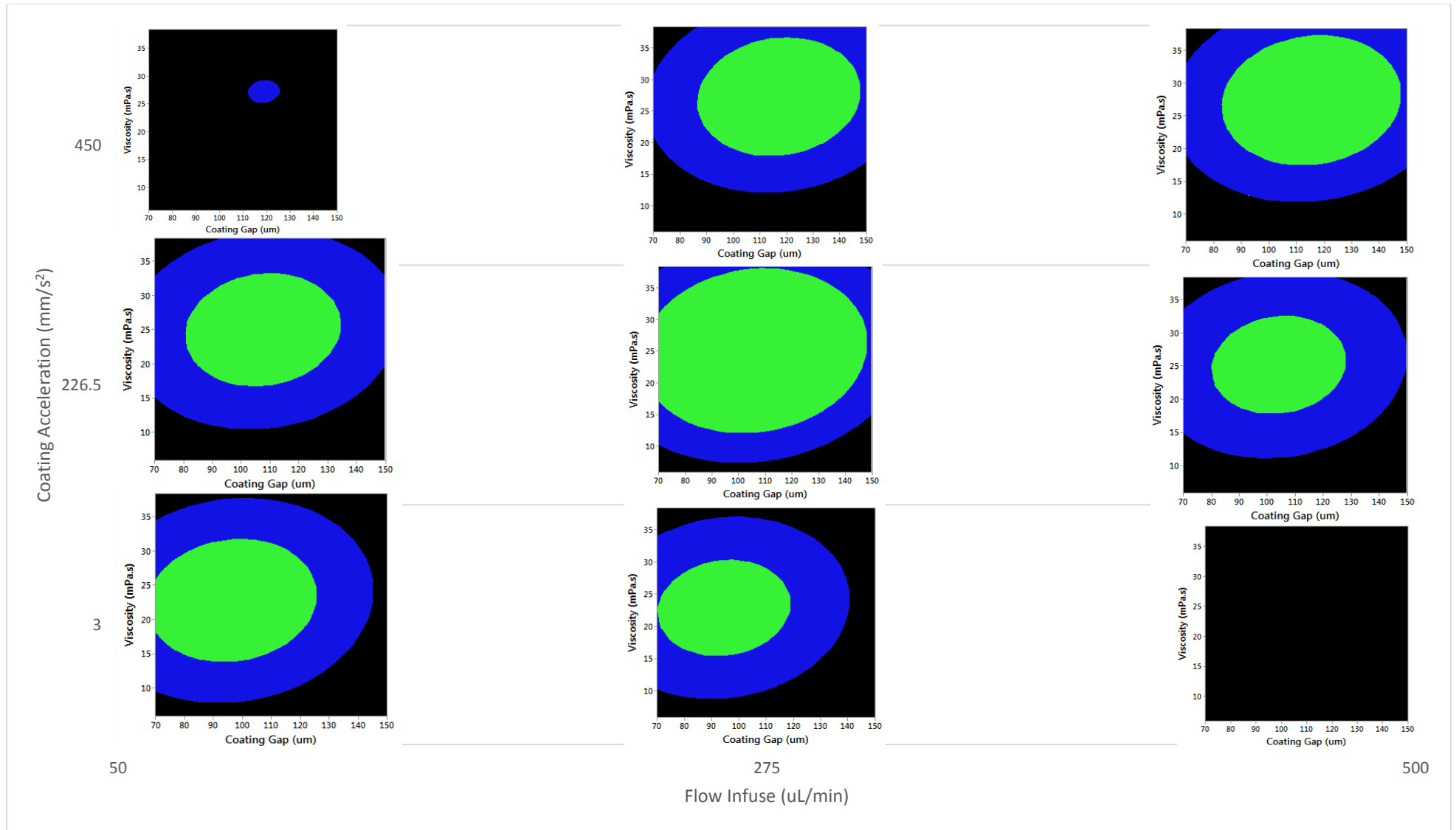
Figure 96: Response surface 1 contour plot results grouped by coating acceleration and flow infuse

There were a number of regions where an acceptable standard deviation could not be achieved, the most notable being the use of a low viscosity fluid. Low viscosity may result in a less stable meniscus, which could be counteracted by using a lower coating gap than was investigated in this study i.e. < 70 µm. Using this rationale high viscosity materials should produce uniform coatings across a larger parameter range due to the higher degree of structure; however this was not the case. High viscosity materials only produced uniform coatings when a mid-point coating gap, mid-high flow infuse and mid-high acceleration were employed. It is possible that with high viscosity materials and low coating gaps the flow rate is too high and causes meniscus instability. The use of lower accelerations and flow infuse rates may reduce the initial flow rate so as not to overwhelm the meniscus.

Generally lower coatings gaps were best paired with low accelerations, higher coating gaps preferred high accelerations.
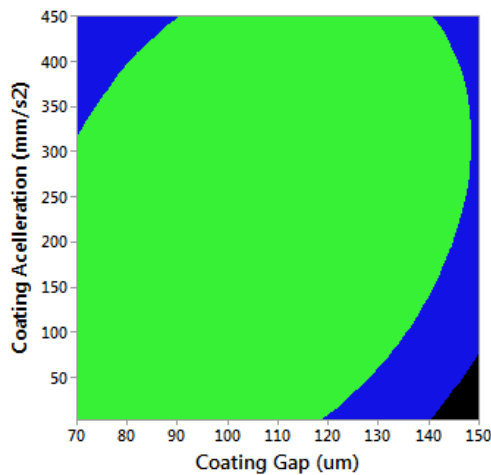
Figure 97: Contour plot for mid-point viscosity and flow infuse

Low flow infuse with high acceleration, as well as high flow infuse and low acceleration did not produce uniform coatings. Mid-range flow rates are preferred for the uniformity of coatings. Yang et al (2009)[60] reported that high flow infuse rates reduced edge effects at the start of coating, producing a more uniform start region. The outer 10 mm of a coating would usually be removed in a device to allow for contact to the electrodes therefore high quality start regions may have to be sacrificed to achieve uniformity across the bulk of the coating. Uniform coatings were not achieved using the highest coating gap, suggesting the meniscus was unstable preventing the fluid from being deposited evenly.

Overall mid-point values were favoured for all factors; optimum values as calculated by MiniTab were:

- Viscosity – 25.2 mPa.s
- Coating acceleration – 246.8 mm/s^2
- Flow infuse – 277.3 μL/min
- Coating gap – 107.2 μm

The experimental design included repeats of middle values to ensure the mid-point was reliable. These plates were checked for repeatability of the thickness (box plot) and standard deviation data (scatterplot), Figure 98.
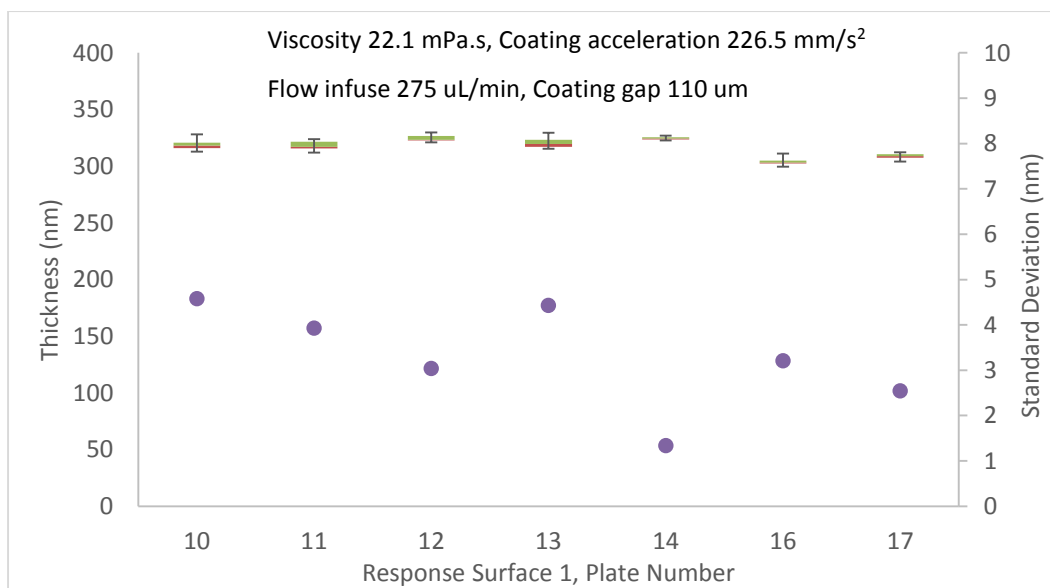

Figure 98: Box plot of thickness data and scatterplot of standard deviation, showing repeatability of mid-point plates for response surface 1

The thickness results were moderately repeatable, the standard deviation results were less so. Repeatability was still an issue when parameters were optimised, suggesting this was inherent to the equipment. However highly uniform coatings were achieved, example profiles shown below:
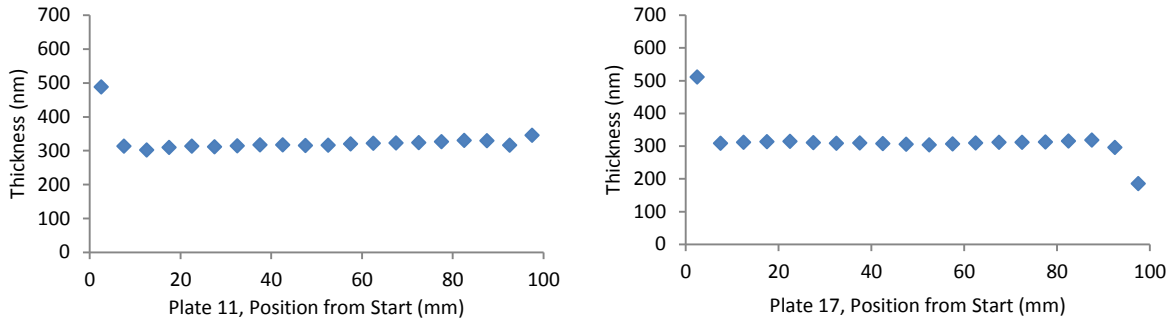
Figure 99: Cross-section of high uniformity coatings achieved in response surface 1

It was also noticed that plates with uniformity issues in the start and stop regions exhibited a poor standard deviation in the middle region.
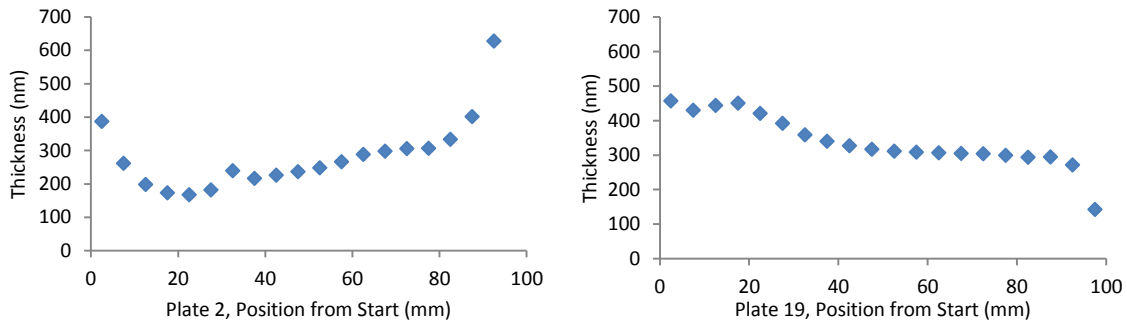
Figure 100: Cross-section of coatings with poor start and stop regions

Though the start and stop regions were not investigated using a surface response design, the effect of instability in these regions does appear to affect the central region. This suggests that by optimising the middle region using the selected parameters, the uniformity of the start and stop regions may also be improved.

The next section describes the effect of viscosity, coating velocity and coating acceleration on the mean thickness of coatings.

b. Response Surface 2

The second response surface carried out was for the Middle Mean and 3 continuous associated factors. The factors and values used are detailed in Table 36. See appendix 6 for the full list of parameter combinations.

Viscosity (mPa.s)	Coating Velocity (mm/s)	Coating Acceleration (mm/s^2)
5.3	6.0	3.0
14.0	8.4	93.6
26.1	12.0	226.5
34.1	15.6	359.4
40.9	18.0	450.0

Table 36: Factor levels selected for response surface 2

Parameters not investigated in this study were set to the following:

- Triton X-100 loading – 0.01 wt%
- Volume infuse – 20 uL
- Flow infuse – 500 uL/min
- Coating gap – 120 um

Based on a uniformity of 5% for the range 310 nm – 332 nm, the accepted values for this response surface study were 293 nm – 349 nm. The results were grouped in blocks of 23 nm for the outer regions and 46 nm for the central region i.e. the desired thickness range. The region of acceptable thickness was coloured green, Figure 101.

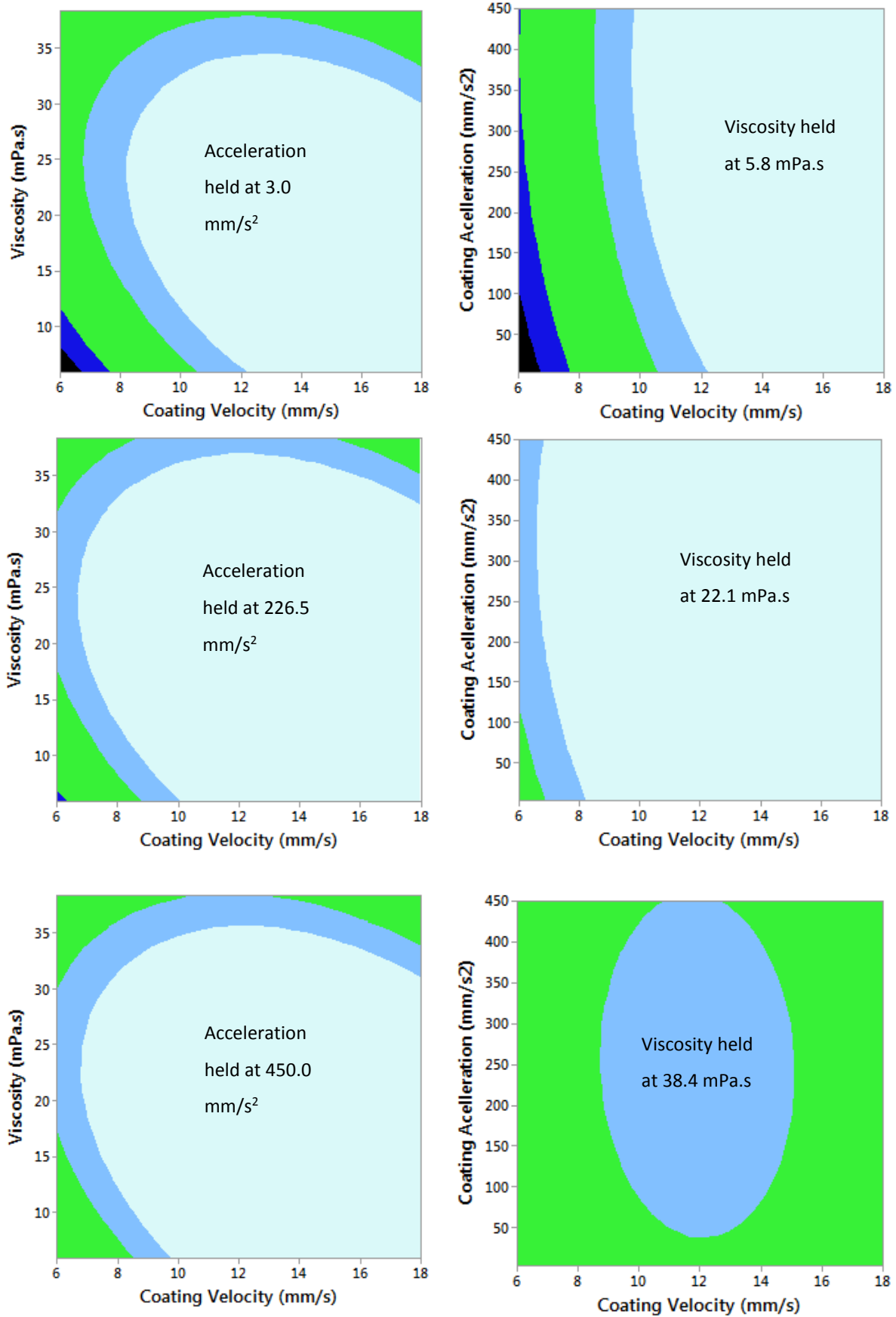Figure 101: Colour key for thickness (nm) of response surface 2 results

Figure 102: Response surface 2 contour plot results

The most noticeable conclusion to draw from the data is that the majority of the parameter combinations resulted in coatings less than 15% thinner of what was expected. The greatest observed effect was the use of high viscosity which resulted in approximately of half the operating window producing coatings of the desired thickness. Coating acceleration was having a minimal effect.

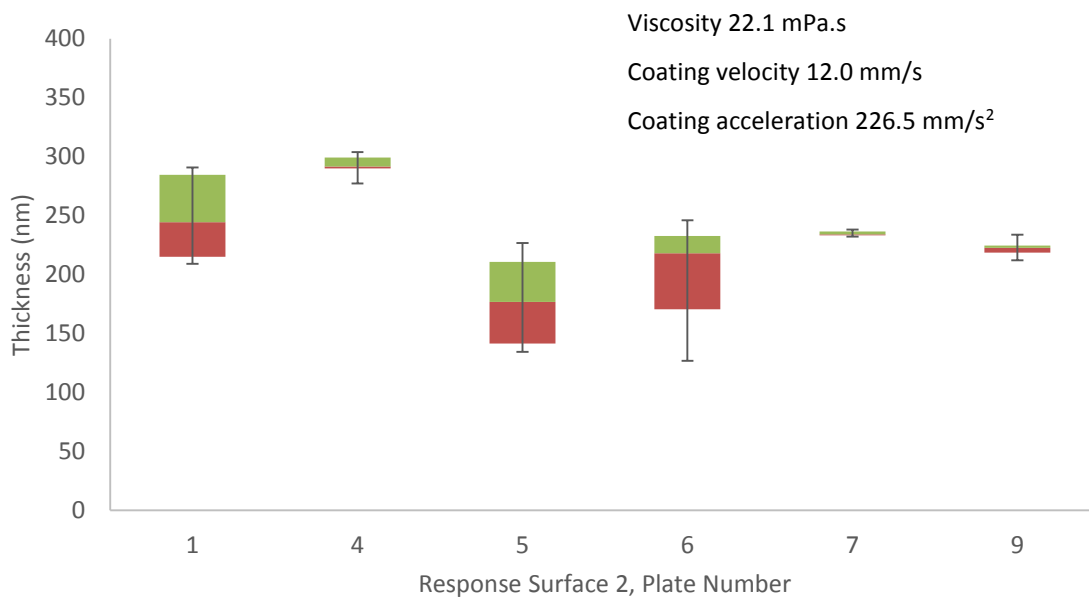As before, the middle point plates were checked for repeatability, Figure 103.

Figure 103: Box plot data showing repeatability of mid-point plates for response surface 2

Repeatability was poor bringing into question the reliability of the results obtained in this response surface. None of the mid-point parameter settings resulted in optimum coating thickness for this study; this suggested that when parameters are not fully optimised this impacts on coating repeatability hence the differences between Figure 98 and Figure 103.

The next section describes the effect of viscosity and coating velocity on the middle mean; coating acceleration was omitted from the study to focus on the other variables.

c. Response Surface 3

The same study was carried out without acceleration to isolate the effects of viscosity and coating velocity; factors and values outlined below. See appendix 7 for the full list of parameter combinations.

Viscosity (mPa.s)	Coating Velocity (mm/s)
5.3	6.0
14.0	7.8
26.1	12.0
34.1	16.2
40.9	18.0

Table 37: Factor levels selected for response surface 3

Parameters not investigated in this study were set to the following:

- Triton X-100 loading – 0.01 wt%
- Coating acceleration – 18 mm/s^2
- Volume infuse – 20 uL
- Flow infuse – 500 uL/min
- Coating gap – 120 um

The effect of coating velocity and viscosity were plotted in a contour plot using the same numerical categories as shown in the previous study, Figure 101. This showed velocity having a minimal effect on mean thickness with the majority of the changes caused by viscosity. This was unexpected.
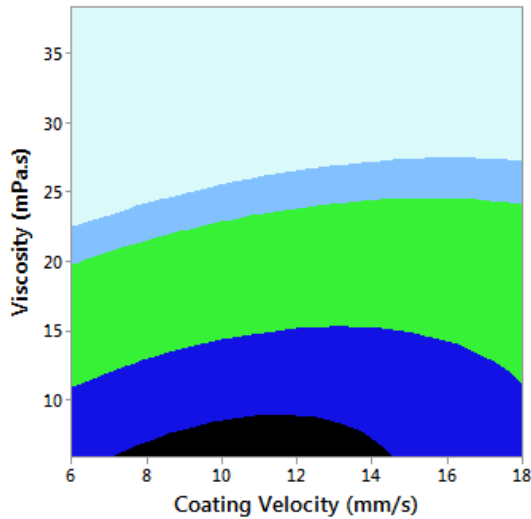
Figure 104: Response surface 3 contour plot results

Again it supported the theory that flow rate was not being properly controlled. It seems the fluid delivery system does not have a feedback loop and the syringe unit provides a flow rate purely based on the desired wet coat thickness without accounting for viscosity and speed.

For response surfaces 1-3 the shim thickness had been changed depending on viscosity, as thinner shims are usually preferred for low viscosities and thick shims are used for high viscosity formulations:

- 5.3 mPa.s fluid – 50 μm shim

- 14.0 mPa.s fluid – 50 μm shim

- 26.1 mPa.s fluid – 100 μm shim

- 34.1 mPa.s fluid – 125 μm shim

- 40.9 mPa.s fluid – 125 μm shim

It's possible that shim thickness was having a larger effect than anticipated on the flow rate. This was analysed in response surface 4.

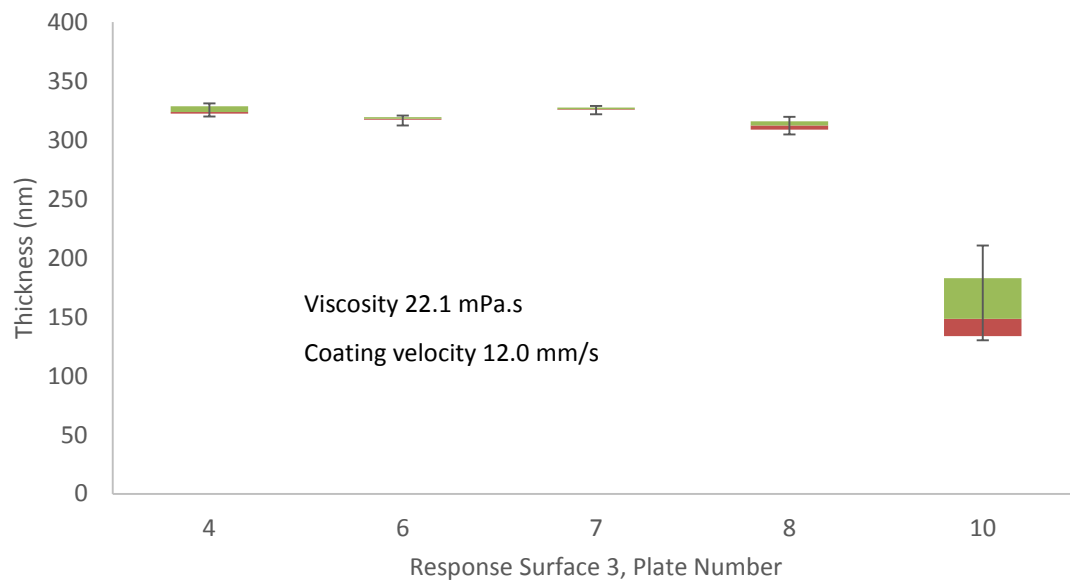Again the middle points were checked for repeatability.

Figure 105: Box plot data showing repeatability of mid-point plates for response surface 3

Results were mostly repeatable with the exception of plate 5, the response surface data was felt to be reliable.

d. Response Surface 4

The final response surface carried out incorporated 2 continuous factors (viscosity and coating velocity) and one categorical factor (shim thickness). Both responses Middle Mean and Middle SD were analysed. See appendix 8 for the full list of parameter combinations.

Viscosity (mPa.s)	Coating Velocity (mm/s)	Shim Thickness (um)
5.3	6.0	50
14.0	7.8	100
26.1	12.0	150
34.1	16.2	
40.9	18.0	

Table 38: Factor levels selected for response surface 4

Parameters not investigated in this study were set to the following:

- Triton X-100 loading – 0.01 wt%
- Coating acceleration – 18 mm/s^2
- Volume infuse – 20 uL
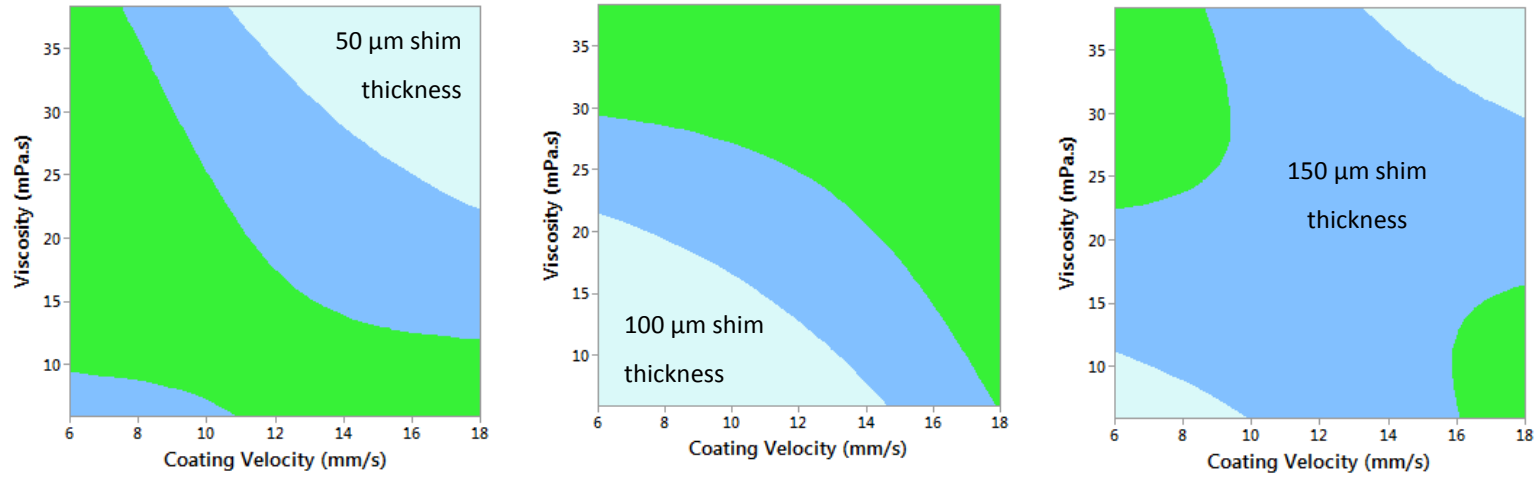- Flow infuse – 500 uL/min
- Coating gap – 120 um

Figure 106: Response surface 4 contour plot results for Middle Mean

The results showed a strong relationship between all three parameters in relation to the response of Middle Mean. Lower viscosities preferred the 50 μm shim and higher viscosities coated better with the 100 μm shim. The 150 μm shim was most favourable for high viscosities paired with low viscosities, as well as low viscosities combined with a high speed. All three shim thicknesses exhibited regions of good coating thickness at high viscosity/low speed and low viscosity/high speed. To better understand the relationships, the impact of flow resistance on flow rate was considered.

Fluid resistance can be calculated using Poiseulle's Law. For a Newtonian fluid passing through a pipe of length 'l' and radius 'r', assuming laminar flow, the fluid resistance is:

$$Rf = \frac{8\eta l}{(\pi r^2)r^2}$$

Equation 27: Fluid resistance in a pipe[61]

where:

- $Rf = Fluid\ resistance$
- $L = Length$

This can be modified for the internal volume of a slot die head. The area of a circle is πr^2, so this section of the equation relates to coating width x shim thickness, and the length is the distance between the bottom of the manifold and the edge of the slot die lips. Equation 4 is a modification of Poiseulle's law relating to internal pressure of a slot die head so the same alterations can be employed.

$$Rf = \frac{12\eta I}{s^3 B}$$

Equation 28: Fluid resistance inside the slot die head

Internal fluid resistance was calculated and plotted on a scatter graph for all combinations of shim thickness and viscosity, Figure 107.
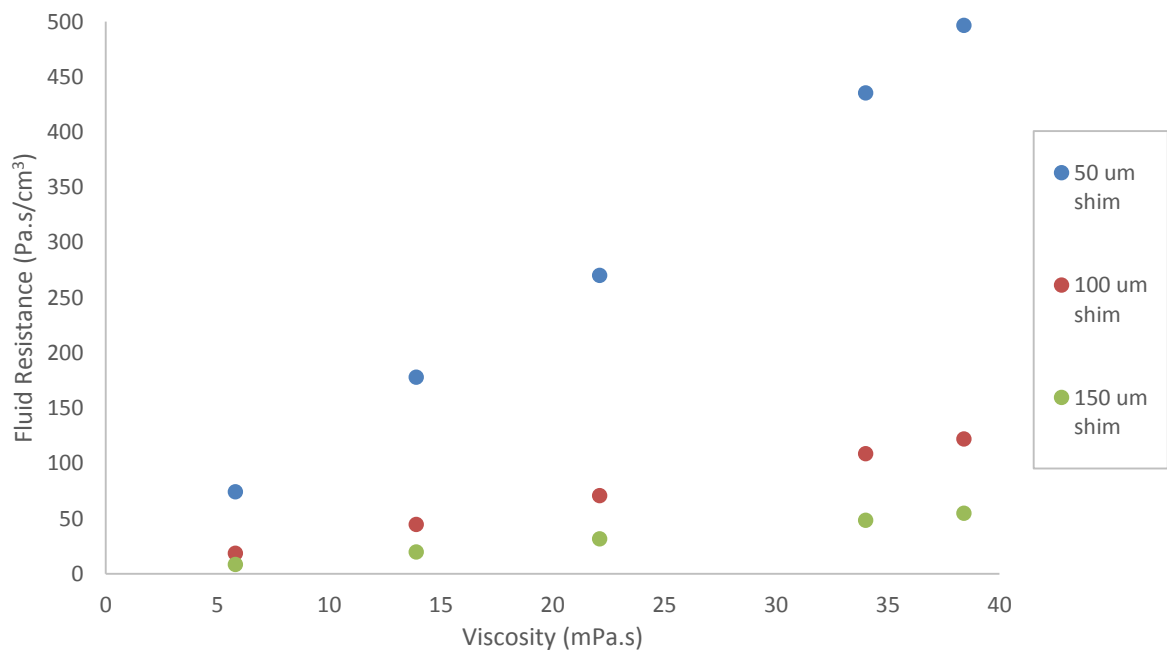

Figure 107: Fluid resistance in the slot die head

Lower shim thicknesses as well as high viscosities will result in higher fluid resistance. Pumping systems incorporating a feedback loop will account for fluid resistance therefore maintaining a consistent flow rate. However it appears the syringe delivery system incorporated into this tool does not regulate the flow rate. Therefore increasing fluid resistance will reduce the flow rate, which will decrease the wet coat thickness and consequently the dry coat thickness.

The effect of fluid resistance on flow rate can be calculated using Equation 29 though without knowing the internal pressure, the flow rate and resultant wet coat thickness (Equation 6) cannot be determined. Values can be calculated for the wet coat thickness, flow rate, fluid resistance and internal pressure using the Middle Mean, however this is not relevant without knowing what the internal pressure and flow rate should be.

$$\frac{dV_p}{dt} = \frac{\Delta p}{Rf}$$

Equation 29: Effect of fluid resistance on flow rate

Analysis of the same data was carried out to determine whether the shim was having any effect on the Middle SD. The same colour scheme was used as in response surface 1, Figure 94.
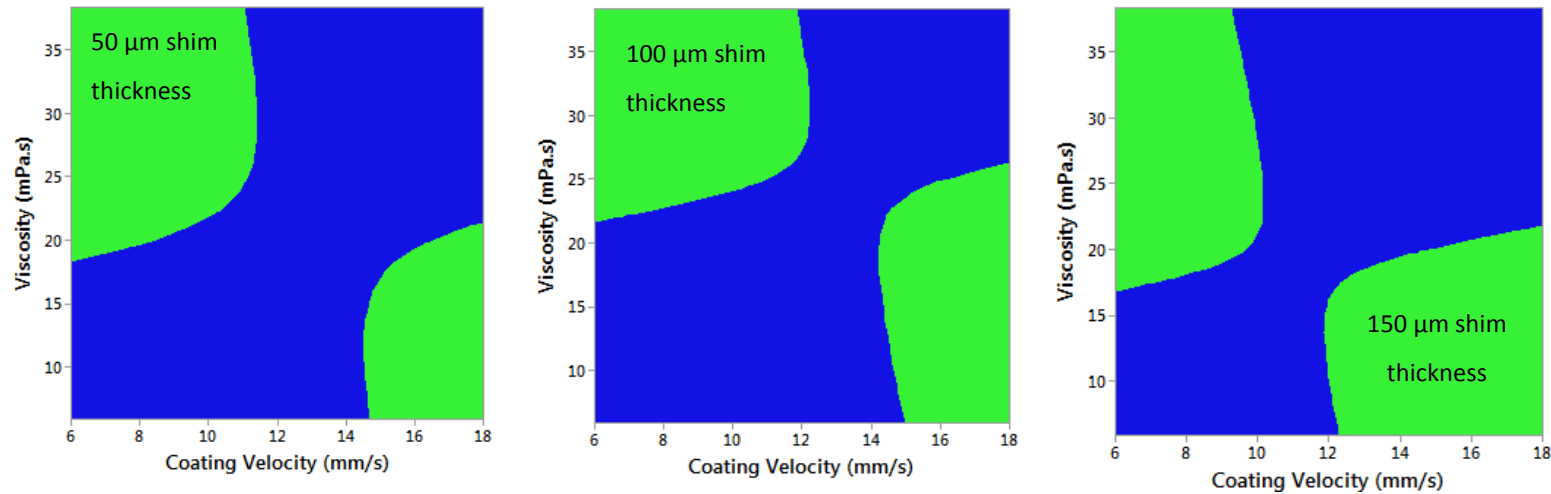

Figure 108: Response surface 4 contour plot results for Middle SD

A similar pattern was observed as for the Middle Mean data; high viscosity coupled with low coating velocity and low viscosity combined with high coating velocity resulted in the most uniform coatings. The response surface has determined an operating window at which the fluid resistance and flow rate are ideally matched to deposit the correct wet coat thickness and stabilise the bead. This is in agreement with the findings of Carvalho and Kheshgi's (2000)[29] that for a low viscosity fluid a flow rate below the flow limit will result in meniscus instability. In this case the speed is used to increase the flow rate, resulting in a stable meniscus.

During this response surface study there was no analysis carried out on the start and stop regions, however it was observed that low viscosities coated with a high shim thickness resulted in a thicker stop region, Figure 109. Shim thickness had a minimal effect on standard deviation, and the effect on the middle mean can be overcome using coating velocity. This means that the original rationale of corresponding shim thickness to viscosity can be employed to optimise start and stop regions.
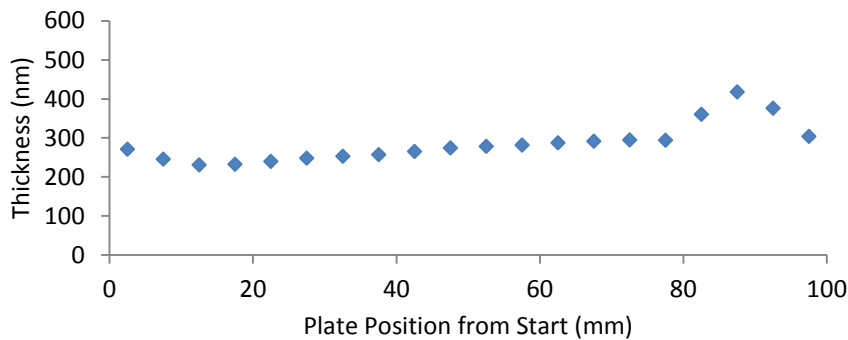

Figure 109: Example cross-section profile for low viscosity formulation coated with a thick shim

Analysis of coating repeatability of the midpoint data was found to be high for the mean thickness. With the exception of plate 23, the standard deviation data was also moderately repeatable. This allowed confidence in the data and conclusions.
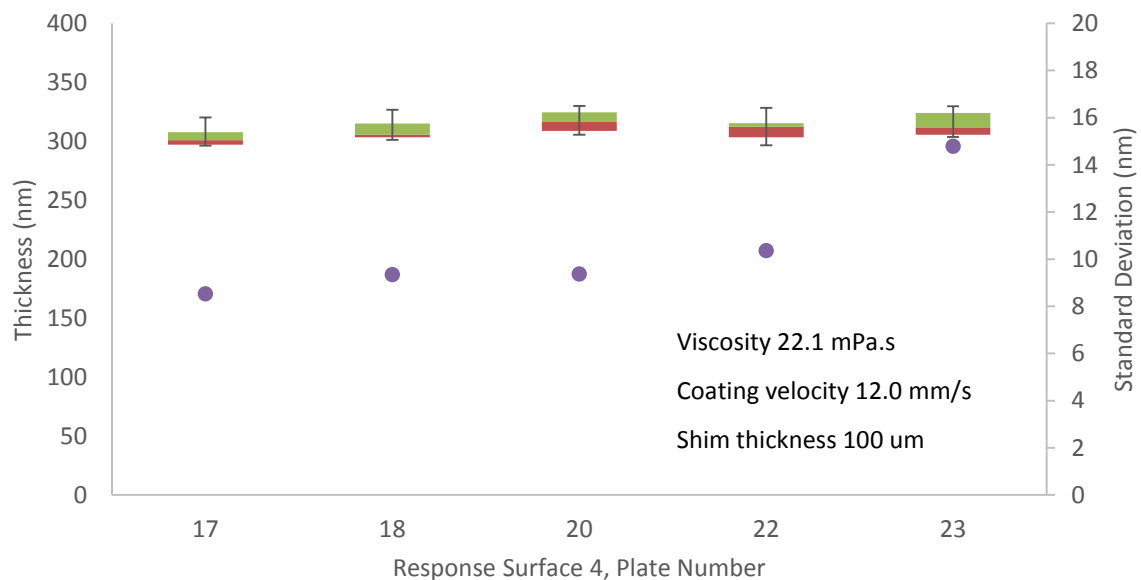

Figure 110: Box plot of thickness data and scatterplot of standard deviation, showing repeatability of mid-point plates for response surface 4

A region within the operating window has been found that will produce high uniformity coatings of the desired thickness.

6. Conclusions

The original aim of this project was to determine the effect of viscosity and surface tension on coating quality, and to assess any potential relationships between parameters in terms of their influence on coating thickness uniformity. This aim has been achieved and a number of models have been created to allow for more streamlined process development and an understanding of requirements when formulating an ink.

Surface tension was shown to have very little effect on the coating performance of the slot die coater, within the range of selected surface tension values. However formulation work was limited by wetting issues; a larger range of surface tension values may have shown a stronger relationship between surface tension and the responses. In hindsight it may have been better to use higher molecular weight polymers such as 400K – 600K molecular weight at a low loading (<2 wt%) to improve wet coat stability, this would have allowed for a lower loading of surfactant (or potentially the use of no surfactant) and therefore higher surface tension values. Surface tension had a small effect on the thickness of the start and the stop region but only when combined with the effects of coating acceleration and coating gap respectively. The influence of coating acceleration and surface tension is thought to be on the stability of the meniscus, there are a number of parameters which should counteract any issues such as coating gap, flow infuse, volume infuse. The effect of surface tension and coating gap on the stop region are expected to reduce the ease of which the material is withdrawn into the head, these effects can be minimised by using a lower gap or by increasing the pump stop offset so there is less material to be removed at the end of the plate. It would be interesting to repeat this study with a wider range of surface tensions, though this study reduces the level of concern over the effect of surface tension on coating uniformity.

It became clear during this project that viscosity has a large effect on the fluid dynamics of slot die coating, by influencing the stability of the bead and contributing to flow resistance. The viscosity and coating speed are inversely proportional and can be used to produce a coating of the correct thickness without compromising uniformity. Response surface 1 showed that it was not possible to achieve a coating of uniformity within ±5% standard deviation within the chosen parameter space due to the instability of the bead. However it may be achievable by using a lower coating gap and coating acceleration. Though it was not highlighted to be significant in the factorial study, a high coating speed was shown, in response surface 4, to exhibit good uniformity for low viscosity fluids. The investigation into the mean thickness was an unanticipated direction of work as it had been assumed early on that the flow rate was being suitably controlled. It is now thought that the flow rate is calculated based on the input values of wet coat thickness, coating speed and coating width, no correction is made to

account for acceleration or fluid resistance. However it was possible to achieve the required wet coat thickness using coating speed to correct for errors in the produced flow rate.

In summary, the effects of surface tension and viscosity can be counteracted using the know-how developed in this project. Where reformulation is possible the viscosity can be modified to allow simpler process development. Where this is not possible the data has shown that, within the operating windows investigated in this study, it is possible to achieve uniform and repeatable coatings of a required thickness.

7. Future Work

Following on from this study I hope to continue this work focussing on the start region, and potentially the stop region as a lower priority. There are a large number of parameters influencing the start region and data has suggested, namely Figure 79, that this is where error is being introduced and having a residual effect on the rest of the plate.
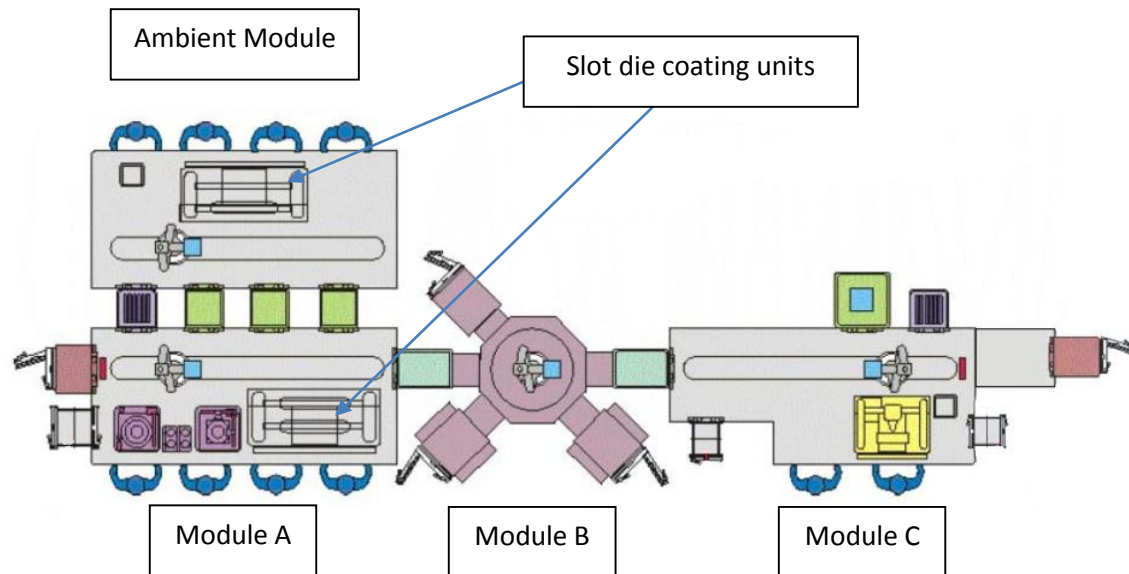
It would be interesting to assess the effects of highly pseudoplastic and thixotropic materials to determine if there was a region in which uniform coatings can be achieved, particularly in relation to electronically active polymers. Khandavalli and Rothstein (2016) report the use of shear thickening to achieve a lower minimum wet coat thickness due to a more stable meniscus. However the modification of formulations to achieve a particular viscosity could hinder electrical performance.

There are plans to purchase a new slot die system at CPI, the specification is being selected to avoid issues observed in this project. The system will cost an excess of £150,000 so specification selection is critical. The new system will incorporate sacrificial glass before and after the substrate so that the start and stop regions are not on the coated substrate, completely removing any issues related to the start and stop region. In addition to this the flow rate will be input to the software and will be regulated by a feedback loop to afford greater fluid control, removing the effects of fluid resistance resulting in variable coating thicknesses. The PEO formulations developed in this project will be used to compare coating quality with the LACE slot die coater.
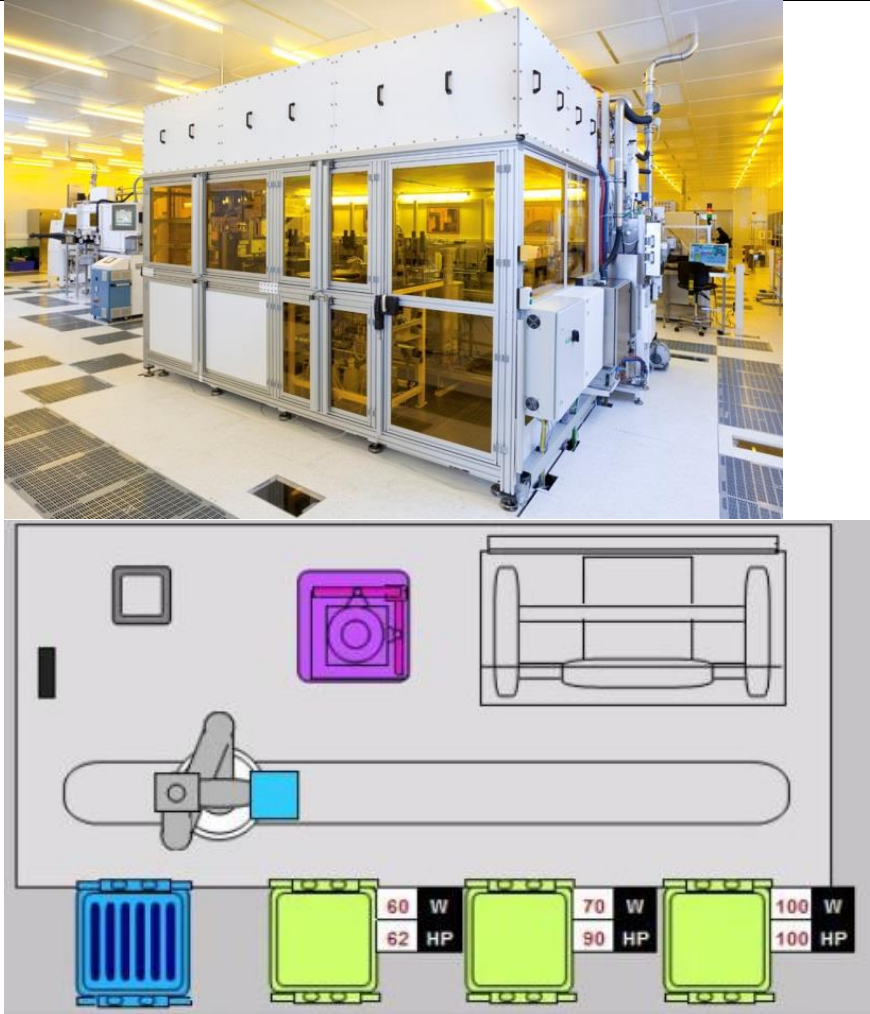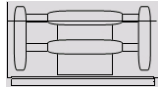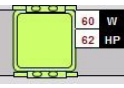
Ideally another study could be carried out using a wider range of surface tension values, potentially using different solvents. Since the new slot die system will have heating capabilities viscosity and surface tension could be controlled using heat.

8. Appendices

Appendix 1 - The LACE Line, plan and front elevation

Ambient Module

Slot die coating units

Module A

Module B

Module C

Appendix 2 – Module descriptions

| Image	Module	Tools
	Ambient Module The ambient module is named so due to processing being carried out in ambient conditions i.e. in air. This unit is used for the solution processing of materials that are not hazardous by inhalation therefore extract is not required; this is usually water-based inks. Coatings are dried in the hotplates and can subsequently be passed through into module A via the hotplates or the UV cleaner for further processing.	Slot die coater (dual head) Edge bead removal tool UV cleaner Hotplates Handling robot Cassette
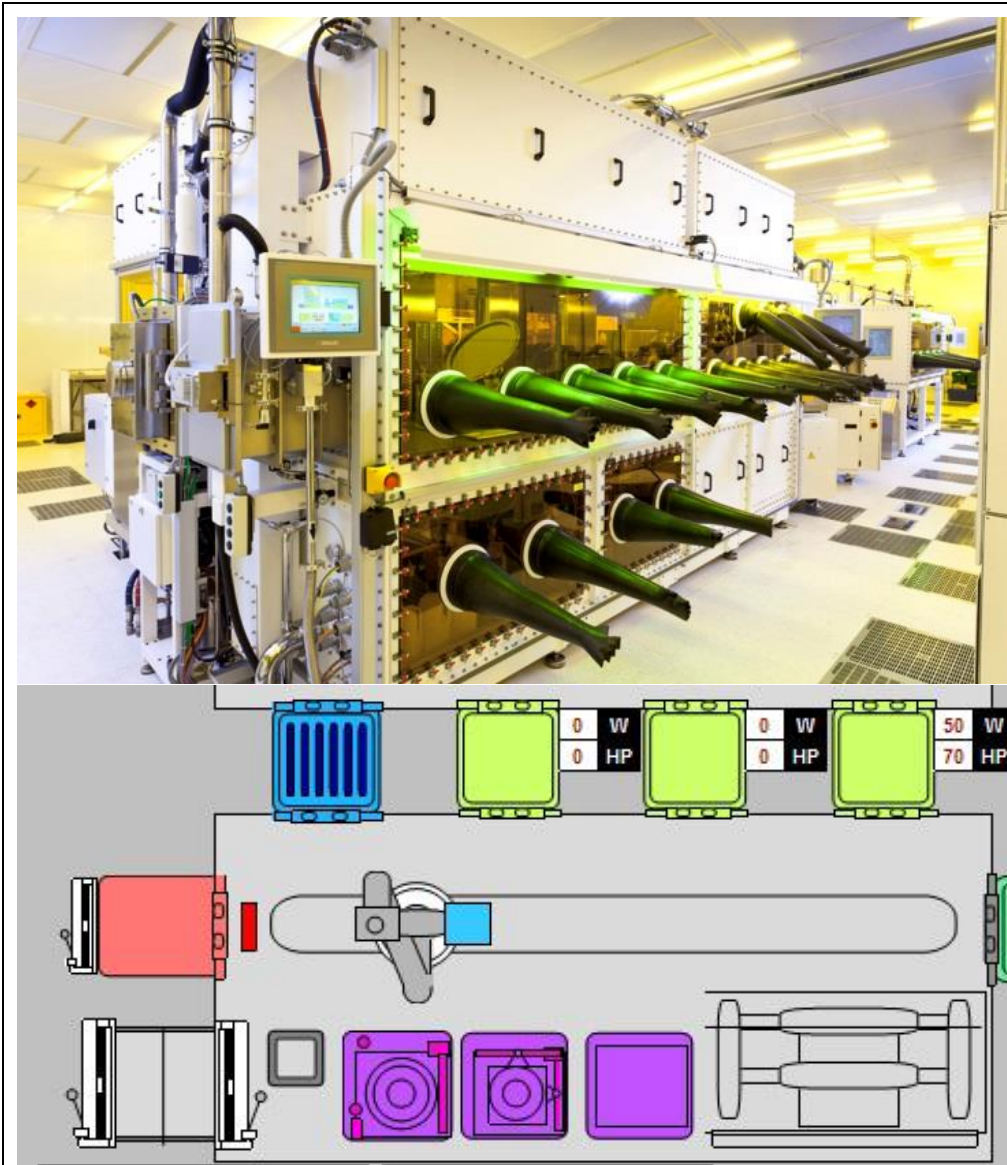
Module A – Inert Coating

Module A is setup as a glovebox configuration. It can be filled with nitrogen for the coating oxygen and moisture sensitive materials. It can also be used in air but with the glovebox glass in place to provide a barrier when hazardous solvents are in use.

Once coatings have been applied the substrate is moved to module B. Prior to this the substrate is inverted using the flip tool and is passed through using the automated robotic system.

Slot die coater (dual head)

Spin coater

Edge bead removal tool

Flip tool

UV cleaner

Hotplates

Convection oven

Handling robot

Antechamber

Cassette
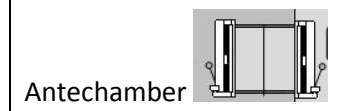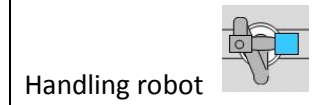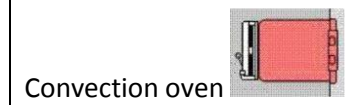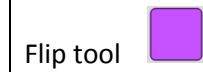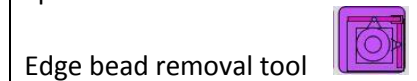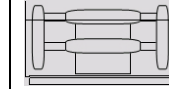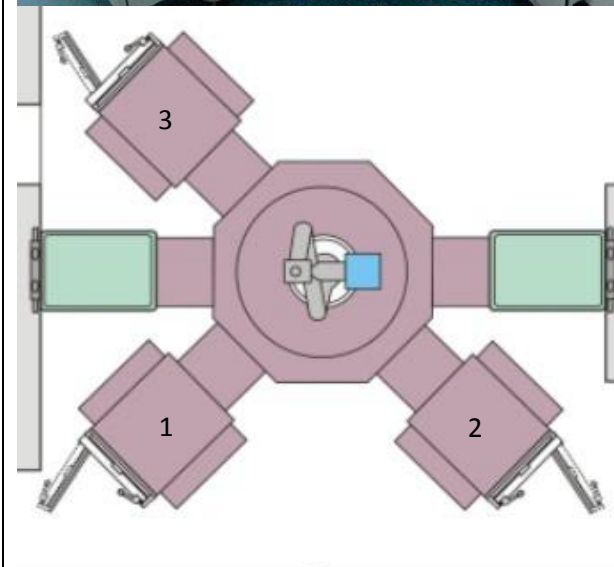
Module B – Evaporation

Metal and organic materials can be evaporated or vacuum deposited through a mask. The substrate can be passed between chambers via the robot in the centre.

Substrates are passed through to module C via the automated robot.

Evaporation module
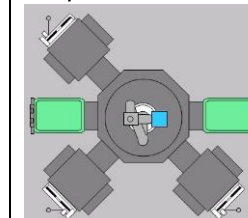
Handling robot
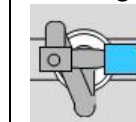
Metal deposition chamber

Organic deposition chamber
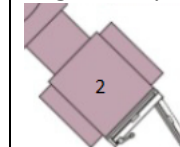
Mask loading chamber
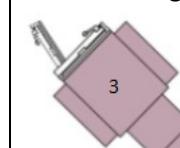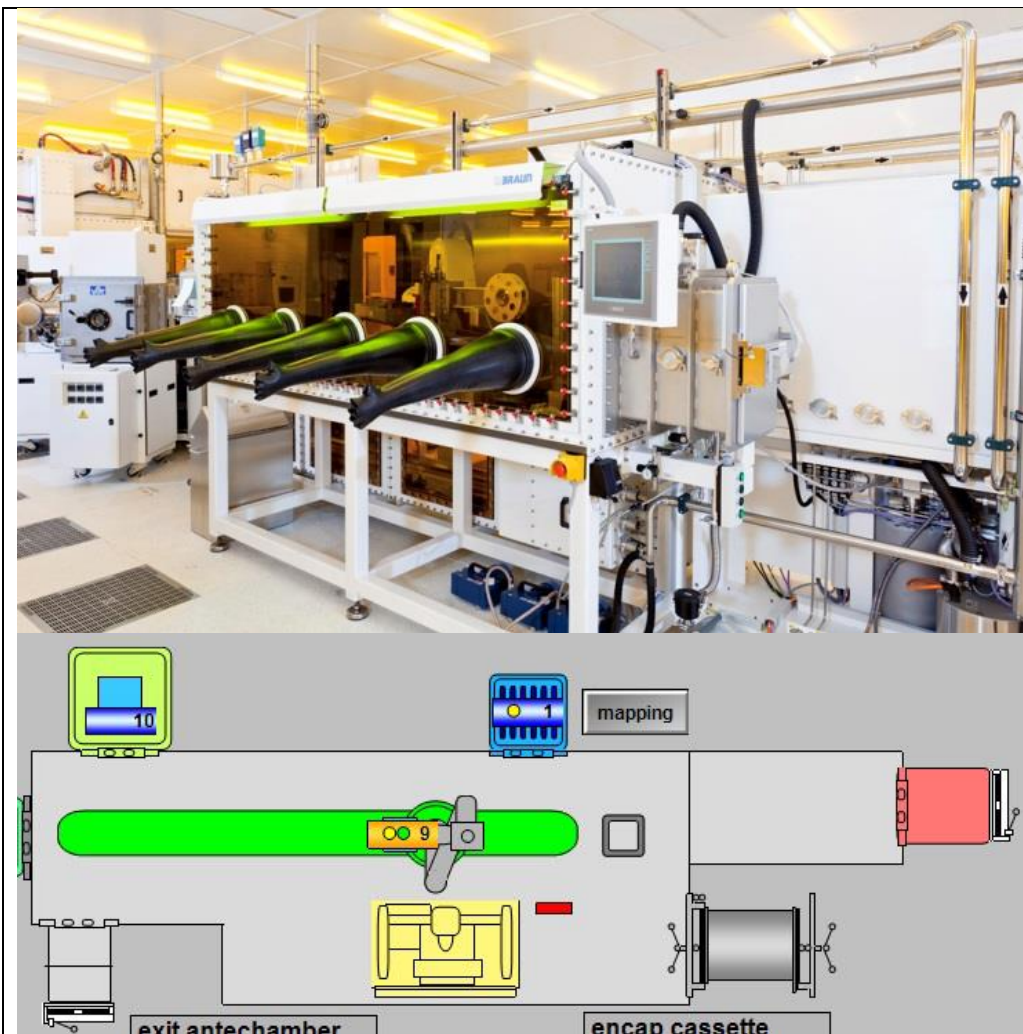
Module C –
Encapsulation

This module always remains under inter conditions.
Encapsulation of processed substrates takes place by applying an epoxy in a chosen pattern, attaching the barrier (usually 1.1 mm thick glass) and curing the epoxy using UV light.
Completed substrates are passed to the exit antechamber for removal from the LACE system.

Encapsulation module

UV-press

UV cleaner

Vacuum oven

Handling robot

Exit antechamber
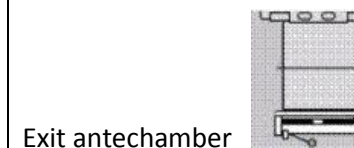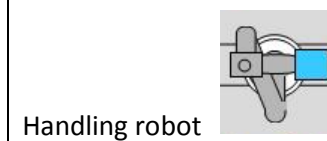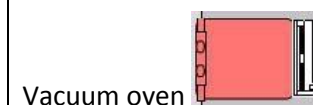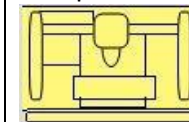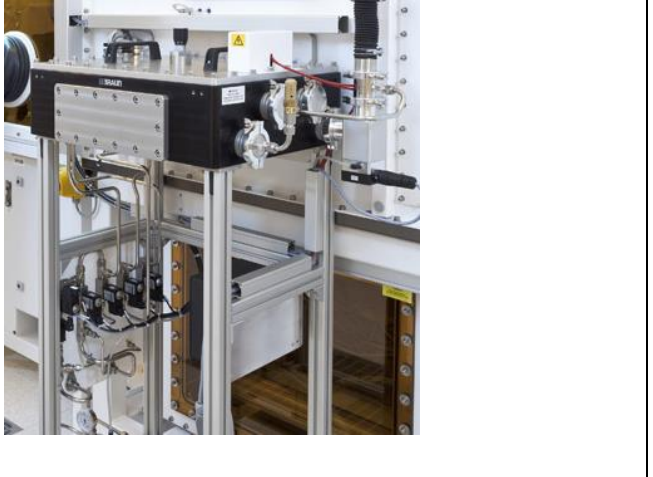
Appendix 3 – Equipment descriptions

Image	Tool	Description	Manufacturer	Specification
	Slot die coater	This is a wet coat deposition technique whereby a fluid is fed through a defined gap in a controlled manner to apply a uniform film. It contains a granite bed that incorporates substrate holders for each substrate size, changes are made in the software to dictate which holder is used.	Mathis Switzerland http://www.mathisag.com/	• Substrate thickness: 0.7 – 1.1 mm • Coating speed: 1 – 30 mm/s

	Spin coater	This is a wet coat deposition technique whereby fluid is dispensed (manually or automatically) onto the centre of the substrate and the substrate is span at a high speed to uniformly push material across the plate.
		
		Substrate holders must be manually changed to switch between substrate sizes.
			Solar Semi
			
			Germany
			
			http://www.solar-semi.com/
				• Substrate thickness: 0.7 – 3.2 mm
				• Max spin speed:
				  o 4" – 3000 rpm
				  o 6" – 1500 rpm
				  o 8" – 1000 rpm

	Edge bead removal tool	This tool removes material a defined distance from the edge using a thin stream of solvent to remove messy edges and to expose metal contacts. Substrate holders must be manually changed to switch between substrate sizes.	Solar Semi Germany http://www.solar-semi.com/	• Substrate thickness: 0.7 – 6 mm • Max edge bead removal: 18 mm

	Flip tool	This inverts the substrate so that it is correctly oriented in the evaporator. It clamps onto 5 mm of the edge of the substrate and rotates it by 180°; the same clamp is used for all substrate sizes.	Solar Semi Germany http://www.solar-semi.com/	• Substrate thickness: 0.7 – 4 mm
	UV cleaner	The UV cleaner uses ultraviolet light to clean residual hydrocarbons from the surface of substrates.	MBraun Germany http://www.mbraun.com/	Not stated in manufacturer documentation.

		Hotplate	Dries or bakes wet coats either under nitrogen or vacuum. Substrate holders must be manually changed to switch between substrate sizes.	VST Services Ltd. Israel www.vacuumltd.com	• Temperature range: 40 - 200°C
		Cluster tool	Applies uniform coatings under high vacuum conditions.	VST Services Ltd. Israel www.vacuumltd.com	Not stated in manufacturer documentation.

	Getter dispenser	Applies adhesive to attach the barrier to the substrate.	Infotech AG Switzerland www.infotech-automation.com	• Axes range o X – 400 mm o Y – 400 mm o Z – 68 mm
	UV Press	Cures the adhesive to bind the substrate to the barrier using UV light.	IST METZ Germany http://www.ist-uv.com/	• UV radiation zone: 180 – 450 nm • Lamp output: 140 W/cm

	Handling robot	Passes the substrate through the entirety of the LACE line.	MBraun Germany http://www.mbraun.com/	• Substrate thickness: 0.7 – 3.2 mm

Appendix 4 – Example fabrication process

Anode
- Pre-prepared before the substrate is loaded into the LACE line via sputter coating.

HIL
- Slot die coated in the ambient module;
- Edge bead removal is carried out in the ambient module;
- Dried in an oven and passed through to Module A.

Emissive layer
- Spin coated or slot die coated in Module A;
- Edge bead removal in Module A;
- Dried in an oven and moved back to Module A;
- Substrate inverted using the flip tool in Module A;
- Passed through to module B.

Cathode
- Cathode material deposited via evaporation in Module B;
- Passed through to Module C.

Adhesive and Barrier Glass
- Adhesive is applied in module C using the encapsulation tool;
- Corresponding barrier glass is added to the stack;
- Adhesive is UV cured;
- Completed substrate is moved to the exit antechamber to be removed from the system.

Appendix 5 – Response surface 1, parameter combinations

Plate	Viscosity (mPa.s)	Coating Acelleration (mm/s^2)	Flow Infuse (uL)	Coating Gap (um)
1	5.8	226.5	275	110
2	13.9	114.8	388	130
3	13.9	338.3	163	130
4	13.9	114.8	388	90
5	13.9	338.3	388	90
6	13.9	114.8	163	130
7	13.9	338.3	388	130
8	13.9	114.8	163	90
9	13.9	338.3	163	90
10	22.2	226.5	275	110
11	22.2	226.5	275	110
12	22.2	226.5	275	110
13	22.2	226.5	275	110
14	22.2	226.5	275	110
15	22.2	226.5	50	110
16	22.2	226.5	275	110
17	22.2	226.5	275	110
18	22.2	450.0	275	110
19	22.2	3.0	275	110
20	22.2	226.5	275	150
21	22.2	226.5	500	110
22	22.2	226.5	275	70
23	34.0	338.3	388	90
24	34.0	114.8	388	90
25	34.0	338.3	163	130
26	34.0	114.8	388	130
27	34.0	114.8	163	130
28	34.0	114.8	163	90
29	34.0	338.3	163	90
30	34.0	338.3	388	130
31	38.4	226.5	275	110

Appendix 6 – Response surface 2, parameter combinations

Plate	Viscosity (mPa.s)	Coating Velocity (mm/s)	Coating Acelleration (mm/s2)
1	22.2	12.0	226.5
2	22.2	12.0	450.0
3	22.2	6.0	226.5
4	22.2	12.0	226.5
5	22.2	12.0	226.5
6	22.2	12.0	226.5
7	22.2	12.0	226.5
8	22.2	18.0	226.5
9	22.2	12.0	226.5
10	22.2	12.0	3.0
11	13.9	15.6	93.6
12	13.9	15.6	359.4
13	13.9	8.4	359.4
14	13.9	8.4	93.6
15	5.8	12.0	226.5
16	34.0	8.4	93.6
17	34.0	15.6	93.6
18	34.0	15.6	359.4
19	34.0	8.4	359.4
20	38.4	12.0	226.5

Appendix 7 – Response surface 3, parameter combinations

Plate	Viscosity (mPa.s)	Coating Velocity (mm/s)
1	5.8	12.0
2	13.9	7.8
3	13.9	16.2
4	22.2	12.0
5	22.2	6.0
6	22.2	12.0
7	22.2	12.0
8	22.2	12.0
9	22.2	18.0
10	22.2	12.0
11	34.0	7.8
12	34.0	16.2
13	38.4	12.0

Appendix 8 – Response surface 4, parameter combinations

Plate	Shim Thickness (um)	Viscosity (mPa.s)	Coating Velocity (mm/s)
1	50	5.8	12.0
2	50	13.9	7.8
3	50	13.9	16.2
4	50	22.2	18.0
5	50	22.2	12.0
6	50	22.2	12.0
7	50	22.2	6.0
8	50	22.2	12.0
9	50	22.2	12.0
10	50	22.2	12.0
11	50	34.0	16.2
12	50	34.0	7.8
13	50	38.4	12.0
14	100	5.8	12.0
15	100	13.9	16.2
16	100	13.9	7.8
17	100	22.2	12.0
18	100	22.2	12.0
19	100	22.2	18.0
20	100	22.2	12.0
21	100	22.2	6.0
22	100	22.2	12.0
23	100	22.2	12.0
24	100	34.0	16.2
25	100	34.0	7.8
26	100	38.4	12.0
27	150	5.8	12.0
28	150	13.9	16.2
29	150	13.9	7.8
30	150	22.2	6.0
31	150	22.2	12.0
32	150	22.2	18.0
33	150	22.2	12.0
34	150	22.2	12.0
35	150	22.2	12.0
36	150	22.2	12.0
37	150	34.0	16.2
38	150	34.0	7.8
39	150	38.4	12.0

9. Reference List

[1] Sivaji Reddy, V. et al (2006) The effect of substrate temperature on the properties of ITO thin films for OLED applications, Institute of Physics Publishing, 21: 1747-1752

[2] Lv, J. (2006) Thermal stability of Ag films in air prepared by thermal evaporation, Applied Surface Science, 253: 7036-7040

[3] Hameed, S. et al (2010), Polymer Light Emitting Diodes – A Review On Materials And Techniques, Review On Advanced Materials Science, 26: 30-42

[4] Höfle, S. et al (2016) Influence of the Emission Layer Thickness on the Optoelectronic Properties of Solution Processed Organic Light-Emitting Diodes, ACS Photonics, 1: 968-973

[5] Grykien, R. et al (2014) A significant improvement of luminance vs current density efficiency of a BioLED, Optical Materials, 36: 1027-1033

[6] Barwick, D. (2012) Organic Electronics: Concepts, OLEDs and Photovoltaics, UK: CPI

[7] Ossila Ltd [2016] Spin Coating: A Guide to Theory and Techniques, available from: https://www.ossila.com/pages/spin-coating#advantages-and-disadvantages-of-spin-coating, UK: Ossila Ltd [accessed 05/12/16]

[8] Discher, David [2014] Piezoelectric Print Heads vs Thermal Print Heads, available from: http://www.aldertech.com/blog/piezoelectric-print-heads-vs-thermal-print-heads/, US: Alder Technology [accessed 05/12/16]

[9] Wierner, M and Roscher, F [2014] Aerosol Jet Printing, available from: http://www.enas.fraunhofer.de/content/dam/enas/de/documents/Downloads/datenblaetter/AerosolJetPrinting_EN_web_NEU-2014.pdf, Germany: Fraunhofer Institute for Electronic Nano Systems [accessed 05/12/16]

[10] Printers' National Environmental Assistance Center [2003] Screen Printing, available from: http://www.pneac.org/printprocesses/screen/, USA: Printers' National Environmental Assistance Center [accessed 15/12/216]

[11] Printers' National Environmental Assistance Center [2003] Print Process Descriptions: Printing Industry Overview: Flexography, available from: http://www.pneac.org/printprocesses/flexography/moreinfo7.cfm, USA: Printers' National Environmental Assistance Center [accessed 15/12/216]

[12] Macaran Printed Products (2009) Flexography 101, available from: http://www.macaran.com/flexo1.html, USA: Macaran Printed Products [accessed 15/12/16]

[13] Printers' National Environmental Assistance Center [2003] Gravure Printing, available from: http://www.pneac.org/printprocesses/gravure/, USA: Printers' National Environmental Assistance Center [accessed 15/12/216]

[14] Siemens [2014] Gravure Printing, available from: http://w3.siemens.com/mcms/mc-solutions/en/mechanical-engineering/printing-machines/gravure-printing-machine/pages/gravure-printing-machine.aspx, Germany: Siemens [accessed 15/12/16]

[15] Holman, R. and McKay, B. (2012) Print and Ink Technology, UK: PRA

[16] Park, J. Shin, K. and Lee, C. (2016) Roll-to-Roll Coating Technology and its Applications: A Review, International Journal of Precision Engineering and Manufacturing, 17: 537-550

¹⁷ Leach, R. H. and Pierce, R. J. (2008) The Printing Ink Manual (5th Ed), The Netherlands: Springer

¹⁸ Crone, Klaus P. (2014) Slot Die Coating for organic photovoltaics and other high tech applications, Germany: Coatema

¹⁹ Sumitomo Chemicals [2013] High Performance Lighting Project, available from: http://www.sumitomo-chem.co.jp/english/pled/project.html, UK: Sumitomo Chemicals [accessed 12/02/16]

²⁰ Zhang, Hongmei [2013] Printed Electrodes for OLED Panels, available from: http://apps1.eere.energy.gov/buildings/publications/pdfs/ssl/zhang_printed_longbeach2013.pdf, USA: Plextronics [accessed 10/02/16]

²¹ Choi, K. et al (2015) Multilayer slot-die coating of large-area organic light-emitting diodes, Organic Electronics, 26: 66-74

²² Raupp, S. et al (2017) An experimental study on the reproducibility of different multilayer OLED materials processed by slot die coating, Chemical Engineering Science, 162: 113-120

²³ Krebs, F. (2009) Polymer solar cell modules prepared using roll-to-roll methods: Knife-over-edge coating, slot-die coating and screen printing, Solar Energy Materials and Solar Cells, 93: 465-475

²⁴ Krebs, F. et al (2013) Freely available OPV—The fast way to progress, 1: 378-381

²⁵ Machui, F et al (2014) Large area slot-die coated organic solar cells on flexible substrates with non-halogenated solution formulations, Solar Energy Materials and Solar Cells, 128: 441-446

²⁶ Siemens [2016] Electrode Coating, available from: http://w3.siemens.com/markets/global/en/battery-manufacturing/applications/electrode-coating/Pages/default.aspx, UK: Siemens AG [accessed 13/02/16]

²⁷ Liu, D. et al (2016) Improvement of Lithium-Ion Batteries Performance by Two-Layered Slot-Die Coating Operation, Energy Technology, In press

²⁸ Lin et al (2010) Operating Window of Slot Die Coating: Comparison of Theoretical Predictions with Experimental Observations, Advances in Polymer Technologu, 29: 31-44

²⁹ Carvalho, S and Kheshgi, H (2000) Low Flow Limit in Slot Coating: Theory and Experiments, AlChE Journal, 46: 1907-1917

³⁰ Romero, O. et al (2006) Slot coating of mildly viscoelastic liquids, Jurnal of Non-Newtonian Fluid Mechanics, 138: 63-75

³¹ Chang et al (2007) Three minimum wet thickness regions of slot die coating, Journal of Colloid and Interface Science, 308: 222-230

³² Goodwin, J.W. & Hughes, R.W. (2000) Rheology for Chemists an introduction, UK: RSC

³³ Mezger, Thomas G. (2014) The Rheology Handbook (4th Ed), Germany: Vincentz Network

³⁴ Cole-Parmer [2015] Viscous Fluid Behavior, available from: http://www.coleparmer.com/TechLibraryArticle/814 London: Cole-Parmer Instrument Co. Ltd [accessed on 22/12/2015]

³⁵ TA Instruments [2016] Determination of the Linear Viscoelastic Region of a Polymer using a Strain Sweep on the DMA 2980, available from: http://www.tainstruments.com/library_download.aspx?file=TS61.pdf, UK: TA Instruments [accessed 10/02/15]

[36] Dealy. J and Plazeck, D (2009) Time-Temperature Superposition – A Users Guide, Rheology Bulletin, 78: 16 - 31

[37] Majumder, M. et al (2012) Overcoming the "Coffee-Stain" Effect by Computational Marangoni-Flow-Assisted Drop-Drying, J.Phys.Chem.B,116: 6536 – 6542

[38] Mittal, K.L. (1993) Contact Angle, Wettability and Adhesion, The Netherlands: VSP

[39] Biolin Scientific [2016] Critical Micelle Concentration, available from: http://www.biolinscientific.com/attension/applications/?card=AA8, Sweden: Biolin Scientific [accessed 02/05/16]

[40] Filmetrics [2012] Taking the mystery out of thin-film measurement, available from: http://www.filmetrics.com/pdf/Filmetrics%20Tutorial%20-%20Thickness%20Metrology%20Guide%20v3N.pdf USA: Filmetrics Inc. [accessed on 01/03/2015]

[41] Kaplonek, Wojciech & Lukianowicz, Czeslaw [2012] Coherence Correlation Interferometry in Surface Topography Measurements, Recent Interferometry Applications in Topography and Astronomy, Dr Ivan Padron (Ed.) available from: http://cdn.intechopen.com/pdfs/33093.pdf, Poland: Koszalin University of Technology, [accessed on 22/12/2015]

[42] RK Print [2015] K Control Coater, available from: http://www.rkprint.com/pdfs/kcontrolcoater.pdf, UK: RK Print-Coat Instruments Ltd. [accessed 31/12/15]

[43] Dyne Technology Ltd. [2011] Vacuum Plasma, available from: http://www.dynetechnology.co.uk/ebooks/vacuumplasma/#/1/, UK: Dyne Technology Ltd. [accessed 15/12/16]

[44] Semicore [2013] What is Sputtering?, available from: http://www.semicore.com/what-is-sputtering, USA: Semicore [accessed 15/12/16]

[45] Sigma Aldrich [2016] Chemical, physical and safety data, available from: www.sigmaaldrich.com, UK: Sigma Aldrich [accessed 21/12/15]

[46] Gilanyi, T et al (2006) Adsorption of poly(ethylene oxide) at the air/water interface: A dynamic and static surface tension study, Journal of Colloid and Interface Science, 301: 428-435

[47] Wu, Y. et al (2010) Alkyl Polyglycoside-Sorbitan Ester Formulations for Improved Oil Recovery, Tenside Surfactants Detergents, 47: 280-287

[48] Anyfantakis, Manos et al (2015) Modulation of the Coffee-Ring Effect in Particle/Surfactant Mixtures: the Importance of Particle–Interface Interactions, 31: 4113-4120

[49] McLeish, T.C.B (2002) Tube Theory of Entangled Polymer Dynamics, Advances in Physics, 51: 1379- 1527

[50] Cowie, G. and Arrighi, V (2007) Polymers: Chemistry and Physics of Modern Materials, Third Edition, US: CRC Press

[51] Biggs, S. and Mulvaney, P. (1996) Surfactant and Polymer Adsorption: Atomic Force Microscopy Measurements, ACS Symposium Series eBooks, 615: 255-266

[52] The University of Iowa (2008) Nanoparticle Mobility in Viscoelastic Media, US: ProQuest

[53] Watanabe, H. (1999) Viscoelasticity and dynamics of entangled polymers, Progress in Polymer Science, 247: 1253-1403

[54] Liu, C. et al (2006) Evaluation of different methods for the determination of the plateau modulus and the entanglement molecular weight, Polymer, 47: 4461-4479

[55] (2012) Polyethylene glycol [MAK Value Documentation, 1998]. The MAK Collection for Occupational Health and Safety, 10: 248–270

[56] Merck Millipore [2016] 818892 | Polyethylene glycol 35000, available from: http://www.merckmillipore.com/GB/en/product/Polyethylene-glycol-35000,MDA_CHEM-818892?ReferrerURL=https%3A%2F%2Fwww.google.co.uk%2F, Germany, Merck Millipore [accessed 22/12/2016]

[57] MiniTab Inc [2016] Factorial designs, available from: http://support.minitab.com/en-us/minitab/17/topic-library/modeling-statistics/doe/factorial-designs/factorial-designs/, US: MiniTab Inc [accessed 08/12/16]

[58] MiniTab Inc [2016] What is a Pareto chart of effects?, available from: http://support.minitab.com/en-us/minitab/17/topic-library/modeling-statistics/doe/factorial-design-plots/what-is-a-pareto-chart-of-effects/US: MiniTab Inc [accessed 06/12/16]

[59] MiniTab Inc [2016] What is a central composite design?, available from: http://support.minitab.com/en-us/minitab/17/topic-library/modeling-statistics/doe/response-surface-designs/what-is-a-central-composite-design/, US: MiniTab Inc [accessed 06/12/16]

[60] Yang et al (2009) Start-Up of Slot Die Coating, Polymer Engineering and Science, 49: 1158-1167

[61] University of Sydney [2004] Fluid Flow, Viscosity, Poiselle's Law, available from: http://www.physics.usyd.edu.au/teach_res/jp/fluids/viscosity.pdf, Australia: University of Sydney [accessed 06/12/16]